Astron Astrophys Rev (2012) 20:52
DOI 10.1007/s00159-012-0052-1

REVIEW ARTICLE

Circumstellar disks and planets

Science cases for next-generation optical/infrared long-baseline interferometers

S. Wolf · F. Malbet · R. Alexander · J.-P. Berger · M. Creech-Eakman · G. Duchêne · A. Dutrey · C. Mordasini · E. Pantin · F. Pont · J.-U. Pott · E. Tatulli · L. Testi

Received: 26 October 2011 / Published online: 29 March 2012

S. Wolf (✉)
Institute for Theoretical Physics and Astrophysics, University of Kiel, Leibnizstr. 15, 24118 Kiel, Germany
e-mail: wolf@astrophysik.uni-kiel.de

F. Malbet · G. Duchêne · E. Tatulli
Institut de Planétologie et d'Astrophysique de Grenoble (IPAG) UMR 5274, UJF-Grenoble 1/CNRS-INSU, Grenoble 38041, France

R. Alexander
Department of Physics & Astronomy, University of Leicester, University Road, Leicester LE1 7RH, UK

J.-P. Berger
European Organisation for Astronomical Research in the Southern Hemisphere (ESO), Casilla, 19001 Santiago 19, Chile

M. Creech-Eakman
Department of Physics, New Mexico Institute of Mining and Technology, 801 Leroy Place, Socorro, NM 87801, USA

G. Duchêne
Astronomy Department, B-20 Hearst Field Annex #3411, UC Berkeley, Berkeley, CA 94720-3411, USA

A. Dutrey
Observatoire Aquitain des Sciences de l'Univers, CNRS, UMR5804, Laboratoire d'Astrophysique de Bordeaux, University of Bordeaux, 2 rue de l'Observatoire, BP 89, 33271 Floirac Cedex, France

C. Mordasini · J.-U. Pott
Max Planck Institute for Astronomy, Königstuhl 17, 69117 Heidelberg, Germany

E. Pantin
CEA/DSM/IRFU/Service d'Astrophysique, CE Saclay, 91191 Gif-sur-Yvette, France

Abstract We present a review of the interplay between the evolution of circumstellar disks and the formation of planets, both from the perspective of theoretical models and dedicated observations. Based on this, we identify and discuss fundamental questions concerning the formation and evolution of circumstellar disks and planets which can be addressed in the near future with optical and infrared long-baseline interferometers. Furthermore, the importance of complementary observations with long-baseline (sub)millimeter interferometers and high-sensitivity infrared observations is outlined.

Keywords Interferometric instruments · Protoplanetary disks · Planet formation · Debris disks · Extrasolar planets

1 Introduction

To understand the formation of planets, one can either attempt to observe them in regions where they are still in their infancy or increase the number of discoveries of mature planetary systems, i.e., of the resulting product of the formation process. Both extrasolar planets and their potential birth regions in circumstellar disks are usually located between 0.1 to 100 AU from their parent star. For nearby star-forming regions, the angular resolution required to investigate the innermost regions is therefore of the order of (sub)milliarcseconds. Furthermore, the temperatures of the emitting inner disk material or close-in planets are in the range of hundreds to thousands of degrees Kelvin. Given these constraints, currently operating optical to infrared (IR) long-baseline interferometers are well suited to investigate the planet-formation process: They provide information at the milliarcsecond (mas) scale in the wavelength range where the emission of these objects has its maximum. In this article, we review the field of protoplanetary disks and exoplanets in the context of high angular resolution techniques, emphasizing the role of optical/IR interferometry. Furthermore, we illustrate the potential of the second generation VLTI[1] instrumentation in this field, taking into account synergies from observations obtained at complementary wavelengths and lower angular resolution.

We first provide a brief review about currently existing theoretical models and observations of protoplanetary disks and exoplanets (resp., Sects. 2 and 3). Based on this knowledge, the scientific potential of optical to mid-IR interferometers and the role of selected complementary observatories are discussed (resp., Sects. 4 and 5).

[1] Very Large Telescope Interferometer.

F. Pont
Astrophysics Group, School of Physics, University of Exeter, Stocker Road, Exeter EX4 4QL, UK

L. Testi
European Organisation for Astronomical Research in the Southern Hemisphere,
Karl-Schwarzschild-Str. 2, 85748 Garching bei München, Germany

2 Theory of disk evolution and planet formation

In this section, we give an introductory overview of the theory of disk evolution and planet formation. As a short introduction, it can necessarily only provide a simplified description of the most important lines of reasoning of these theories and many important aspects have to remain unaddressed. Instead, relevant comprehensive reviews are referred to if necessary. The objective is to have an overall understanding of planet formation from the disk stage to mature planets.

2.1 Evolution of protoplanetary disks

The most common means of observing disks around young stars is the detection of continuum emission from warm dust in the disk. This emission is brighter than the stellar photosphere at IR and even more at longer wavelengths, and such “excess” emission is usually associated with the presence of a dust disk at ∼AU radii (Kenyon and Hartmann 1995; Haisch et al. 2001).

Observing gas in disks is much more difficult, as the trace dust component dominates the disk opacity. We can detect line emission from atoms and molecules of heavy elements, or from the warm surface layers of the disk, but the most common means of observing gas in disks is through signatures of accretion onto the stellar surface. Typically we detect either the accretion luminosity, observed as UV continuum emission or veiling of photospheric lines, or broad emission lines (such as Hα) that originate in the hot accretion flow (Hartigan et al. 1995; Gullbring et al. 1998; Muzerolle et al. 2000). There is a near one-to-one correspondence between solar-mass objects showing accretion signatures (usually referred to as classical T Tauri stars, henceforth CTTs) and those showing the IR excess characteristic of inner dust disks (IR Class II). In addition, recent non-detection of warm H_2 emission sets very strict upper limits to the gas mass around non-accreting, also called weak-lined T Tauri stars (WTTS; Ingleby et al. 2009), suggesting that the mechanism for clearing inner disks is very efficient indeed.

The vast majority of young stars fall into the categories of disk-bearing CTTs or disk-less WTTs, but some show properties intermediate between these two states. These latter objects were named “transitional” disks by Strom et al. (1989), and typically show evidence of inner disk clearing. These objects are rare, accounting for $\lesssim$10 % of the TT population, and this relative lack of objects between the CTT & WTT states has long been interpreted as evidence that the transition from disk-bearing to disk-less is rapid, occurring on a time scale 1–2 orders of magnitude shorter than the Myr disk lifetime (Skrutskie et al. 1990; Kenyon and Hartmann 1995; Simon and Prato 1995; Wolk and Walter 1996). In recent years, it has become clear that the transitional disks are not a homologous class of objects (Salyk et al. 2009), and a number of different mechanisms have been proposed for their origin (Najita and Muzerolle 2007; Chiang and Murray-Clay 2007; Ireland and Kraus 2008; Alexander 2008a; Cieza et al. 2008; Alexander and Armitage 2009). It is clear, however, that transitional disks have undergone significant evolution, and further investigation of them may be crucial to our understanding of disk evolution and clearing.

Protoplanetary disks typically live for a few Myr, with a spread of lifetimes of at least an order of magnitude. Disks have been found to cover a mass range of $\sim$0.1–0.001 $M_\odot$ (Andrews and Williams 2005), and to possess accretion rates of $\sim 10^{-7}$–10^{-10} $M_\odot\,yr^{-1}$ (Hartigan et al. 1995; Gullbring et al. 1998; Muzerolle et al. 2000). The relative lack of objects seen between the disk-bearing Class II and diskless Class III states implies that the dust clearing time scale is short ($\sim 10^5$ yr), and recent observations suggest that this two-time-scale constraint applies to the gaseous component of the disk also (Ingleby et al. 2009). Models of disk evolution must satisfy all of these constraints. Moreover, the mass budget demands that all gas giant planets must form before their parent disks are dispersed, and thus understanding protoplanetary disk evolution is crucial to understanding how planetary systems are formed.

2.1.1 Role of accretion in the standard disk theory

Angular momentum conservation is fundamental to the evolution of protoplanetary disks. Disks form because angular momentum is conserved during protostellar collapse, and estimates of the rotational velocities of molecular cores (Goodman et al. 1993) imply that young stars should be surrounded by centrifugally supported disks of tens to hundreds of AU in size (as observed). Material in such a disk must lose angular momentum if it is to accrete, so further evolution requires the transport of angular momentum through the disk. Understanding how angular momentum is transported is therefore crucial to understanding how protoplanetary disks evolve. The theory of protoplanetary disk evolution has been discussed in depth in a number of review articles in recent years (Dullemond et al. 2007; Alexander 2008a; Lodato 2008; Armitage 2007, 2010); here we present only a brief summary of the salient points.

Classical accretion disk theory invokes a fluid viscosity as the source of angular momentum transport (Shakura and Sunyaev 1973; Lynden-Bell and Pringle 1974), but from an early stage it was clear that ordinary molecular viscosity is many orders of magnitude too inefficient to be responsible for the accretion we see in real astrophysical disks. Early models side-stepped this problem by appealing to turbulence in the disk as a source of angular momentum transport, but the physical origin of such turbulence remained elusive. The seminal work of Shakura and Sunyaev (1973) introduced the famous alpha-prescription, where the efficiency of angular momentum transport is given by the expression $\nu = \alpha c_{\mathrm{s}} H$ where ν is the kinematic viscosity, c_s is the local sound speed, and H is the scale height of the disk. The quantity $\alpha \leq 1$ is a dimensionless parameter which characterizes the strength of the turbulence (formally the ratio of the turbulent stress to the local pressure), and essentially encapsulates all that one does not understand about how angular momentum is transported in accretion disks. However, simple models of this type provide considerable insight into how disks around young stars evolve, and the basic paradigm of viscous disk accretion is broadly consistent with the observed data. Angular momentum is transported outward, which allows mass to be accreted. In the absence of infall onto the disk the disk mass and accretion rate decline with time, while the disk spreads radially to conserve angular momentum (Lynden-Bell and Pringle 1974; Pringle 1981; Hartmann et al. 1998).

We now know of a number of potential mechanisms for angular momentum transport in disks, the most relevant of which are magneto-hydrodynamic (MHD) turbulence (driven by the magneto-rotational instability, MRI; Balbus and Hawley 1991; Balbus 2009), and gravitational instabilities (GIs; Toomre 1964; Lodato and Rice 2004, 2005). Disks become unstable to GIs if they are sufficiently massive and/or cold. Detailed calculations suggest that protoplanetary disks are only likely to be gravitationally unstable if they have masses $\gtrsim$0.1 $M_\odot$ (Rafikov 2009; Clarke 2009), and even then GIs can only occur in the cold, outer regions of the disk. Disk masses decline with time as the disk accretes onto the star, and consequently GIs dominate only at very early times. Angular momentum transport by GIs may well be responsible for the accretion of much of the stellar mass through the disk at early times, but they cannot be significant for the majority of the disk lifetime.

By contrast, the MRI is expected to operate in any weakly magnetized shear flow, provided that the gas is sufficiently ionized to couple to the magnetic field. However, in protoplanetary disks it is not clear that this ionization threshold is always met. The disk is thermally ionized very close to the star, and cosmic rays and stellar X-rays ionize a moderately thick surface layer, but MRI-"dead" zones can exist at the midplane at $\sim$AU radii (Gammie 1996; Armitage et al. 2001; Zhu et al. 2009). The rate of angular momentum transport due to the MRI remains the subject of current research, but numerical simulations of MHD turbulence suggest that it can transport angular momentum with an efficiency of $\alpha \sim 0.001$–0.1 (Stone et al. 1996).

Observations provide us with only limited insight into how angular momentum is transported in protoplanetary disks. Accretion histories of CTTs are generally consistent with simple, constant-α viscous accretion disk models, but the data do not give strong constraints on the model parameters. Hartmann et al. (1998) showed that the viscous accretion models of Lynden-Bell and Pringle (1974) can reproduce the observed decline in CTT accretion rates with time, and estimated a typical $\alpha \sim 0.01$. The basic paradigm of viscous accretion in protoplanetary disks remains broadly consistent with the observed accretion histories of T Tauri stars (Sicilia-Aguilar et al. 2010).

Where pure accretion disk models fail, however, is in the final clearing stage. Viscous accretion disk models predict that the various observable quantities (mass, accretion rate, surface density) should decline as power laws in time, and thus the time required for a viscous disk to evolve from one state into another is always of order the disk age. This is dramatically inconsistent with the rapid disk clearing observed in T Tauris, and strongly suggests that some other mechanism plays a dominant role in the latter stages of protoplanetary disk evolution. At present, the favored process is that of disk photoevaporation.

2.1.2 Importance of photoevaporation in disk evolution

The basic principle of photoevaporation is simple: high-energy (UV or X-ray) photons heat the disk surface, and beyond some radius the hot surface layer contains sufficient thermal energy to escape the stellar gravitational potential and flow as a wind. The critical length-scale for photoevaporation (the "gravitational radius" R_g)

can be estimated by equating the thermal energy (per particle) of the heated layer with the gravitational binding energy, so $R_g = GM_*/c_{\rm hot}^2$ where M_* is the stellar mass, and $c_{\rm hot}$ is the sound speed in the hot surface layer. Careful consideration of the pressure forces tells us that the bulk of the mass loss in fact comes from a factor of a few inside R_g (Liffman 2003; Font et al. 2004), and the resulting winds are analogous to, for example, Compton-heated winds from the disks around AGNs (Begelman et al. 1983).

The temperature of the heated layer, and thus the value of $c_{\rm hot}$, depends on the nature of the irradiation. In the case of protoplanetary disks, there are three important cases to consider: extreme ultraviolet (EUV) ionizing photons; far-ultraviolet (FUV); and X-rays. EUV irradiation creates an ionized layer on the disk surface, akin to an HII region, with $T \simeq 10^4$ K and $c_{\rm hot} \simeq 10$ km/s, so the critical length-scale for EUV photoevaporation is typically ≃1–2 AU. Heating by FUV or X-rays is more complex, leading to a range of temperatures in the disk atmosphere, but in general the critical radii range from a few AU to a few tens of AU, depending on the flux and spectrum of the incident radiation field. The irradiation can arise from the star irradiating its own disk, or come from external sources such as nearby O-stars. External irradiation is observed to drive disk photoevaporation in some cases, such as the "proplyds" in the Orion Nebula (Johnstone et al. 1998), but for most T Tauri disks irradiation from the central star dominates.

In general, computing the structure of photoevaporative winds is a complicated problem in both radiative transfer and hydrodynamics. In the EUV case the wind structure has been computed by Hollenbach et al. (1994) and Font et al. (2004). It gives rise to a wind rate which is given by $\dot{M}_{\rm w} \simeq 10^{-10} \Phi_{41}^{1/2} (M_*/M_\odot)^{1/2}\ {\rm M_\odot\ yr^{-1}}$ (where Φ_{41} is the stellar ionizing flux in units of 10^{41} ionizing photons per second). The ionizing luminosities of T Tauri stars are in general not well known, but typical estimates suggest values in the range 10^{40}–10^{42} photons/s (Alexander et al. 2005; Herczeg 2007). The bulk of the ionizing emission from T Tauri stars arises in the stellar chromosphere (Alexander et al. 2004, 2005) and is thus largely independent of the evolutionary state of the disk, so the wind rate is approximately constant over the Myr disk lifetime.

When combined with viscous evolution of the disk, EUV photoevaporation gives rise to rather surprising behavior. At early times, the accretion rate through the disk exceeds the wind rate by several orders of magnitude, so the wind is negligible. However, the accretion rate declines with time, and eventually (typically after a few Myr) reaches the same level as the (constant) wind rate. The mass loss due to the wind is concentrated at radii of a few AU, so at this point the wind cuts off the inner disk from re-supply. The inner disk then drains on its (short) viscous time scale, leaving an ∼AU-sized "hole" in the disk (Clarke et al. 2001). As it drains, the inner disk becomes optically thin to EUV photons, which increases the wind rate by a factor of ∼10, and the wind then clears the disk from the inside-out in $\sim 10^5$ yr (Alexander et al. 2006a, 2006b). This rapid clearing after a long lifetime appears to be consistent with observations of disk evolution (Alexander et al. 2006b; Alexander and Armitage 2009), and due to the role of the wind in precipitating disk clearing, this class of models are often referred to as "UV-switch" models (Clarke et al. 2001).

Photoevaporation by FUV radiation and/or X-rays is a much more complex problem (both in terms of radiative transfer and hydrodynamics), and consequently models of X-ray and FUV photoevaporation are not yet as advanced as for EUV photoevaporation. However, significant progress has been made in this area recently, using sophisticated radiative transfer codes and numerical hydrodynamics (Ercolano et al. 2009; Gorti and Hollenbach 2009; Gorti et al. 2009; Owen et al. 2010, 2011). Models of both X-ray- and FUV-driven winds suggest maximum wind rates as high as $\sim 10^{-8}\ M_{\odot}\,yr^{-1}$, and when coupled with viscous evolution these models predict a similar "switch" behavior to the EUV case, albeit at a much higher accretion rate (Gorti et al. 2009; Owen et al. 2010). Such high wind rates are unlikely to occur in all objects, however, and it remains to be seen how these results scale with various model parameters. These results all suggest that photoevaporation plays a dominant role in disk evolution at late times. This theoretical view is supported by recent observations of blue-shifted forbidden emission lines from some T Tauri stars (Pascucci and Sterzik 2009; Pascucci et al. 2011). These observations unambiguously detect a slow ($\sim$10 km/s), ionized wind, and are broadly consistent with the predictions of photoevaporation models (Alexander 2008b; Ercolano and Owen 2010); further such data will provide important new insight into the processes driving disk clearing.

2.2 Formation of planets

While the structure and evolution of protoplanetary disks has been discussed in the previous section, these objects are now considered as the environment for the formation of planets therein. For more comprehensive reviews, we refer the reader to Lissauer (1993), Papaloizou and Terquem (2006), Armitage (2007), and the book of Klahr and Brandner (2006).

2.2.1 Observational constraints

The guidelines to understand the physics involved in the different stages of planet formation come from observational constraints derived from three different classes of astrophysical objects. The first one is our own planetary system, i.e. the Solar System. Studies of the Solar System include remote observations of the Sun, the planets and the minor bodies, laboratory analysis of meteorites, in-situ measurements by space probes, possibly including sample returns, as well as theoretical work and numerical modeling.

The second class of astrophysical objects leading to important constraints on planetary formation are protoplanetary disks. As planets are believed to form in protoplanetary disks, the conditions in them are the initial and boundary conditions for the formation process. As already discussed in Sect. 2.1, the fraction of disk-bearing stars is a roughly linearly decreasing function of cluster age, disappearing after about 4–6 Myr. Giant planets must have formed at this moment. This represents a non-trivial constraint on classical giant planet-formation models.

The third class are finally the extrasolar planets, which can all be regarded as different examples of the final outcome of the formation process (see Sect. 3.2). Especially the fact that many extrasolar planets were found exactly where one did not expect to find them pointed towards a serious gap in the understanding of planet formation derived from the Solar System alone, so that the mentioned orbital migration which we will address in Sect. 2.2.6 is nowadays regarded as an integral component of modern planet-formation theory.

The already large number of extrasolar planets also gives us the possibility to look in a new way at all these discoveries: to see them no more just as single objects, but as a population with distributions of extrasolar planet masses, semimajor axes, host star metallicities and so on, as well as all kinds of correlations between them. A theoretical study of these statistical properties of the exoplanet population is done best by the method of planetary population synthesis (Ida and Lin 2004a, 2004b; Mordasini et al. 2009a, 2009b).

2.2.2 From dust to planetesimals

The first stage of planetary growth starts with roughly micro-meter sized dust grains, similar to those found in the interstellar medium. These tiny objects are well coupled to the motion of the gas in the protoplanetary disk via gas drag. With increasing mass, gravity becomes important also, and the particles decouple from the pure gas motion. This stage involves the growth of the dust grains via coagulation (sticking), their sedimentation towards the disk midplane, and their radial drift towards the star. In this context, the gas and the solid particles move around the star at a slightly different orbital speed. The reason for this is that the gas is partially pressure supported (both the centrifugal force and the gas pressure counteract the gravity), and therefore moves slightly slower (sub-Keplerian) around the star. The resulting gas drag in turn causes the drift of the solid particles towards the star.

In the picture of classical coagulation, bodies grow all the way to kilometer size by two-body collisions. While growth from dust grains to roughly meter sized bodies can be reasonably well modeled with classical coagulation simulations as for example in Brauer et al. (2008a), two significant problems arise at the so-called “meter barrier”:

- For typical disk properties, objects which are roughly meter sized drift extremely quickly towards the central star where they are destroyed by the high temperatures. The drift time scale at this size becomes in particular shorter than the time scale for further growth (Klahr and Bodenheimer 2006), so that growth effectively stops.
- The second problem arises from the fact that meter sized boulders do not stick well together, but rather shatter at the typical collision speeds which arise from the turbulent motion of the disk gas, and the differential radial drift motion.

First ideas on how to bypass the critical meter size were put forward already a long time ago, and invoke the instability of the dust layer to its own gravity, which can produce full blown planetesimals from small sub-meter objects. In the classical model of Goldreich and Ward (1973), dust settles into a thin layer in the disk midplane. If the concentration of the dust becomes sufficiently high, the dust becomes unstable to its own gravity and collapses to form planetesimals directly. The turbulent speed of the grains, however, must be very low to reach the necessary concentration. This condition is difficult to meet, as the vertical velocity shear between the dust disk rotation at the Keplerian frequency and the dust poor gas above and below the midplane rotating slightly sub-Keplerian causes the development of Kelvin–Helmholtz instabilities.

The resulting turbulence is sufficiently strong to decrease the particle concentration below the threshold necessary for the gravitational collapse. This is why self-gravity of the dust, and gas turbulence, either due to the Kelvin–Helmholtz mechanism, or due to the magneto-rotational instability (Balbus and Hawley 1998), were for a long time thought to be mutually exclusive.

In recent years, however, significant progress has been made in the direction of planetesimal formation by self-gravity (Johansen et al. 2006; Cuzzi et al. 2008). In particular, it was understood that turbulence can actually aid the formation of planetesimals, rather than hindering it. The reason is that turbulence can locally lead to severe over-densities of the solid particle concentration by a factor as high as 80 compared to the normal dust to gas ratio on large scales of the turbulence (Johansen et al. 2006) or by $\sim 10^3$ on small scales (Cuzzi et al. 2008). Further concentration can occur thanks to the streaming instability (Youdin and Goodman 2005), which all together can lead to the formation of gravitationally bound clusters with already impressive masses, comparable to dwarf planets (Johansen et al. 2007), on a time scale much shorter than the drift time scale. This so-called gravoturbulent planetesimal formation should leave imprints visible in the Solar System distinguishing it from the classical pure coagulation mechanism. The recent work of Morbidelli et al. (2009) finds that the observed size frequency distribution in the asteroid belt cannot be reproduced with planetesimals that grow (and fragment) starting at a small size. It rather seems that planetesimals need to get born big in order to satisfy this observational constraint, with initial sizes between already 100 and 1000 km. On the other hand, too large initial sizes for the majority of the planetesimals might not be desirable either, as this could slow down the formation of giant planet cores, at least if the planetesimal accretion occurs through a mechanism similar as described in Pollack et al. (1996). This is due to the higher random velocities of massive planetesimals, and the less effective capture of larger bodies by the protoplanetary gaseous envelope.

2.2.3 From planetesimals to protoplanets

At the size of planetesimals (∼kilometers), gravity is clearly the dominant force, even though the gas drag still plays a role. However, the growth stage from planetesimals to protoplanets (with radii of order a thousand kilometers) remains challenging to study because of the following reasons:

- The initial conditions are poorly known since the formation mechanism and, thus, the size distribution of the first planetesimals are not yet clearly understood (see previous section).
- The very large number of planetesimals to follow prevents any direct N-body integrations with current computational capabilities. For example, a planet with a mass of about ten Earth masses consists of more than 10^8 planetesimals with a radius of 30 km.
- The time sequence to be simulated (typically several million years) is very long, equivalent to the same number of dynamical time scales (at 1 AU).
- The growth process is highly non-linear and involves complex feedback mechanisms since the growing bodies play an increasing role in the dynamics of the system.

– The physics describing the collisions which are ultimately needed for growth is non-trivial and includes for example shock waves, multi-phase fluids and fracturing.

The planetesimals-to-protoplanets growth stage has therefore been modeled with different methods, each having different abilities to address the listed issues. Here, we only address the most basic approach. Other, more complex methods which yield a more realistic description of this stage are statistical methods (Inaba et al. 2001) or Monte Carlo methods (Ormel et al. 2010).

In the *rate equations* approach, the growth of a body is described in the form of a rate equation which directly gives the mass growth rate dM/dt of a body as a function of several quantities. Usually it is assumed that one large body (the protoplanet) collisionally grows from the accretion of much smaller background planetesimal (see e.g. Goldreich et al. 2004). These background planetesimals are characterized by a size (or a size distribution), a surface density and a dynamical state (eccentricity and inclination). The growth rate is then described with a Safronov (1969) type equation,

$$\frac{dM}{dt} = \pi R^2 \Omega \Sigma_{\mathrm{p}} F_{\mathrm{G}} \tag{1}$$

where Ω is the Keplerian frequency of the large body at an orbital distance a around the star of mass M_*, and Σ_{p} is the surface density of the field planetesimals, R is the radius of the large body, and F_{G} is the gravitational focusing factor. It reflects the fact that due to gravity, the effective collisional cross section of the body is larger than the purely geometrical one, πR^2, since the trajectories get bent towards the large body. The focusing factor is the key parameter in this equation, as it gives raise to different growth regimes: *runaway*, *oligarchic* or *orderly growth*, which come with very different growth rates (Rafikov 2003). Its value depends on the random velocity of the small bodies v_{ran} relative to the local circular motion. It scales with their eccentricity and inclination. The small bodies are mutually affected by the encounters between them, and by the large body (which increases the random velocity) and the damping influence by the gas (which decreases it).

In the simplest approximation, where one neglects the influence of the star, F_{G} is given as $1 + v_{\mathrm{esc}}^2/v_{\mathrm{ran}}^2$, where v_{esc} is the escape velocity from the big body. One notes that if the planetesimals have small random velocities in comparison with v_{esc}, then F_{G} is large and fast accretion occurs. The mass accretion rate is then proportional to R^4, i.e. strongly nonlinear. This is the case in the so-called runaway growth regime, where massive bodies grow quicker than small ones, so that these runaway bodies detach from the remaining population of small planetesimals (Weidenschilling et al. 1997). However, with increasing mass, these big bodies start to increase the random velocities of the small ones, so that the growth becomes slower, and the mode changes to the so-called oligarchic mode, where the big bodies grow in lockstep (Ida and Makino 1993).

As the planet grows in mass, the surface density of planetesimals must decrease correspondingly (e.g. Thommes et al. 2003). As the growing protoplanet is itself embedded in the gravitational field of the star, one finds by studying the restricted three body problem that a growing body can only accrete planetesimals which are within its gravitational reach (in its feeding zone), i.e. in an annulus around the body which has a half width which is a multiple (∼4) of the Hill sphere radius $R_{\mathrm{H}} = (M/3M_*)^{1/3}a$ of the protoplanet. Without radial excursions (migration), a protoplanet can therefore grow in situ only up to the so-called isolation mass (Lissauer 1993).

The outcome of this growth stage is the inner part of the planetary system with a high number of small protoplanets, with masses between 0.01 and 0.1 $M_\oplus$, which are called *oligarchs*. When the gas disk is present, growth is stalled at such masses since gas damping hinders the development of high eccentricities which would be necessary for mutual collision between these bodies (Ida and Lin 2004a). In the outer part of the planetary system, i.e. beyond the iceline, a few 1 to 10 $M_\oplus$ protoplanets form.

2.2.4 From protoplanets to giant planets

For the formation of the most massive planets, the gaseous giants, two competing theories exist. The most widely accepted theory is the so-called core accretion–gas capture model. However, we will first discuss the direct gravitational collapse model.

Direct gravitational collapse model In this model, giant planets are thought to form directly from the collapse of a part of the gaseous protoplanetary disk into a gravitationally bound clump. As we will see below, this requires fairly massive disks, so that it is thought that this mechanism should occur early in the disk evolution. For the mechanism to work, two requirements must be fulfilled:

1. The self-gravity of the disk (measured at one vertical scale height) must be important compared to the gravity exerted by the star (D'Angelo et al. 2010). The linear stability analysis of Toomre (1981) shows that a disk is unstable for the growth of axisymmetric radial rings if the Toomre parameter $Q < 1$. The disks become unstable when they are cold and massive. Hydrodynamical simulations show that disks become unstable to non-axisymmetric perturbations (spiral waves) already at slightly higher Q values of about 1.4 to 2 (Mayer et al. 2004). At the orbital distance of Jupiter, the surface density of gas must be about 10 times larger than in the minimal mass solar nebula[1] (MMSN), for the disk to become unstable.
2. In order to allow for fragmentation into bound clumps, the time scale on which a gas parcel in the disk cools and thus contracts must be short compared to the shearing time scale, on which the clump would be disrupted otherwise, which is equal to the orbital time scale (Gammie 2001). If this condition is not fulfilled, only spiral waves develop leading to a gravoturbulent disk. The spiral waves transport angular momentum outward, and therefore let matter spiral inward to the star. This process releases gravitational binding energy, which increases the temperature, and reduces the gas surface temperature, so that the disk evolves to a steady state of marginal instability only, without fragmentation.

[1] In the MMSN model (Weidenschilling 1977; Hayashi 1981) it is assumed that the planets formed at their current positions, and that the solids found in all planets of the Solar System today correspond to the amount of solids available also at the time of formation. The total disk mass is then found by adding gas in the same proportion as observed in the star.

From the time-scale arguments, we see that the correct treatment of the disk thermodynamics is of central importance to understand whether the direct collapse model can operate. Radiation hydrodynamic simulations give a confused picture, where different groups find for similar initial conditions both fragmentation (Boss 2007) and no fragmentation (Cai et al. 2010). This illustrates that the question whether bound clumps can form is still being debated. It is usually thought that it is unlikely that disk instability as a formation mechanism can work inside several tens of AU. This is due the fact that the two necessary conditions discussed above lead to the following dilemma, as first noted by Rafikov (2005): a disk that is massive enough to be gravitationally unstable is at the same time too massive to cool quickly enough to fragment, at least inside say 40–100 AU. Outside such a distance, the situation might be different as the orbital time scales become long (Boley 2009).

In contrast to the subsequently discussed core-accretion model, giant planet formation is extremely fast in the direct collapse model, as it occurs on a dynamical time scale.

Core-accretion model The basic setup for the core-accretion model is to follow the concurrent growth of a initially small solid core consisting of ices and rocks, and a surrounding gaseous envelope, embedded in the protoplanetary disk. This concept has been studied for over thirty years (Perri and Cameron 1974; Mizuno et al. 1978; Bodenheimer and Pollack 1986). Within the core-accretion paradigm, giant planet formation happens as a two step process: first a solid core with a critical mass (of order 10 $M_\oplus$) must form, then the rapid accretion of a massive gaseous envelope sets in.

The growth of the solid core by the accretion of planetesimals is modeled in the same way as described in Sect. 2.2.3. The growth of the gaseous envelope is described by one-dimensional hydrostatic structure equations similar to those for stars, except that the energy released by nuclear fusion is replaced by the heating by impacting planetesimals, which are the main energy source during the early phases. The other equations are the equation of mass conservation, of hydrostatic equilibrium, of energy conservation and of energy transfer. Boundary conditions (Bodenheimer et al. 2000; Papaloizou and Nelson 2005) are required to solve these equations. We have to distinguish two regimes:

– At low masses, the envelope of the protoplanet is attached continuously to the background nebula, and the conditions at the surface of the planet are just the pressure and temperature in the surrounding disk. The radius of the planet is given in this regime approximately by the Hill sphere radius. The gas accretion rate is given by the ability of the envelope to radiate away energy so that it can contract and in turn new gas can stream in.
– When the gas accretion obtained in this way becomes too high as compared to the externally possible gas supply, the planet enters the second phase and contracts to a radius which is much smaller than the Hill sphere radius. This is the detached regime of high-mass, runaway (or post-runaway) planets. The planet now adjusts its radius to the boundary conditions that are given by an accretion shock on the surface for matter falling onto the planet from the Hill sphere radius, or probably more realistically, by conditions appropriate for the interface to a circumplanetary

disk. In this phase, the gas accretion rate is no more controlled by the planetary structure itself, but by the amount of gas which is supplied by the disk and can pass the gap formed by the planet in the protoplanetary disk (Lubow et al. 1999).

Pollack et al. (1996) have implemented the aforementioned equations in a model that we may call the baseline formation model. They assumed a constant pressure and temperature in the surrounding disk, and a strictly fixed embryo position, i.e. no migration. Figure 1 shows the formation and subsequent evolution of a Jupiter mass planet fixed at 5.2 AU for initial conditions equivalent to case J6 in Pollack et al. (1996). In the calculation shown here the core density is variable, the luminosity is spatially constant in the envelope, but derived from total energy conservation (Papaloizou and Nelson 2005). The limiting maximum gas accretion rate is simply set to 10^{-3} $M_\oplus\,yr^{-1}$, and accretion is completely stopped once the total mass is equal to one Jupiter mass. In a full simulation (Alibert et al. 2005a), the maximum limiting accretion rate, as well as the termination of gas accretion is given by the decline of the gas flux in the disk caused by the evolution of the protoplanetary nebula.

The top left panel shows that three phases can be distinguished. In phase I, a solid core is built up. The solid accretion rate is large, as shown by the top right panel. The phase ends when the planet has exhausted its feeding zone of planetesimals, which means that the planet reaches the isolation mass, which is of order 11.5 $M_\oplus$. In phase II, the accretion rates are low, and the planet must increase the feeding zone. This is achieved by the gradual accretion of an envelope: an increase in the gas mass leads to an increase of the feeding zone of solids. Therefore the core can grow a little bit. This leads to a contraction of the external radius of the envelope. Gas from the disk streams in, leading to a further increase of the envelope mass. In phase III, runaway gas accretion occurs. It starts at the crossover mass, i.e. when the core and envelope mass are equal (about 16.4 $M_\oplus$ in this simulation). At this stage, the radiative losses from the envelope can no more be compensated for by the accretional luminosity from the impacting planetesimals alone. The envelope has to contract, so that the new gas can stream in (note the quasi exponential increase of the gas accretion rate), which increases the radiative loss as the Kelvin–Helmholtz time scale decreases strongly with mass in this regime, so that the process runs away, quickly building up a massive envelope.

The existence of such a critical mass is intrinsic to the core-envelope setup and not dependent on detailed physics (Stevenson 1982; Wuchterl 1993). The critical core mass is typically of the order of 10–15 $M_\oplus$, but it can amount to 1–40 $M_\oplus$ in extreme cases (Papaloizou and Terquem 1999).

Shortly after the beginning of runaway gas accretion phase, the limiting gas accretion rate is reached. The collapse phase starts which is actually a fast, but still hydrostatic contraction (Bodenheimer and Pollack 1986; Lissauer et al. 2009) on a time scale of $\sim 10^5$ years. The planet surface detaches now from the surrounding nebula. The contraction continues quickly down to an outer radius of about 2 $R_{Jupiter}$ (bottom left panel).

Over the subsequent billion years, after the final mass is reached, slow contraction and cooling occurs. The different phases can also be well distinguished in the luminosity of the planet (bottom right curve), in particular the two maxima when a

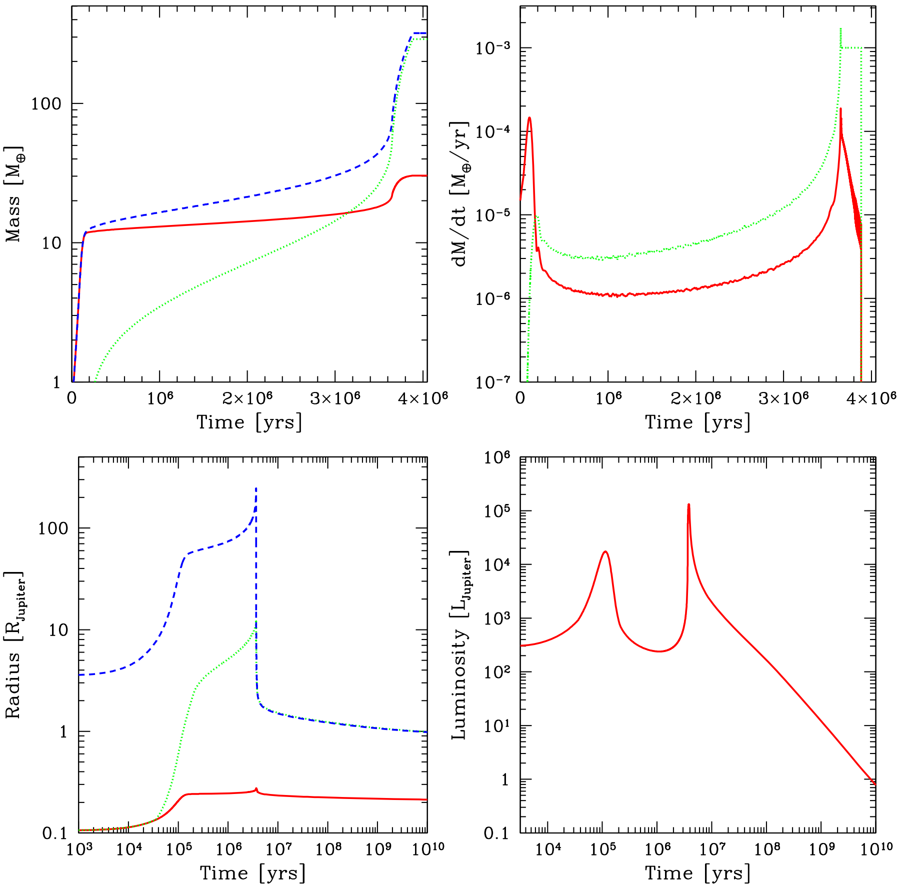

Fig. 1 Simulation for the in-situ formation of Jupiter. *The top left panel* shows the evolution of the core mass (*red solid line*), the envelope mass (*green dotted line*) and the total mass (*blue solid line*). *The top right panels* shows the accretion rate of solids (*red solid line*) and of gas (*green dotted line*). The limiting gas accretion rate is set to 10^{-3} $M_\oplus$ yr^{-1}. Note that the model is allowed to overshoot this value for a few time steps. *The bottom left panel* shows the evolution of the core radius (*red solid line*), the total radius (*blue dashed line*) and the capture radius (*green dotted line*). The latter radius is relevant for the capture of planetesimals. It is larger than the core radius due to the braking effect of the envelope. The outer radius is initially (during the attached regime) very large, as it is equal to the Hill sphere radius. At about 4 Myrs, it detaches from the nebula and collapses to a radius of initially about 2 Jupiter radii. Afterwards, there is a slow contraction phase. *The bottom right panel* shows the internal luminosity of the planet. *The first peak in the curve* is due to the rapid accretion of the core, and *the second* to the runaway gas accretion/collapse phase

significant amount of gravitational binding energy is released during the rapid accretion of the core and during the runaway gas accretion and collapse phase.

The baseline formation model has many appealing features, producing a Jupiter-like planet with an internal composition similar to what is inferred from internal structure model in a four times MMSN in a few million years. Note that in the calculation shown here it was assumed that all planetesimals can reach the central core. In reality, the shielding effect of a massive envelope prevents planetesimals of 100 km in radius as assumed here to reach directly the core for core masses larger than about 6 $M_\oplus$ (Alibert et al. 2005b), and the planetesimals get dissolved in the envelope instead.

The largest part of the evolution is spent in phase II. The length of this phase becomes uncomfortably close to protoplanetary disk lifetimes for lower initial solid surface densities, or for higher grain opacities in the envelope (Pollack et al. 1996). This is the so-called time-scale problem. However, once migration is included, this problem can be overcome (Alibert et al. 2004).

2.2.5 From protoplanets to terrestrial planets

For terrestrial planets, the requirement that they form within the lifetime of the gaseous protoplanetary disk ($\leq$10 Myrs) can be dropped. Indeed, we recall the final outcome of the planetesimal to protoplanets stage discussed in Sect. 2.2.3 in the inner part of the protoplanetary nebula, i.e. inside the iceline: a large number of oligarchs with masses between 0.01 to 0.1 $M_\oplus$.

Once the eccentricity damping caused by the gas disk or by a sufficiently large population of small planetesimals is finished, these oligarchs start to mutually pump up their eccentricities, and eventually the orbits of neighboring protoplanets cross, so that the final growth stage up to the final terrestrial planets with masses of order of the mass of Earth starts. The system of large bodies evolves through a series of giant impacts to a state where the remaining planets have a configuration close to the smallest spacings allowed by long-term stability over Gyr time scales (Goldreich et al. 2004). This long-term stability manifests itself in the form of a sufficiently large mutual spacing of the bodies in terms of mutual Hill spheres, with typical final separation between the planets of a few ten Hill radii (Raymond et al. 2008). Interestingly, such basic architectures now become visible in the recently detected multi-planet extrasolar systems consisting of several low-mass planets (Lovis et al. 2011).

In the inner Solar System, simulations (now based on direct N-body integration) addressing this growth stage must concurrently meet the following constraints (Raymond et al. 2009): the observed orbits of the planets, in particular the small eccentricities (0.03 for the Earth); the masses, in particular the small mass of Mars; the formation time of the Earth as deduced from isotope dating, about 50–100 Myrs; the bulk structure of the asteroid belt with a lack of big bodies; the relatively large water content of the Earth with a mass fraction of 10^{-3} and last but not least, the influence of Jupiter and Saturn.

Figure 2 shows as an example six snapshots in time for the terrestrial planet formation in the inner Solar System by Raymond et al. (2009). This simulation starts with roughly 100 0.01-to-0.1 $M_\oplus$ oligarchs, plus additional background planetesimals, as well as Jupiter and Saturn. One notes in the first panel the well defined eccentricity excitations at the places of mean motion resonances with the giant planets. In panel two and three, this resonant excitation spreads out. During the stage of chaotic growth (until about 100 Myr), substantial radial mixing occurs, bringing water-rich bodes in the inner system, as visible in the last three panels. At the end, four terrestrial planets with masses between about 0.6 and 1.8 $M_\oplus$ have formed. The orbital distances, eccentricities, masses, formation time scales, and water content found in this simulation are approximatively in agreement with the actual Solar System, but

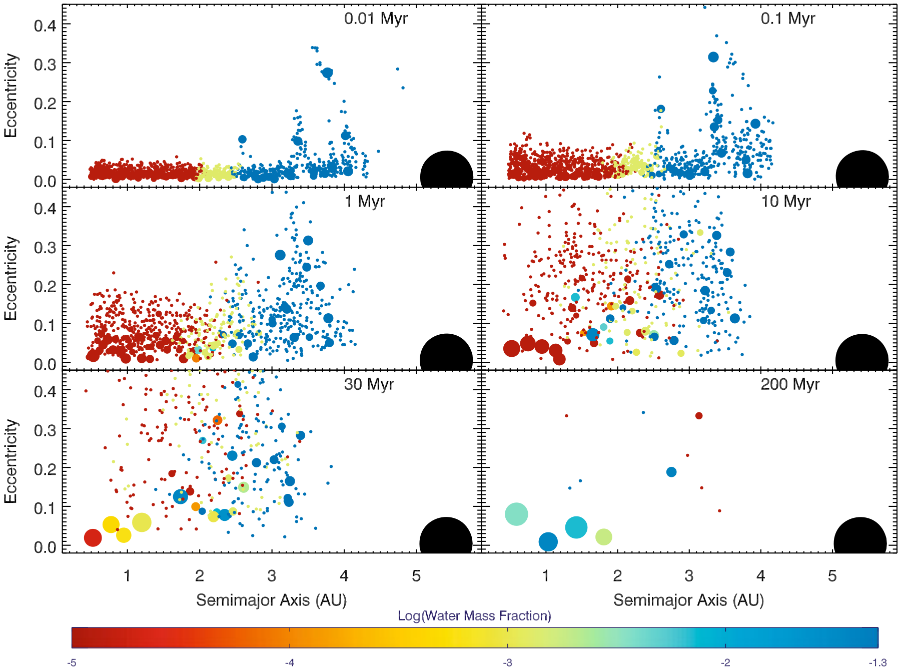

Fig. 2 Six snapshots in time for an N-body simulation of terrestrial planet formation by Raymond et al. (2009). The size of each body is proportional to its mass, while *the color* corresponds to the water content by mass, going from *red* (dry) to *blue* (5 % water). Jupiter is indicated as a *large black circle* while Saturn is not shown. (Reprinted with permission from Elsevier)

the Mars analogue is too massive, and there are three additional bodies in the asteroid belt. This simulation thus reproduces many important observed aspects, but not all of them. A main complication arises: the positions, eccentricities and masses of the giant planets at each moment in time are not exactly known, but significantly influence the formation of the terrestrial planets.

2.2.6 *Orbital migration*

Orbital migration occurs through the gravitational interaction of the planet with the protoplanetary disk. If the resulting torques exerted by the different parts of the disk onto the planet do not sum up to exactly zero, the planet will react on them by adjusting its angular momentum, i.e. its semimajor axis. Two major types of migration have been identified:

1. Low-mass planets migrate in so-called type I migration (Goldreich and Tremaine 1980; Tanaka et al. 2002).
2. Massive planets which can open a gap in the gaseous disk migrate in type II migration (Lin and Papaloizou 1986).

Migration can be both a threat and a benefit for planet formation: on the one hand, if migration happens on a time scale shorter than the growth time scale, planetary cores fall into the star before they can significantly grow (e.g. Mordasini et al. 2009b). On the other hand, it allows planetary cores to grow beyond the isolation mass as cores always get into new regions of the disk where there are still fresh planetesimals to accrete, which reduces the formation time of giant planets, as the lengthy phase II in core accretion is skipped (Alibert et al. 2004). Numerical simulations of the migration process (e.g., Paardekooper et al. 2010; Kley et al. 2009; Crida and Morbidelli 2007) have shown that depending on the local disk properties like the temperature and surface density gradients, both in- and outward migration can occur. The disk model is therefore of very high importance. It was also found that migration and accretion can strongly interact: for example, inward migration without significant gain in planetary mass occurs when a planet migrates through a part of the disk which it has previously emptied from planetesimals while migrating outward. On the other hand, gas runaway accretion and the associated mass growth can cause the switch to another migration regime. Note that hot Jupiters form as the isolation mass limitation in the inner system can be overcome thanks to migration.

2.3 Selected key questions

2.3.1 Surface density distribution?

As mentioned above, understanding angular momentum transport is critical to understanding how protoplanetary disks evolve, and without detailed knowledge of the processes of angular momentum transport all of our models are necessarily idealized. We can tune the free parameters of viscous accretion models to match observed timescales and accretion rates, but such models are necessarily phenomenological and are consequently rather lacking in predictive power.

The single most important observation we could make in this area would be to determine the (gas) surface density distribution $\Sigma(R)$. Coupled to a measurement of the accretion rate, this would allow one to determine directly the efficiency of angular momentum transport as a function of radius (as $\dot{M} = 3\pi\nu\Sigma$ in a quasi-steady disk). Deriving $\nu(R)$ would provide us with critical insight into how angular momentum is transported, and would also allow a significant refinement of the disk evolution models.

Directly observing $\Sigma(R)$ in gas in the potential planet-forming region is likely to be beyond our capabilities for some years yet, but recent observations have made significant progress in determining spatially resolved dust surface density profiles on scales of tens of AU (Andrews et al. 2009, 2010; Isella et al. 2009). Extending these results down to AU scales would be of significant interest, both in terms of disk evolution and for models of planet formation. Recent attempts to measure the turbulent velocity field in T Tauri disks may also provide important insight into this problem (Hughes et al. 2011).

2.3.2 Resolve transitional disks?

In addition, spatially resolved studies of the so-called transitional disks are likely to be key to understanding the processes that drive both planet formation and disk clearing. Current IR observations allowed one to resolve some transitional disk structures

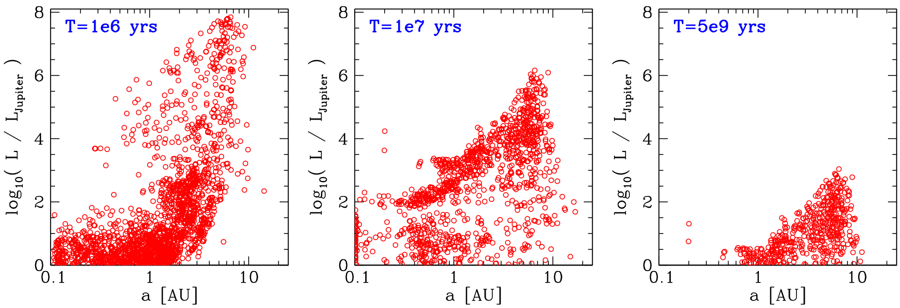

Fig. 3 Luminosity for a population of synthetic planets forming and evolving around a solar like star. The luminosity in units of Jupiter's luminosity today (8.7×10^{-10} $L_\odot$) is shown as a function of distance, for three moments in time. *The left panels* is during the formation epoch, *the middle panel* soon after the protoplanetary disks have disappeared, and *the right panels* shows the situation after 5×10^9 yrs. Note that outward migration, or outward scattering is impossible in these simulation by construction, which likely leads to an underestimation of giant planets at large semimajor axes (from Mordasini et al. in prep.)

on scales of a few AU (Eisner et al. 2006; Ratzka et al. 2007; Olofsson et al. 2011; Tatulli et al. 2011), and similar observations of small numbers of objects have also been made at mid-infrared to millimeter wavelengths (Hughes et al. 2007, 2009; Brown et al. 2009; Gräfe et al. 2011). Extending these results to large, unbiased samples of transitional disks will potentially allow one to distinguish between different models for disk clearing, and perhaps even directly detect newly formed planets (Wolf and D'Angelo 2005).

2.3.3 *Luminosities of young planets?*

A key property for several detection methods of extrasolar planets like direct imaging or interferometric methods is the luminosity of (young) giant planets (Absil et al. 2010). As outlined in Sect. 2.2.4, the luminosity is a strong function of time (and of planetary mass?). The highest luminosities occur during the gas runaway accretion and collapse phase. For fast gas accretion one finds very high peak luminosities, up to $\sim$0.1 $L_\odot$ for a Jupiter mass planet, but the phase of high luminosity is only very short, about 10^4 yrs. Lower peak luminosities are found if the gas accretion rate is low, but the duration of the phase is longer (Lissauer et al. 2009). This local energy input into the disk leads to the formation of a hot blob ($T \sim 400$–1500 K) around the planet, with a size equal to a few Hill spheres of the planet, corresponding to 0.1–1 AU for a growing giant planet a 5 AU. Such a feature should be detectable in the mid-IR, and might even cast shadows (Klahr and Kley 2006; Wolf 2008).

For observational surveys looking for planetary companions, it is relevant to know the distance–luminosity distribution as a function of time. Figure 3 (Mordasini et al. in prep.) shows this for a synthetic population of planets forming around a solar like star. Note that outward migration is not yet possible by construction in this set of models, which might be relevant in the context, as it leads to an underestimation of giant planets at large semimajor axes which are prime targets for such surveys. Note further that the luminosity of young giant planets is in general a topic which is still being debated (Fortney et al. 2005). The left panel shows the distance–luminosity plane at an age of the protoplanetary disks of 10^6 yrs. There are some very bright planets with luminosities up to about 0.06 $L_{\odot}$. They are found somewhat outside the current position of Jupiter, at 6–7 AU. These are massive planets forming in solid rich disk, which get early in the gas runaway accretion/collapse phase, so that high gas accretion rates are possible. The much lower luminosities of the planets at smaller distances (inside about 1 AU) is caused in contrast by the accretion of planetesimals. The middle plot shows the situation at 10 million years, thus after all gaseous protoplanetary disks have disappeared. Gas accretion onto the planets has therefore ceased, but the planets are still quite luminous in this early phase of contraction. At the present age of the Solar System (as shown in the right panel) luminosities have decreased by several orders of magnitude. The highest luminosities are caused by some $\sim$30 Jupiter mass objects. Two massive planets relatively close to the star are also visible.

2.3.4 Where in the disk do giant planets form?

The rate equations for solid accretion (Sect. 2.2.3) indicates that a position not far outside the iceline is the sweet spot for giant planet formation within the core-accretion paradigm, as massive cores can form still relatively quickly. This is confirmed by more complete simulations (Mordasini et al. in prep.), which compute the initial location of planets that eventually grow more massive than 300 $M_{\oplus}$ (about 1 Jupiter mass) relative to the position of the iceline in their parent protoplanetary disk: the typical position from where giant planet come is indeed a few AU outside the iceline, especially for low and medium [Fe/H] disks. At high [Fe/H], giant planets can form both inside, as well as clearly outside the iceline (see also Ida and Lin 2004a).

The location of the iceline itself is set, at least initially, by the energy production due to viscous dissipation in the disk, and its radiation at the disk surface. Fits to the location of the iceline as a function of disk and stellar mass in this regime can be found in Alibert et al. (2011). For a solar-type star, it lies between roughly 2 to 7 AU. At later stages, when the disk becomes optically thin, the location of the iceline becomes determined by the energy input from the star (Ida and Lin 2004a), and lies at about 3 AU. In the observed semimajor axis distribution of the extrasolar planets, there is an upturn in the frequency at a semimajor axis of about 1 AU, which could be caused by this preferred starting position close to the iceline, and subsequent orbital migration (Mordasini et al. 2009b; Schlaufman et al. 2009). This would thus be a direct imprint of disk properties on planetary properties. But one should keep in mind that the temperature and solid surface density structure in the disks might be in reality much more complicated (Dzyurkevich et al. 2010) than assumed in the simple models used here.

3 Observing disks and exoplanets

One of the immediate goals in planet formation research is to determine the statistics, properties, and large- and small-scale structures of circumstellar disks and exoplanets. Ultimately, the study of disks spanning across the pre- to the post-planet formation phases over a range of stellar masses will help identifying the most profound trends, hence the relevant physics, that are central to planet formation. In this section, we briefly outline the current state-of-the-art in spatially resolved observations of circumstellar disks and exoplanets (see also Absil and Mawet 2010). In particular, we aim at outlining the specific observing methods that are available and the extent to which they can be used to infer the properties of an individual disk or exoplanet.

3.1 Circumstellar disks

Spatially unresolved photometry is by far the easiest way to assess the presence and determine some of the properties of a circumstellar disk. Over the last three decades, this approach has been used to determine the typical ∼5 Myr time scale for disk survival (Fedele et al. 2010), hence planet formation, as well as to assess the presence of dust grains 1 mm in size or larger in the majority of protoplanetary disks (Natta et al. 2007). Similarly, recent *Spitzer* surveys have established that 10–50 % of young main sequence stars host a debris disks (Trilling et al. 2008; Meyer et al. 2008; Lestrade et al. 2009), confirming that the formation of planetesimals is a very common outcome of disk evolution, in line with the high proportion of detected exoplanets around nearby stars (Udry and Santos 2007).

However, analyses of spectral energy distributions of these objects are limited to some very simple questions (Is the disk present or absent? Is it optically thin or thick?) as a result of numerous ambiguities between the various physical parameters that describe a given disk (Chiang et al. 2001). To give a simple example, determining that a debris disk system is characterized by black-body excess emission only firmly establishes the temperature of this dust population. Its physical location around the star, which could then be compared to an exoplanetary system or to planet formation theories, can only be inferred by making an assumption about the distribution of size and composition of the dust grains.

3.1.1 Observing circumstellar disks

Before addressing particular observing techniques, it is useful to discuss the ways in which disks can be studied if they can be spatially resolved. This will help to highlight the complementarity of the various observing techniques and to identify the areas in which long-baseline interferometry can provide a unique contribution.

Scattered light imaging At optical wavelengths, circumstellar disks are not significant emitters since their temperature does not exceed the dust sublimation temperature (typically ∼1500 K). At these wavelengths, a disk can only be imaged in scattered light, i.e. stellar photons that have scattered off a dust grain in the disk prior to reaching the observer. As demonstrated by McCabe et al. (2003), disks can be imaged in scattered light up to the mid-IR regime. However, depending on the stellar effective temperature and luminosity as well as the dust properties, the relative contribution of the thermal emission becomes important at near- to mid-IR wavelengths (e.g., Pinte et al. 2008), i.e., the main source of scattered photons is the hot dust in the innermost disk regions itself. Consequently, not only the stellar photosphere, but also these inner regions have to be hidden from direct view if the goal is to obtain large-scale disk images in the optical to mid-IR wavelength range.

Scattered light images are powerful tools to determine the *overall geometry* of a disk. First of all, an image usually provides a direct estimate of the disk *inclination*. Furthermore, it provides a lower limit to the disk *outer radius*. Because it does not rely on intrinsic disk emission, scattered light can be detected up to large distances from the central star (up to 1000 AU) with sensitive enough detectors. In the case of debris disks, which are optically thin, scattered light images directly trace the structure of disks with surface brightness enhancements in regions of higher density. In fact, surface brightness profiles can be inverted into *surface density profiles*, making it possible to infer the presence of planets through gaps, asymmetries or resonant trapping of dust particles. On the other hand, protoplanetary disks are optically thick and scattered light only probes the upper surface of the disk. Indeed, surface brightness profiles inform us on the geometry of the disk surface: a flat or shadowed disk does not produce substantial scattered light, for instance. In the specific case of edge-on disks, it is possible to infer the *vertical scale height* of the dust component. If the vertical extent of the dust component is deemed too small compared to the prediction for a disk in hydrostatic equilibrium, this can be interpreted as a sign of settling compared to the gas component. Scattered light images of optically thick disks, however, suffer from ambiguous interpretation: lateral asymmetry can be either due to an intrinsic large-scale asymmetry in the disk or an illumination disparity, possibly because of asymmetry in the innermost regions of the disk.

Because of the nature of scattering, optical and near-IR images of disks also inform on the nature of the dust grains: grains much smaller than the observing wavelength scatter isotropically while large grain are strongly forward-throwing. Dust properties, especially the possibility of porous or non-spherical grains, also play a role in setting the scattering "phase function". If the viewing geometry of a system, hence the scattering angle at each position in the disk, can be determined, it is possible to map the phase function. This can in turn be used to probe the *grain size distribution*, under some assumption about the dust composition. While multiple combinations of dust compositions (including porosity) and size distributions can yield the same scattering asymmetry, one can take advantage of a multi-wavelength approach to map this asymmetry as a function of wavelength, which can help disentangle the effects of *dust composition* and grain size distribution. Finally, if the dust grains have a sufficiently strong spectral feature in their albedo function (such as the water ice feature around 3 μm), it is possible to use scattered light imaging to constrain the dust composition independently of the phase function and of the disk optical depth.

In optically thin disks, *grain sizes* can also be constrained by the observed color of the disk relative to the central star. Indeed, very small grains have an albedo function that drops significantly towards longer wavelengths, making the disk "blue", whereas disks containing larger grains are typically neutral or slightly "red". The intensity scattered off a dust grain is actually the product of the albedo and the phase function, so it is critical to obtain a resolved image to disentangle the two effects.

As a final note, scattered photons are generally highly linearly polarized, with details depending on the photon wavelength, dust size, shape and composition. Therefore, maps of linear polarization vectors or, second-best as this induces a loss of information, polarized intensity images also convey insight on the dust properties. Polarized imaging offers the added benefit that the central star is essentially unpolarized, which alleviates dramatically the high-contrast problem posed by scattered light imaging.

Thermal emission mapping At near- and mid-IR and longer wavelengths, disks are imaged via their dust thermal emission. Dust grains are heated by the central star and re-emit as gray bodies depending on their equilibrium temperatures. The inner few AUs of a disk emit mostly in the near- and mid-IR range whereas the outer regions (beyond 10 AU) emit primarily in the far-IR and (sub)millimeter wavelength regimes. Therefore, it is possible to discern details in the immediate vicinity of the central star in the mid-IR regime if the spatial resolution is high enough, gaining insight on the disk *inner radius*, as well as the geometry of the inner regions of the disk.

At the longest wavelengths, most of the disk is optically thin, so that the surface brightness of a disk is a direct measure of the $\kappa_\nu \Sigma(r) B_\nu(T)$ product, where κ_ν is the dust opacity, $\Sigma(r)$ the surface density and $T(r)$ the dust temperature. A surface brightness map can therefore be used to determine the *surface density profile* of a disk if its temperature profile can be estimated or assumed. Furthermore, the ratio of surface brightnesses at independent wavelengths is only dependent on the opacity ratio, which itself is a function of the *grain size distribution*. This method has first been used with unresolved observations to probe the presence of dust grains as large as 1 mm. If the wavelength-dependent resolution can be accounted for properly, resolved maps can be used to study spatial variations in the grain size distribution.

Because debris disks are optically thin at all wavelengths, it is possible to take advantage of the inescapable rule of thumb that observables are most sensitive to grains whose size is comparable to the observing wavelength. If grains of various sizes have different spatial distributions as a consequence of size-dependent forces exerted on the grains, this can translate into significantly different morphologies as a function of wavelength for a given disk, for instance from mid-IR to millimeter wavelengths.

As a final note, it is worth emphasizing that the scattered light and thermal emission regimes overlap in wavelength which, in the case of optically thick disks, leads to a combination of different "photon histories" that contribute to the observed image and must be disentangled, generally by comparing observations to predictions of complex radiative transfer models. Debris disks offer the possibility of more straightforward interpretations as all photons received by the observed only interact once with the disk.

Other approaches In addition to these two generic approaches, there are several other methods that can provide spatially resolved information about disks. First of all, disks around some Herbig Ae/Be stars have been spatially resolved in near- to mid-IR PAH[2] observations. PAH grains are stochastically heated by the UV radiation of early-type stars and emit in a few bands between 3 and 12 μm. Comparing the morphology of disks in these bands and in adjacent continuum bands has revealed that PAH grains can be excited up to very large distances (well beyond 100 AU in some cases) in the surface layers of flared disks. As such, they provide key information

[2]Polycyclic aromatic hydrocarbons.

regarding the *global structure* of disks on the large scale (vertical height, flaring), akin to scattered light images.

An unexpected source of *spatial* information about protoplanetary disks comes from photometric time series, which reveal variability from the optical to the to mid-IR on timescales of a few days to a few months. At least some of these variations arise from inhomogeneities and/or asymmetries in the inner regions of disks, at a distance from the star determined by the observed time scale via Keplerian rotation. This approach can be used to probe the structure of disks within a few AU at most of the central star.

The various approaches outlined so far focus on the dust component of disks, which is the common element to protoplanetary and debris disks. However, most of the mass of protoplanetary disks is in gaseous form which can also be spatially resolved. For instance, the rotational lines of many molecular species lie in the (sub)-millimeter regime, so that they can be mapped with the same instruments as their adjacent continuum. While this is currently limited to the most massive disks because of sensitivity limitations, this method can be used to study the chemical structure of disks as well as to measure the Keplerian rotation of circumstellar disks, hence the mass of the central star. At much shorter wavelengths, it is possible to apply the "spectro-astrometric" method to near-IR molecular emission lines. The objective is then to measure a spatial displacement of a source photocenter across a spectral emission line, revealing the emission from the hot gas component of the disk, which is located in the inner few AU.

Observational techniques Protoplanetary disks are too distant to be imaged with simple, ground-based imaging techniques at optical or IR wavelengths. Diffraction-limited devices (adaptive optics on large ground-based telescopes, or the Hubble Space Telescope) are necessary to image disks, providing a typical linear resolution of 5–10 AU, insufficient to discern details in the innermost regions of disks. Furthermore, except in the special cases of edge-on disks or polarized imaging, a coronagraph is required to block the light of the central star which, with the unwanted side effect of masking out the inner 50–100 AU of the disk as well. Nonetheless, an increasingly number of disks (currently about three dozens) has been imaged in scattered light using these techniques. Debris disks, which are located much closer (down to a few pc from the Sun), can be imaged with very high linear resolution, up to 1 AU, and as close as a few AU from their parent star in favorable cases. Such images, typically dominated by scattered light can typically be obtained from the near-UV to the near-IR regime (2–5 μm). Also, it is possible to use a back-end spectroscopic instrument (long-slit or integral field unit) to search for spectro-astrometric signatures of hot gas in the inner region of disks.

In the far-IR to millimeter regime, the spatial resolution afforded by single-dish telescopes is insufficient to resolve any protoplanetary disk, and only a handful of nearby debris disks have been resolved.[3] Long-baseline interferometers working in the (sub)millimeter range (VLA, IRAM Plateau de Bure, CARMA, ATCA, SMA) provide subarcsecond resolution, sufficient to resolve disks. Such instruments have

[3] It must be noted that the *Herschel Space Observatory* is now rapidly expanding this list.

been used to map the continuum thermal emission of protoplanetary disks in the outer regions of disks, specifically in the disk midplane which contains the highest density of dust particles. With the exception of rare cases, these interferometers are not sensitive enough to detect debris disks, however.

Long-baseline interferometric techniques in the optical, near- and mid-IR regimes have also been used extensively in recent years to map the innermost regions of protoplanetary and debris disks. The spatial resolution achieved by an interferometer is defined as λ/B where λ is the wavelength and B the *baseline*, that is, the distance between the telescopes. For a typical baseline of 100 m, the interferometric spatial resolution is ∼4 and ∼20 mas for the K and N bands, respectively, thus in adequacy with the angular sizes involved in our science case. The exquisite resolution these interferometers provide allows one to resolve the inner radius of many protoplanetary disks, although in most cases analyses are limited to comparison of interferometric data with synthetic model images of disks with simple morphological structures. In all cases, because of their intrinsically small field-of-view, as well as the use of an observing wavelength $\lambda \leq 15$ μm, only the inner few AU of disks can be studied through such observations.

3.1.2 Inner disk regions: observational findings

To date, well over 100 protoplanetary disks and over two dozen debris disks have been spatially resolved at one or more wavelengths.[4] We summarize some of the main findings resulting from these images for protoplanetary and debris disks, with a focus on findings that are related to planet formation.

Herbig Ae/Be stars: thermal emission of the dusty inner rim Monnier et al. (2005), Vinković and Jurkić (2007) have shown on a sample of Herbig Ae/Be stars that the interferometric size of the K band emission was correlated with the star luminosity, as illustrated on Fig. 4 (left). From this correlation they have demonstrated that the near-IR excess of such stars was—with the exception of the most luminous ones—arising from the thermal emission of the inner part of the dusty circumstellar disk, located at the dust sublimation radius (roughly $T \sim 1500$ K for silicates), assuming that the dust is in equilibrium with the radiation field. If this scenario works well for Herbig Ae stars and late Be, it however fails to interpret the size of the IR excess emission region for the early Be, the inner rim being too close to the star regarding their high luminosity. In this case, one likely interpretation is that the gas inside the dust sublimation radius is optically thick to the stellar radiation, hence shielding a fraction of the stellar light and allowing the dusty inner rim to move closer to the star.

T Tauri stars: a strong contribution of the scattered light Together with the last improvements of interferometers in terms of sensitivity, it is only recently that the same kind of study could have been performed on the less luminous T Tauri stars. And the results that have been obtained were somewhat surprising, the size of the near-IR emission being *larger* than predicted (Akeson et al. 2005;

[4] An up-to-date list is maintained at the http://www.circumstellardisks.org/ website.

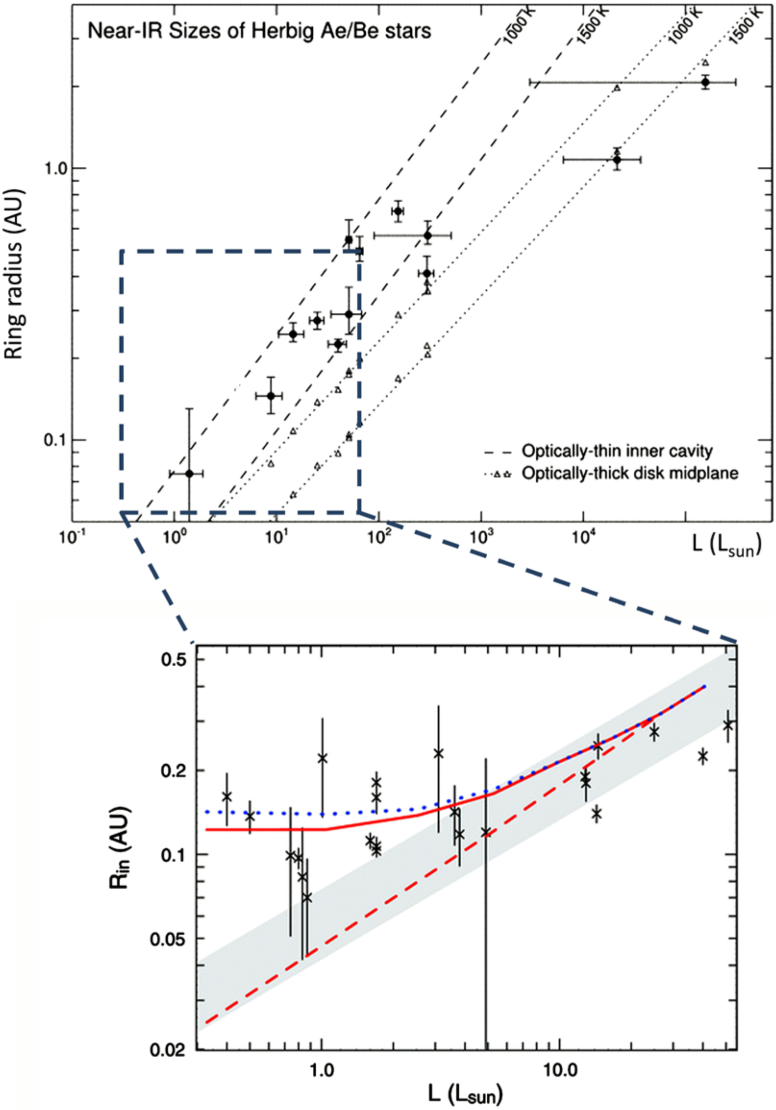

Fig. 4 K band interferometric size–luminosity relationship for intermediate (*top*, adapted from Monnier et al. 2005) and low (*bottom*, adapted from Pinte et al. 2008) mass young stars. We can see that for the T Tauri regime, considering the thermal emission only (*dashed line*) does not reproduce the correlation whereas taking into account both the thermal and scattered light emission with the same disk model (*solid line*) does. (Reproduced by permission of the AAS)

Eisner et al. 2005, 2007b). Many hypotheses were invoked such as lower sublimation temperature $T_{sub} \sim 1000$ K, fast dissipation of the inner disk, magnetospheric radii bigger than dust sublimation ones hence defining the location of the inner rim; until Pinte et al. (2008) had shown that when the luminosity of the star decreases, the contribution of the scattered light, in addition to that of the thermal emission, could not be neglected anymore. As a consequence these authors have convincingly demonstrated that the model of the inner disk located at the dust sublimation radius was holding for the T Tauri regime as well, and that no alternative scenario was required as long as the radiative transfer in the disk was thoroughly studied (thermal + scattered light).

The shape of the dusty inner rim As it is directly and frontally irradiated by the star, it was quickly suggested that the inner rim would be probably thicker than the disk straight behind it which at the contrary only receives a grazing star light. As a result, the inner rim is expected to be "puffed-up", hence casting a shadow on the outer part of the disk. However, how big and sharp the puffed-up rim is and how pronounced the shadow behind appears remain open questions. In the past years, various models with increasing complexity have been developed to address this issue. After the first simple models by Natta et al. (2001) and Dullemond et al. (2001) in which the rim was assumed to exhibit a vertical wall, approximate 1-D (e.g. D'Alessio et al. 2004; Isella and Natta 2005) and full 2-D radiative transfer models (e.g. Dullemond and Dominik 2004; Tannirkulam et al. 2007; Kama et al. 2009) have progressively shown that the rim was most likely rounded off, although the true vertical profile of the rim is hard to determine as it is highly dependent on dust and gas properties.

From an observational point of view, provided that the source is seen under a large enough inclination angle, images of its near-IR emission should all the more deviate from axisymmetry than the inner rim is sharp. Using three telescopes simultaneously, interferometry enables to measure such a level of asymmetry through the so-called "closure phase" observable (Monnier 2000), the bigger the closure phase, the bigger the departure from axisymmetry. In this framework, observations with the 3-telescope IOTA interferometer of a sample of 16 young stars (Monnier et al. 2006) have mostly revealed sources with small closure phases, hence ruling out the sharp vertical wall hypothesis and favoring a smooth rounded off structure for the inner rim. New observations with higher closure phase accuracy should be extremely fruitful to further constrain the shape of the inner rim.

The hot gas inside the dusty inner rim Though dust is mostly dominating the near-IR continuum emission of young stars, there are some cases where the dust rim cannot account for the entire near IR excess observed in the SED. Particularly, in the case of stars where the accretion rate is high enough (roughly $>10^{-7}$–10^{-8} $M_\odot\,yr^{-1}$) the contribution of the hot gaseous component to the near-IR excess cannot be neglected. Since the hot gas is located between the star and the dust sublimation radius, we expect its region of emission to be *hotter* and *more compact* than that of the dusty inner rim. As a consequence, observing at shorter wavelengths or longer baselines appears to be well suited to probe this region. This was first achieved by Isella et al. (2008) which have observed the Herbig Ae star MWC 758 with the AMBER instrument on the VLTI, both in the H and K bands. They have shown that, if the K band observations alone are well interpreted by the classical dusty puffed-up inner rim (Isella and Natta 2005), it fails to reproduce the H band observations for which the emission is less resolved than expected by this model. Furthermore, with this single model, the SED cannot be fitted successfully, showing a lack of energy in the H band. Conversely, by adding an unresolved hotter component (of $T = 2500$ K) to the model, they managed to reproduce both the H and K bands measurements jointly. Given the temperature and the size ($\leq$0.1 AU) of this emission region, the unresolved component was then interpreted as arising from the hot gas accreting close to the star, an hypothesis reinforced by models of accreting gas (Muzerolle et al. 2004) which allowed for a satisfactory fit of the shape of the SED by filling the lack of energy in the H band. A somewhat similar strategy was used by Eisner et al. (2007a) who observed different Herbig Ae/Be stars with the Keck interferometer (KI), using moderate spectral dispersion (R = 25) within the K band. They have found that for several stars of their sample, single-temperature ring could not reproduce the data well, and that models incorporating radial temperature gradients or two rings should be preferred, supporting the view that the near-IR emission of Herbig Ae/Be sources can arise both, from hot circumstellar dust and gas. For example, the interferometric data of AB Aur require the presence of one dust inner rim together with a more compact and hotter component ($T \sim 2000$ K) interpreted as coming from the hot dust-free inner gas. And as a matter of fact, this scenario was also proposed by Tannirkulam et al. (2008) who observed the same star with the very long baselines (300 m) of the CHARA interferometer, hence probing smaller emission region and showing the need of adding smooth hot ($T > 1900$ K) emission inside the dust inner rim, contributing to 65 % of the K band excess.

However, as an increasing number of interferometric observations led to the direct detection of gas inside the dust sublimation radius, a careful analysis of the expected gas continuum emission shows that such a conclusion is eventually not straightforward. In the specific case of the Herbig Ae star HD 163296, Benisty et al. (2010) have indeed pointed that neither gas LTE[5] opacities—which produce strong molecular bands absent in the observed spectrum—nor H^- non-LTE opacity—where the resulting continuum emission is too weak and presents an inconsistent wavelength dependence—could account for the extra IR excess not filled by the emission of the (silicate) dusty rim. Conversely, the presence of refractory grains inside the inner rim, such as iron, corundum, or graphite which can survive at much higher temperatures could be a satisfactory alternate interpretation. Similarly, the supposedly detection by interferometry of hot water molecular emission (MWC 480, Eisner 2007) inside the dust sublimation radius was soon after invalidated by high-resolution spectroscopy single-dish observations of the same source which did not show the strong molecular lines expected (Najita et al. 2009). In one case, the young Be star 51 Oph, Tatulli et al. (2008) confirmed that the strong observed CO overtone emission was originating from a region located at 0.15 AU from the star—that is, in the gaseous rotating disk—, but it seems that in a general manner this inner gaseous disks may be poorer in molecules than expected and the composition of the matter responsible for the continuum emission from inside the dusty rim remains unclear and more complex than first contemplated. The above puzzling examples emphasize the need to accompany interferometric measurement with (as long as possible) simultaneous high-resolution spectroscopic observation in order to avoid misinterpretation of the interferometric data. Whenever possible, directly recording dispersed interferograms with the appropriate spectral resolution obviously remains the best-suited solution, at it is discussed in the next section.

[5] Local thermal equilibrium.

Accretion/ejection phenomena with gas line observations One major achievement in interferometry in the past years is the capacity of spectrally dispersed the interferogram across the wavelength range, with resolution high enough (AMBER/VLTI: R = 1500, see Petrov et al. 2007, and KI: R = 250, 1700, see e.g. Wizinowich et al. 2004; Ragland et al. 2008) to spatially resolve the lines emission regions and separate them from that of the continuum, that is, to directly probe—through their emission lines—the gaseous species which constitute 99 % of the mass of the circumstellar matter. Among all the IR emission lines that are seen in young stars, the atomic transition of the hydrogen Brγ is by far the most observed in spectro-interferometry for it is the brightest and can therefore be studied with rather good signal to noise ratio (SNR). Two main scenarios are commonly in balance to interpret the origin of this emission line, scenarios for which the extension of the emission region will differ:

– *Magnetospheric accretion*: If the line is emitted in accreting columns of gas (Hartmann et al. 1994), then the region of emission lies roughly between the star and the corotation radius, that is, *the line emission region is much more compact than that of the continuum* which comes from the dust sublimation radius.
– *Outflowing winds/jets*: At the contrary, if the line arises from outflows (Shu et al. 1994; Casse and Ferreira 2000; Sauty et al. 2004), one expects the *line emitting region to be of the same size or bigger than that of the continuum*.

By measuring the size of the emitting regions responsible for both the emission line and the surrounding continuum and compare their relative size, IR spectro-interferometry enables to disentangle between both scenarios and to constrain the origin of Brγ in young stars. Such an effect was investigated in parallel by both spectro-interferometric IR instruments AMBER and KI, first on single young stars (Tatulli et al. 2007; Malbet et al. 2007) and subsequently on surveys (Kraus et al. 2008; Eisner et al. 2009, 2010), and these author have found a large variety of spatial scales for the Brγ emission region, both smaller and bigger than that of the adjacent continuum. A complete comprehension of the phenomena at stake yet remains to be elaborated. However, these results have already suggested two distinct trends for the low- and intermediate-mass young stars, respectively: if the correlation between magnetospheric-accretion and Brγ emission seems well established for T Tauri stars, it appears that for Herbig Ae/Be stars we are mostly probing outflows phenomena, the Brγ line being probably in this case an indirect tracer of accretion through accretion-driven mass loss (Kraus et al. 2008). Spectro-interferometry thus enables to spatially locate the emitting regions of IR lines in young stars, although in practice only the brightest one, Brγ, has been deeply investigated so far. With the regular increase in sensitivity of interferometers, this promising field is expected to move one step forward along two main axes:

1. The observation of weaker lines such as Paβ to probe the geometry of the region at the interface between accretion and the stellar surface, the structure of this interface playing a crucial role in mass loss and angular momentum regulation phenomena (Dougados et al. 2003), the iron line [FeII] to put further constraints on the MHD models on jets and their launching region (Pesenti et al. 2003), or several other lines directly tracing the hot rotating gas such as the CO molecule.

2. The interferometric observation at very high spectral resolution (typically R ∼ 8000) in order to spatially *and spectrally* resolve the lines, thus tracing the various emitting regions along the lines from the wings towards the central part and accessing the kinematics and velocity maps of these regions, in order to directly measure the rotation at the base of the jets (Bacciotti et al. 2003; Dougados 2009) as well as quantify the (Keplerian?) disk rotation of the hot gas around young stars.

The size of the 10 μm region as a proxy for the disk vertical structure Following through the circumstellar disk further away from the star than the inner rim, the middle disk—located roughly from one to few AUs and radiating at temperatures of a few ∼100 K—is adequately probed by interferometry at mid-IR wavelengths. Particularly, such a technique has enabled to unveil its vertical structure as well as the composition of its surface layer.

By observing a sample of Herbig Ae/Be stars with the MIDI/VLTI instrument, Leinert et al. (2004) have measured the radius of the 10 μm emission region of the whole young stars and compared them with their mid-IR color. It was shown that the more red objects were displaying more extended emission than that of the more blue sources. Such a result is consistent with the classification of Meeus et al. (2001) where the group I flared disks are redder and of which mid-IR emission appears larger, whereas the group II flat self-shadowed disks present a more compact mid-IR emission.

Radial evolution of the disk mineralogy Mid-IR interferometry can also provide spectrally dispersed interferograms (e.g. MIDI/VLTI, R ∼ 230) in a wavelength range perfectly suited to study the silicate feature at ∼10 μm, which allows one to probe the radial composition of the disk atmosphere. One finds that the surface of the inner disk has larger and more crystalline (crystallinity fraction of 40 % to 100 %) silicate grains than that of the outer part, being smaller and more amorphous. Remarkably enough, such a property holds for a large range of stellar masses, from the intermediate Herbig Ae/Be stars (van Boekel et al. 2004) to less massive T Tauri stars (Ratzka et al. 2007; Schegerer et al. 2008, 2009).

The connection to the outer disk regions Scattered light images and thermal emission maps have confirmed that many disks have outer radii beyond 100 AU although there is a large object-to-object scatter (Watson et al. 2007). In a handful of disks in which the inner regions have been depleted of small dust grains, millimeter mapping with interferometers has provided sufficient resolution to resolve the inner radius of the disk at a few tens of AU, typically (Piétu et al. 2006; Sauter et al. 2009; Hughes et al. 2009). This came as a direct confirmation of the prediction based on the peculiar SED of "transition" disks. In one case, the inner region has also been tentatively imaged in scattered light (Thalmann et al. 2010). It is generally believed that the inner hole in at least some transition disks is the result of carving by a forming planet, although this remains to be confirmed. More surprisingly, inner holes have been discovered in disks in which no prior evidence existed for such a structure (Isella et al. 2010). Once again, this emphasizes the crucial importance of high-resolution observations in the analysis of any particular disk.

The outer structure of protoplanetary disks imaged in scattered light is flared (Burrows et al. 1996; Lagage et al. 2006; Perrin et al. 2006b; Okamoto et al. 2009), in accordance with simple models based on hydrostatic equilibrium, implying that stellar illumination is the only significant source of heating for the outer disk regions. It must be emphasized, however, that more than half of all known protoplanetary disks around T Tauri stars in nearby star-forming regions have *not* been detected in scattered light, despite multiple surveys using the Hubble Space Telescope or adaptive optics devices (Stapelfeldt and Ménard, priv. comm.). Because our current knowledge is biased towards flared disks which are much easier to detect since they intercept more starlight, it is possible that undetected disks represent a more advanced, settled state in disk evolution. In the specific case of intermediate-mass Herbig Ae stars, SED analyses have led to a picture in which, for so-called "group II" (Meeus et al. 2001), the outer disk lies in the shadow cast by the inner regions, reducing the chances to detect the disk in scattered light. Indeed, only two of the 10 disks imaged in scattered light around Herbig stars pertain to the group II discussed above. However, it remains unclear whether this phenomenon is related to the non-detection of many disks around T Tauri stars, for which no clear-cut distinction is seen in SED analyses. If confirmed, this could indicate strong evolution towards a geometrically thin, dense midplane which would provide appropriate conditions for planet formation.

The small number of resolution elements across the disk offered by currently operating (sub)millimeter interferometers prevents detailed studies of their surface density profile. Fitting power-law models to data indicates that the global density profile is typically $\Sigma(r) \propto r^{-0.5\cdots-1}$, significantly flatter than the Minimum Mass Solar Nebula model (Kitamura et al. 2002; Andrews and Williams 2007). Typical surface densities at a radius of 100 AU are on the order of a few $\mathrm{g\,cm^{-3}}$. Recent work at the highest achievable resolution supports a picture in which the density profile is not well described by a single power law (Wolf et al. 2008), but is tapered towards the outermost regions (Isella et al. 2009; Guilloteau et al. 2011). Because none of these observations actually probe the region in which planets are thought to form (inside of 10 AU), current estimates of the actual surface density in the inner regions are strongly dependent (by more than two orders of magnitude) on inward extrapolation of the outer density profile, so that it remains impossible to directly assess whether the density in the midplane of a given disk is high enough to sustain planet formation.

Beyond these global characteristics, spatially resolved observations of disks have revealed a slew of asymmetries and small-scale structure in many disks (Mouillet et al. 2001; Fukagawa et al. 2004; McCabe et al. 2011). Spiral arms and gaps may be related to the presence of embedded protoplanets, although their interpretation is often ambiguous due to the large optical depth of the disks. Density perturbations induced by an outer stellar companion or a self-gravitating disk are equally plausible in many cases (Reche et al. 2009). Lateral large-scale asymmetries are generally thought to trace the inhomogeneous structure of the inner disk that affects the illumination pattern of the outer disk. The clearest illustration of this phenomenon is the variability seen in the images and integrated polarization signal of the HH 30 edge-on disk (Watson and Stapelfeldt 2007; Durán-Rojas et al. 2009). This phenomenon may be related to the quasi-periodic shadowing observed in AA Tau, in which the inner wall of the disk is warped and the base of the accretion column onto the star periodically occults our line of sight to the star (Bouvier et al. 2007). Recent photometric timeseries obtained with the *CoRoT* telescope revealed that this phenomenon may indeed be common among T Tauri stars, with a frequency as high as 30 % (Alencar et al. 2010).

While millimeter observations of disks have unambiguously established that the largest dust grains in the midplane are at least millimeter-sized, it is still extremely challenging to probe their radial dependencies. Early attempts indicate little-to-no differences as a function of radius (Isella et al. 2010; Guilloteau et al. 2011). In the disk upper layers, scattered light images indicate that their optical properties are grossly similar to those of interstellar grains, although in several cases, power-law size distributions have to be extended up to a maximum grain size of a few micron to better reproduce the data (Burrows et al. 1996; Stapelfeldt et al. 1998; McCabe et al. 2003; Duchêne et al. 2004; Sauter et al. 2009). Nonetheless, power-law distributions with a maximum grain size of 10 μm or larger are systematically excluded, indicating that the dust properties are significantly different from those of the midplane (Duchêne et al. 2002; Wolf et al. 2003; Pinte et al. 2008b). Polarization mapping of protoplanetary disks has also revealed high degrees of polarization, typical of small dust grains (Silber et al. 2000; Glauser et al. 2008; Perrin et al. 2009). A stratified structure is a common prediction to models of grain growth and settling, whereby larger grains reside much lower than small ones due to their weaker coupling to the gas. Detailed multi-wavelength studies of at least a handful of disks have confirmed such a settled disk structure (Duchêne et al. 2004; Pinte et al. 2008b). In some disks, this picture is also supported by a dust scale height that is smaller than expected based on an hydrostatic equilibrium gas structure (Watson et al. 2007). Finally, water ice coating of dust grains in the disk outer regions has been confirmed in scattered light imaging taken in and out of the 3 μm absorption band for several disks (Terada et al. 2007; Honda et al. 2009; McCabe et al. 2011) or spatially resolved spectra (Schegerer and Wolf 2010). In all cases, these conclusions apply to the outer disk, tens of AU away from the star. It is natural to assume that this is also true in the inner disk, but it cannot be confirmed directly with current observations.

Debris disks As discussed above, the closer distance to many debris disks enables much higher linear resolution, down to sub-AU scales. At this resolution, many disks show significant departures from smooth, axisymmetric structures: gaps, warps, dual midplanes, lateral density asymmetries have all been identified (Mouillet et al. 1997; Golimowski et al. 2006; Fitzgerald et al. 2007a; Kalas et al. 2007b; Schneider 2009). Some of these structures, namely gaps and warps, are frequently interpreted as evidence for the presence of undetected planetary objects. This interpretation has recently been strikingly confirmed in two debris disks, whose structure led to a correct prediction of the semimajor axis of the putative planet, which was subsequently directly imaged (Kalas et al. 2008a; Lagrange et al. 2009). Several other debris disks show similar structures although no planet has been found to date (Koerner et al. 1998; Schneider et al. 1999). Furthermore, some disks have shown to be eccentric or off-centered, which is most easily explained by the influence of an unseen massive body on an eccentric orbit (Kalas et al. 2005; Buenzli et al. 2010).

Scattered light images of many disks, especially when coupled with SED analyses, have allowed one to locate precisely the location of a "parent" body ring. Semimajor axes range from a few AU to up to 100 AU from the central star, indicating that planetesimal formation can occur over a broad range of radii or, alternatively, that migration mechanisms, along with resonance trapping with full-size planets, can carry planetesimals over large distances after their formation.

In the parent body ring, planetesimals constantly collide with each other, producing vast amounts of small dust grains which are subsequently carried away from the ring via radiation pressure or stellar wind pressure. Only grains smaller than ∼mm/cm can be directly detected, so studies of debris disks are limited to the analysis of this secondary dust population. In the rare cases where the same disk has been imaged over two or more orders in wavelengths (any combination of scattered light imaging, mid-IR imaging and submillimeter mapping), striking differences in morphology have been observed, indicating that grains of different sizes follow different spatial distributions (Fitzgerald et al. 2007b; Maness et al. 2008). When coupled with a dynamical model of the disk, this can be used to infer more robustly the location of the various components of the disk.

As is the case for protoplanetary disks, scattered light images of a debris disk allow one to constrain the grain size distribution, most notably the size of the smallest grains in the disk. Generally speaking, these are in the 0.1–5 μm range and in good agreement with the expected blow-out size given the central star luminosity and/or stellar wind (Boccaletti et al. 2003; Clampin et al. 2003; Golimowski et al. 2006; Kalas et al. 2007a). It is arguable whether a strict power-law size distribution should be expected in a collisional cascade (Thébault and Augereau 2007). Here, scattered light images at multiple wavelengths can provide constraints for the grain size distribution. Most importantly, departures from spherical compact grains has been identified in one disk and suggested in at least another one (Schneider et al. 2006). In particular, polarimetric imaging of the debris disk surrounding AU Mic has revealed that the smallest dust grains are highly porous (Graham et al. 2007; Fitzgerald et al. 2007a). It is likely that this property was inherent to the colliding parent bodies, raising the question of the efficiency of grain compaction during the growth phase of dust grains. Because porous grains have a much smaller density, they react differently to the various forces exerted on them during the evolution of disks, so this property could be important for planet formation theories. Unfortunately, it is extremely challenging to demonstrate that small dust grains are indeed porous in earlier stages of disk evolution (Pinte et al. 2008b; Perrin et al. 2009).

3.2 Exoplanets

The analysis of the structure of extrasolar planetary systems and the analysis of basic characteristics of exoplanets since the mid-1990s allow one now to approach the question of planet formation from the perspective of the "results" of this process. For this reason, a brief overview about the current state of planet detection capabilities and results is summarized in this section.

A recurrent feature in the field of exoplanet observation is that model expectations have been repeatedly challenged and overhauled by observations. The majority of planetary systems detected to date have turned out to be strikingly different from the Solar System in several fundamental ways. However, before briefly evoking these results in more details below, it is important to keep in mind that our present knowledge is strongly constrained by the detection biases of the observing techniques, and that it is still possible that our Solar System is representative of the most common types of planetary systems.

About 700 planets are known with a radial-velocity signature, spanning periods between less than a day and several years, and masses from the brown dwarf limit to a few Earth masses (see *exoplanets.org*, *exoplanet.eu*). More than 1000 transit candidates, a majority of them probably bona fide planets, have been identified by the Kepler mission, down to sizes of 1 Earth radius (see, e.g., Lissauer et al. 2011). Other techniques have identified planets in lower numbers, but in interesting regions of parameter space: very light planets around pulsars, distance planets with microlensing, free-floating planets and wide systems with imaging.

Planet diversity The planets detected today practically fill all the volume in parameter space allowed by physical constraints and detection limits, and this is arguably the most impressive and unexpected result of the first ∼15 years of exoplanet research. The Solar System features three types of planet: cold gas giants and ice giants, and warm rocky planets, all orbiting on relatively circular orbits, aligned with the rotation plane of the Sun, and with internal compositions compatible with accumulation of condensate material and accreted gas at or near their present orbital distance.

By contrast, (a) the eccentricity distribution of exoplanet orbits is very broad, much closer to that of binary stars than of the Solar System, with circular orbits being exceptional (except very close to the star where tidal forces had time to circularize the orbit), (b) close-in planets are common, down to the shortest orbital distances allowed by tidal destruction, (c) the orbit of many close-in planets is not aligned with the rotation plane of the star, (d) giant planets with much higher masses than Jupiter exist, all the way to the Brown Dwarf limit around 12 M_{Jup} and higher, (e) many close-in gas giants are much larger than predicted by models, (f) planets with masses between ice giants and rocky planets are not uncommon, and (g) the composition of planets does not correlate much with the material available in the protoplanetary disk at their present orbital distance.

The one point of agreement between observations and previous expectation is the basic prediction of core-accretion theory. A clear link is observed between the presence of heavy planets around a star and the host star's content of heavy elements (Santos et al. 2004; Fischer and Valenti 2005), thus presumably the abundance of dust in the protoplanetary disk. Furthermore, high-density planets with masses below the critical mass of accretion of hydrogen and helium are abundant. The ensemble features of the planet population confirm the basic tenets of the core-accretion models. Although the competing scenario for giant planet formation—formation by disk gravitational instability—has not been ruled out entirely, it seems to be confined to a minority of cases, at least in the regions of parameter space probed by present surveys.

Giant planets Because of their enhanced detectability, the most extensively studied category of giant planets is the so-called "hot Jupiters", gas giants on close orbits (inside 0.1 AU). Their statistical properties are now well known and outlined in the next paragraphs. Hot Jupiters accompany around one solar-type star in 200 (Gould et al. 2006; Howard et al. 2010). At larger orbital distances, gas giants get more common as the orbit get wider, reaching a frequency of about 5 % of solar-type stars out to radii of 2–3 AU (Marcy et al. 2005). As radial-velocity surveys do not seem to have reached the mode of the gas giant frequency distribution yet, the actual frequency including Jupiter analogues could be comparable or much higher. At the other extreme in orbital distance, imaging surveys show that giant planets are also present at distances larger than the Neptune orbit (Marois et al. 2008; Kalas et al. 2008a). The statistics of this population will emerge in the coming years as imaging surveys like GPI and SPHERE get in full swing. One intriguing early indication from the HR8799 system is that cold gas giants are not analogous to brown dwarfs of the same temperature, but differ drastically in colors, a possible indication of different cloud coverage (Bowler et al. 2010).

Hot Jupiters are found at all orbital distances down to a few multiple of the distance at which the planet would fill its Roche lobe (P = 1–3 days depending in the mass), and seem to accumulate against this limit. A "pile-up" of orbits is observed near P = 3 days for gas giant lighter than Jupiter, with a mass dependence leading to periods near 1–2 days near masses of 2 M_{Jup} (Mazeh et al. 2005). The pile-up seems absent for higher masses (Pont 2009). The angle between stellar spin and planetary orbit—measured for transiting planets by the radial-velocity anomaly observed during the transit, the "Rossiter–Mc Laughlin effect"—shows a very wide distribution, all the way from aligned orbit to polar or entirely retrograde orbits, again with the exception of very close orbits which are generally aligned (Winn et al. 2010). Because of these last two observations, the balance of evidence to explain the presence of hot Jupiters and close-in planets generally has recently been tilting away from explanations involving inward migration in the protoplanetary disk, towards dynamical evolution after the disk has dissipated. The leading explanation now invokes planet–planet dynamical interactions and planet-star tidal interactions to bring planets inward and explain where they end up (Naoz et al. 2011). Only violent dynamical interactions seem able to account for the high level of disorder in the distribution of spin–orbit angles, although scenarios invoking disk–planet interactions have also been invoked (Lai et al. 2011).

Many hot Jupiters have a much larger radius—as measured by the depth of the brightness dip during transits—than predicted by structure models. Several explanations have been proposed, and as more transiting planets have been discovered it is now clear that the size anomaly is closely related to the amount of incoming irradiation received from the host stars. Hot Jupiter atmospheres seem able to transfer a significant fraction of the incoming radiative energy into internal entropy, via one or several processes that may or may not include ohmic dissipation (Batygin and Stevenson 2010), or eddy dissipation (Showman and Guillot 2002; Youdin and Mitchell 2010). Other explanations have been proposed for the anomalous radii but do not account for the observed dependence with stellar irradiation.

Observations have been gathered on the atmospheres of hot Jupiters during transits, secondary eclipses or phase variations, and it appears that there is more than one type of hot Jupiter atmosphere. This field is still in its infancy and there are few robust observations. For most objects, the data consist of a series of secondary eclipse depth measurements in a subset of the *Spitzer* telescope channels of 3.6–24 μm, giving a broad outline of the energy distribution of the day-side thermal irradiation of the planet. Tentative indications from these observations include the following: some atmospheres have a temperature inversion in the lower layers and other do not (Fortney et al. 2008a), the general atmospheric circulation is dominated by eastward jets (Knutson et al. 2009), some hot Jupiters are very dark and others reflective (Cowan and Agol 2011), the fate of the incoming stellar light can be dominated by alkali metal absorption (Na and K) (Singa et al. 2008), or by scattering from a haze layer. Explanations for these features are yet very tentative, including the presence of a layer of titanium oxide vapor for the temperature inversion, and silicate dust grains for the high-altitude haze.

Spectra are now being collected for much colder planets discovered by direct imaging, and the study of gas giant atmospheres at the other end of the temperature range can be expected to blossom soon. Already, as mentioned earlier, the preliminary indication that the clouds on the planets of HR8799 do not behave like those on brown dwarfs of the same temperature is very tantalizing.

Terrestrial planets The NASA Kepler mission is bringing a quantum leap in our knowledge of lower-mass exoplanets. The veil on statistical properties of 10–20 $M_{\oplus}$ planets that was slowly moving one planet at a time, was lifted in one sweep by the results of the first year of Kepler data.

The initial Kepler results indicate that the abundance of planets keeps increasing towards smaller masses and towards larger orbital distance. From around 0.5 % for hot Jupiters orbiting sun-like stars, the frequency of planets increases tenfold towards masses in the 10–20 $M_{\oplus}$ range, and tenfold again from short orbital distances to 1 AU. These results offer, qualitatively, strong support for the standard core-accretion scenario of planet formation, although they differ markedly in detail. Population synthesis using core-accretion models and disk migration predicted a gap in mass between gas giants and planetary embryos near the critical mass for runaway accretion of hydrogen and helium (15 $M_{\oplus}$), but such a gap is not observed. The size distribution of more than 1000 planet candidates from Kepler is rather smooth, suggesting that the neat separation in the Solar System between gas giants, ice giants and terrestrial planets is not a universal outcome of planet formation.

With apparently continuous distributions in mass and orbital distance, it is tempting to extrapolate the present distribution towards Earth analogues. If the power-law parametrization of the presently observed distributions are extrapolated to approximately 1 $M_{\oplus}$ and 1 AU, they amount to a star-to-planet ratio near unity (obviously counting the fact that a single star can have more than one planet)—a very remarkable result that would imply that terrestrial planets are an extremely common outcome of star formation. The Kepler mission will soon reach this regime and be able to provide a solid answer.

The sparser results from microlensing surveys, probing large orbital distances, and even the few known cases of terrestrial planets orbiting pulsars, are also broadly supporting these abundance estimates.

Planetary systems Another remarkable outcome of radial-velocity and transit surveys is the finding that systems with more than one planet are common. The Kepler mission has discovered more than one hundred systems with two or more transiting planets, and up to six transiting planets in the same systems. Given the geometric bias requiring alignment of the orbital planes with the line of sight for the transits to be observable, the high occurrence rate of systems with multiple transits is remarkable and was not expected. Radial-velocity surveys have also uncovered systems with more than four planets, although the exact number is often difficult to establish given the sparse data sampling and the superposition of all the orbital signals, and the lowest-mass candidates are usually doubtful.

When the selection effects are taken into account, it appears that planets are very commonly found in systems. Interestingly, it seems that many systems are quite close to the stability limit, "dynamically full" in the sense that the addition of one major planet would lead to short term instability and catastrophic dynamical evolution. This, together with the misaligned spin–orbit angles of many hot Jupiters, has lent support to the speculation that planet formation was in some sense "too efficient" and initially leading to over-crowded systems which would later evolve by dynamical interaction, possibly leading to the formation of close-in planets and the ejection of free-floating planets. This is a powerful constraint from planet formation model, which struggle to understand how the formation process clears all the hurdles between dust grain and full-fledge planet, let alone the problem to form planets in such abundance.

Some known planetary systems exhibit orbital resonance between two or more planets, but as an exception rather than a rule, perhaps suggesting that violent dynamical interactions are more common than orderly inward migration of several planets together.

Habitability The concept of habitable planets has generated an abundant literature, but based on a single example and few data, it has yet to demonstrate its relevance. While there is general agreement as to which orbital ranges are favorable to the presence of liquid water on the surface of a terrestrial planet, there is much variation in the details, and clear determinations of habitability are difficult to achieve in specific cases (Selsis et al. 2007). It is not clear that the concept of habitability extends to non-solar stellar types in a straightforward manner. For example, M stars are strong sources of UV radiation which may be a second important parameter aside of temperature for the permanence of liquid water and a substantial atmosphere (Raymond et al. 2007). Furthermore, it is not obvious if a mild temperature, resulting from equilibrium with the stellar radiation, is the only or even the main source of habitability (the greenhouse and anti-greenhouse effects can maintain surface temperatures very far from the equilibrium temperature on a planet with a thick atmosphere, and geothermal or tidal energy are able to keep a surface ocean liquid even with low stellar irradiation). Therefore, even though the $M \sim 1\ \mathrm{M}_{\oplus}$, $T_{\mathrm{eq}} \sim 300$ K region is obviously a soft spot for planet searches from the point of view of habitability and from a parochial perspective, there is nothing in our present knowledge that makes compelling the belief that this is very tightly connected to habitability or astrobiological interest (see also Lammer et al. 2009).

4 Scientific potential of optical to mid-IR interferometers

With the background of the theoretical models for the disk evolution and planet formation and corresponding observational findings, we now discuss the role of near-future long-baseline interferometers working from optical to the mid-IR wavelengths.

In this section, we will first review quickly the capabilities of coming interferometric instruments (Sect. 4.1) before outlining selected science cases in Sect. 4.2. These discussions are complemented by an outlook on synergy effects expected from observations with near-future large observatories and interferometers both in the IR and the (sub)millimeter domain in the subsequent section (Sect. 5).

4.1 Selected near-future interferometric instruments

To a great extent, current knowledge about the inner part of protoplanetary disks has been obtained with interferometric instruments that are presently in operation: AMBER[6] (Petrov and The AMBER Consortium 2003) and MIDI[7] (Leinert et al. 2003) on the VLTI (Glindemann et al. 2003), MIRC[8] (Monnier et al. 2004), CLIMB[9] and VEGA[10] (Mourard et al. 2010) on CHARA[11] (ten Brummelaar et al. 2005), and SPR[12] and the N band nuller (Millan-Gabet et al. 2011) on the KI (Perrin et al. 2006a). Furthermore, the PTI[13] (Pedretti et al. 2008) and IOTA[14] (Pedretti et al. 2008) have been used for circumstellar disk studies until recently. For selected results obtained with these interferometers and instruments, we refer to Sect. 3. Here, we present the near-future instruments that will be available on the VLTI, the Keck telescopes, and will discuss, exemplarily, the new optical/infrared interferometer MROI.

4.1.1 VLTI/PRIMA

PRIMA is a facility that will soon provide the VLTI both with a new instrumental capability and an enhancement of the existing instruments AMBER and MIDI (Delplancke 2008). It results from the joint effort of ESO and the ESPRI[15] (Launhardt 2009). It will offer the following new observing functionalities:

[6] Astronomical Multi-beam Combiner: the near-infrared/red focal instrument of the VLTI.

[7] Mid-infrared interferometric instrument.

[8] Michigan Infrared Combiner.

[9] Classic Infrared Multiple Beamcombiner.

[10] Visible spectrograph and polarimeter.

[11] Center for High Angular Resolution Astronomy.

[12] Self-phase referencing.

[13] Palomar Testbed Interferometer.

[14] Infrared Optical Telescope Array.

[15] ESPRI is a consortium led by the Observatoire de Genève (Switzerland), Max Planck Institute for Astronomy, and Landessternwarte Heidelberg (Germany).

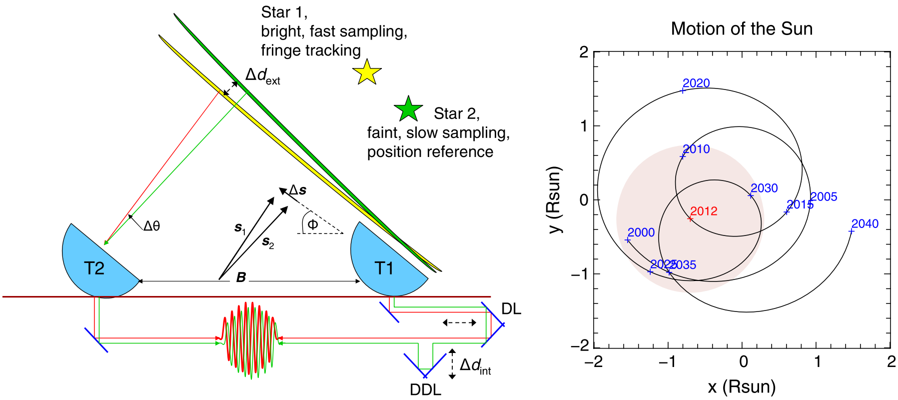

Fig. 5 *Left*: Schematic principle of dual-star narrow-angle astrometry (from Launhardt 2009). *Right*: Astrometric wobble of the Sun under the influence of Solar System planets (in solar radii). (Reproduced with permission from Elsevier)

1. Astrometric detection with accuracy expected to be down ∼50 μas;
2. Faint object observation with MIDI and AMBER;
3. Phase-referencing imaging with MIDI and AMBER.

PRIMA implements a narrow-angle dual-star astrometric capability to the VLTI. The schematic principle of narrow-angle astrometry can be seen in Fig. 5 (see also Shao and Colavita 1992). Two telescopes are used to observe interferometrically and simultaneously two objects in the sky. By using internal metrology and a proper knowledge of the telescope array localization it is possible to provide a measurement of the astrometric distance between the two objects.

PRIMA'a success relies on the inclusion of several new subsystems at VLTI and their joint operation. These subsystems are the building blocks of a proper astrometric system. They include:

1. Star Separator Systems at each Auxiliary Telescope focus (possibly extended to the Unit Telescope array). This system will allow one to observe simultaneously two objects in the isoplanatic sky patch: the science target and a reference object.
2. Two Fringe Sensing Units (FSU A and B). These instruments allow one to track simultaneously interference fringes on two objects.
3. Differential Delay Lines (DDL) that compensate for the optical path difference between the two objects therefore allowing one their simultaneous observation.
4. A Metrology System (PRIMET) that allows the angular distance between the science target and the reference to be measured.

With all these systems in place, PRIMA should be able to track on a reference star and monitor the astrometric wobble of the science target. As of July 2011 all PRIMA subsystems that have been installed on the mountain are almost all individually operational. Their common operation is now the focus of all the efforts. Once ready, PRIMA will be offered to the astronomical community.

4.1.2 VLTI/GRAVITY

GRAVITY (Gillessen et al. 2010) is a second generation instrument for the VLTI. It has been designed specifically to observe highly relativistic motions of matter close to the Galactic Center where a massive black hole gravity reigns.

To reach its final purpose, observing the astrometric motion of the faint near-IR flare at the center of the Milky way, GRAVITY will have to reach an unprecedented sensitivity. It will offer the possibility to observe with four telescopes in imaging and narrow-angle astrometric mode. It will add to the VLTI infrastructure near-IR sensitive adaptive optics and the capability to fringe track on a reference object within one telescope field-of-view (i.e. $2''$ for the UTs). GRAVITY will allow objects of magnitude up to $K \sim 18$ to be observed as long as a suitable off-axis reference object is available ($K \sim 10$). In on-axis mode the sensitivity will be $K \sim 10$.

In its imaging mode GRAVITY/VLTI will offer the measurement of interferometric observables (visibility, differential phases, closure phases, and triple amplitudes) on six baselines with ∼mas resolution. With time and earth-induced projection effects the *uv* plane can be properly sampled, therefore paving the way for conventional aperture synthesis image reconstruction. Three spectral resolution modes in the K band will be accessible i.e. $R \sim 22$, 500, 4000.

In its astrometric mode, using a newly implemented metrology system, GRAVITY will allow the measurement of angular distances with accuracies as low as 10 μas. Detecting a displacement of 10 $\mu\mathrm{as\,yr}^{-1}$ corresponds to ∼7 m/s at 150 pc, a typical distance for star-forming regions.

4.1.3 VLTI/MATISSE

MATISSE[16] (see, e.g., Lopez et al. 2009; Wolf et al. 2009) is a mid-infrared spectro-interferometer combining the beams of up to four UTs or ATs of the Very Large Telescope Interferometer (VLTI). MATISSE will measure closure phase relations and thus offer an efficient capability for image reconstruction. In addition to this, MATISSE will open two new observing windows at the VLTI: the L and M band in addition to the N band. Furthermore, the instrument will offer the possibility to perform simultaneous observations in separate bands. MATISSE will also provide several spectroscopic modes. In summary, MATISSE can be seen as a successor of MIDI by providing imaging capabilities in the mid-infrared domain. The extension of MATISSE down to ∼3 μm as well as its generalization of the use of closure phases makes it also an extension of AMBER. Thus, in many respects MATISSE will combine and extend the experience acquired with two first generation VLTI instruments—MIDI and AMBER.

MATISSE will extend the astrophysical potential of the VLTI by overcoming the ambiguities often existing in the interpretation of simple visibility measurements. The existence of the four large apertures of the VLT (UTs) will permit to push the sensitivity limits up to values required by selected astrophysical programs such as the study of AGNs and extrasolar planets. Moreover, the existence of ATs which are

[16] Multi Aperture Mid-Infrared SpectroScopic Experiment.

relocatable in position in about 30 different stations will allow for the exploration of the Fourier plane with up to 200 meters baseline length. Key science programs using the ATs cover for example the formation and evolution of planetary systems, the birth of massive stars as well as the observation of the high-contrast environment of hot and evolved stars.

The primary goal of MATISSE is to allow image reconstruction in the mid-infrared wavelength range with an unprecedented spatial resolution of ∼10 mas. A sufficient uv coverage will be reached on the basis of 3–5 different AT configurations (with 1 night of observation per AT configuration). Constrained by the dynamical evolution of MATISSE targets on ∼mas scale, the different AT configurations (i.e., a complete set of observations for a given target) should be scheduled within a period of two–four weeks. The comparison between models and visibility points and phases in the Fourier plane is considered as an alternative approach for the data analysis. This approach will profit from the combination of the experience gained with MIDI (data analysis in the N band) and radio interferometry (simultaneous analysis of many uv data points).

In the N band, the sensitivity of MATISSE depends on the number of combined beams but is in general comparable to MIDI. The type and number of astronomical sources per object class is therefore comparable to those of MIDI. MATISSE will allow one to investigate the expected complex nature of the small-scale structures traced with MIDI. These observations are expected to significantly improve our understanding of fundamental astrophysical processes in various classes of objects (e.g., planet formation/planet-disk interaction, structure of AGN tori).

In the L&M bands, observations will allow one to trace regions with higher characteristic temperatures. The physical conditions and chemical environment can therefore be studied in different regions (e.g., in protoplanetary disks, or stellar winds). While N band observations are clearly dominated by the thermal emission of warm and cool dust, L/M band continuum images are expected to be dominated by the scattering and thermal emission of radiation of hot dust grains. Thus, MATISSE will provide complementary information about the structure of the dusty environment of the various astrophysical objects, but also about the dust properties. Furthermore, in L band the highest sensitivity is expected due to the reduced background emission.

MATISSE will provide a spectral coverage from the L band (∼3 μm) to the N band (∼13 μm) with spectral resolutions of R ∼ 30 (L/N), 100–300 (L/N), and 500–1000 (L). Beside an individual analysis of measurements in different bands, the combination of data from multiple bands is expected to provide much stronger constraints on models of science targets than data from a single band alone. This is due to the different regions (spatial resolution), different physical conditions and processes (temperature), and origin of the radiation (reemission, scattering) of the MATISSE targets that can be traced in L to N band the wavelength range.

4.1.4 VLTI/VSI

The VLTI Spectro Imager (VSI; Malbet et al. 2008) instrument has been proposed in 2006 to ESO as a possible VLTI 2nd generation instrument dedicated to spectro-imaging at the milliarcsecond scale of various compact astrophysical sources in the near-infrared. Compared to GRAVITY, it would bring the J and H bands, high spectral resolution and the possibility to use 6 VLTI beams at the same time offering an imaging snapshot capability within a night.

VSI will provide the astronomical community with spectrally resolved near-infrared images at angular resolutions down to 1.1 mas and spectral resolutions up to R = 10000 to 30000. Targets as faint as K = 13 will be imaged without requiring a brighter nearby reference object; fainter targets can be accessed if a suitable off-axis reference is available. This unique combination of high-dynamic-range imaging at high angular resolution and high spectral resolution for a wide range of targets provides the opportunity for breakthroughs in many areas at the forefront of astrophysics, especially for the formation of stars and planets.

VSI will probe the morphology of the dusty close environment of pre-main-sequence stars at NIR where the temperature of the emitting material is close to the dust sublimation temperature. Therefore it will focus on the central radiation field in the environment structure, i.e. the exact shape of the sublimation surface/rim and inner cavity. It will permit to correlate the morphology with dust properties, but also to detect possible planetary orbiting companions which open cavities in the central disk region. This information is important to understand the influence of planetary companions on the planet formation and migration scenarios. The structure of the inner disk revealed by the capacity of image reconstruction with VSI can help to understand the initial conditions for planet formation.

The most remarkable feature of VSI is its capacity to get snapshot images of these environments within a night, opening the path to time-dependent morphology. At Taurus distance, the Earth orbit is located at 7 mas. Therefore, all motions within this radius will have time constants of the order of months and even less. For the first time a systematic study of the orbital evolution of the dusty environment will be feasible and compared to numerical simulations. By comparing objects at different evolutionary stages, the time scales for the morphological evolution and dissipation can be addressed. With VSI, a considerable advance in PMS stellar evolution models is expected and more precise timing of the central stars will be available. The spectral capacity of VSI in the NIR domain will allow the estimation of the stellar mass. This mass directly affects the central radiation field and the dusty environment via sublimation/heating and radiation pressure.

4.1.5 KI/ASTRA

The KI[17] combines the two 10 m Keck telescopes with a baseline separation of 85 m. The resulting resolution of $\lambda/2B \sim 2.7$ mas at 2.2 µm is about a factor 3 better than the diffraction limit of the planned ∼30 m class next generation of ground-based telescopes currently under development. The opto-mechanical complexity of the imaging process of 30 m telescopes (Gilmozzi and Spyromilio 2008) will make it difficult to match and outperform the high precision of *interferometric* astrometry with *imaging*

[17]Unfortunately, NASA has currently decided to cease operations funding for the KI for budgetary reasons. Please check for more up-to-date information the Keck Interferometer support page: http://nexsci.caltech.edu/software/KISupport/.

astrometry. Recent developments include the addition of nulling interferometry and improved sensitivity (Colavita et al. 2008).

ASTRA, which stands for the *ASTrometric and phase-Referenced Astronomy*, is a major development effort to broaden the astrophysical applications of the KI (Woillez et al. 2010). There are three modes of ASTRA which implement continuous corrections for phase distortions by increasing degree of complexity: the self-referenced spectroscopy (SPR) stabilizes fringes *on-axis* directly on the science target and enable higher spectral resolution up to a few thousands; dual-field phase-referenced visibility measurements (DFPR) stand for integration beyond the atmospheric coherence time to reach $K = 15$ mag on science targets while locking the fringe tracker on an offset guide star; the narrow-angle astrometry mode (AST) eventually will measure distances between a pair of stars within the isopistonic patch to a precision of 50 μas. The three ASTRA steps, or modi of operation, gradually increase the technological complexity. The SPR mode (Woillez et al. 2010; Pott et al. 2010) is already in operation and we focus here in the two other coming developments.

Dual-field operation The dual-field operation is a natural extension of the SPR mode. Two fringe cameras run in parallel. The first one tracks the fringes for good piston and vibration correction, enabling much longer integration times at the second camera to increase the SNR. But in contrast to SPR, the dual-field phase-referencing mode focuses on increasing the limiting magnitude of the low-dispersion mode by about 5 magnitudes to allow one pointing the second fringe camera on a faint star within the isopistonic patch around a bright star. The key difference in the implementation between these first two phases is that for the dual-field operation the light has to be split already in the image plane at the Nasmyth foci of the telescopes. After this field separation, the light travels along two separate beam trains down to the beam combining laboratory, thus a doubled delay line infrastructure is needed. The additional delay lines are already in regular use for the operation of the KI nuller instrument. The advantage of the dual-field operation is two-fold. The atmospheric differential piston, as measured on the bright star in the primary field, can be applied to both fields to stabilize the fringe motion. This correction is effective as long as the star separation is smaller than the isopistonic angle. But monitoring helper systems are needed to ensure that the non-common path after the beam separation does not suffer from vibration induced decorrelation and differential tip-tilt. DFPR operation will also allow one to use the one (unresolved) star as phase reference against the other. An unresolved star, used as phase reference, has no intrinsic visibility phase, so the measured phase derives entirely from the atmosphere and the instrument. This knowledge can be used to calibrate and retrieve the intrinsic phase information from the (fainter) companion in the second field. This will allow the measurement of imaging information about the object in the second field, as long as its position and the related astrometric phase is known. For instance asymmetric dust distributions would produce intrinsic phase signals. First on-sky tests validated the ASTRA dual-field hardware during the summer 2010, and separate fringes on two stars were recorded.

Astrometry For the phase-referenced visibility measurement (DFPR), the absolute fringe location does not matter, as long as the geometrical delay is corrected for well enough to ensure that the fringe pattern stably ends up on the detector. The visibility information is encoded in the *contrast* of the interference signal. But astronomical information is also contained in the differential fringe *location* which encodes the absolute separation between two stars. ASTRA-AST (Pott et al. 2009; Woillez et al. 2010) is designed to measure the differential optical path difference (OPD) between both stars. ASTRA-AST will provide the KI with an internal laser metrology system precise enough to measure Δ OPD at the 10 nm level, which transforms into a precision better than 50 μas for stars separated closely enough that the differential atmospheric phase distortions do (nearly) cancel out, i.e. for two stars from within the isopistonic angle. Note that the actual *astrometric* baseline of the observation is defined by the endpoints of the internal metrology system used to measure the precise differential fringe delay. This astrometric baseline typically does not exactly coincide with the conventionally calibrated wide-angle baseline. Since the astrometric baseline is typically not defined in the primary space of the telescope, it is difficult to measure it at a precision of about 50 μm, which is required to achieve the goal of 50 μas astrometry. To avoid the difficulty of knowing the astrometric baseline, the technique of differential narrow-angle astrometry (DNA) was developed for ASTRA-AST. This technique relaxes the requirements on the precision of the astrometric baseline to a few millimeter, and still achieves the goal of 50 μas astrometry when observing nearby calibrator binaries of similar orientation and separation on the sky (Woillez et al. 2010). Such a precision level is provided by the KI due to the stability of the Keck telescope pivots over the night.

Laser guide star aided interferometry The second of the two Keck telescopes will be equipped with a powerful sodium layer laser beacon to allow for adaptive optics correction independent of a bright visible guide star (Chin et al. 2010). This will put the KI in the unique position of being able to offer laser guide star-AO aided operations of targets too faint in the visible to feed the current wave front sensor. In the context of young-stellar objects (YSO) and their disks, this is particularly interesting for deeply dust embedded objects and edge-on disk systems, which delivered no or poor AO-correction so far.

4.1.6 MROI/SIRCUS

The Magdalena Ridge Observatory Interferometer (MROI) is an optical/near-IR interferometer being built west of Socorro, New Mexico, on a mountain at 3500 m and overlooking the site of the EVLA (Fig. 6). The entire interferometer has been optimized for a high-sensitivity imaging mission. The baselines for MROI range from roughly 8 to 345 meters, allowing it to access angular resolutions of 30 mas down to 0.3 mas. First fringes for the facility are scheduled for 2013, with more telescopes coming online shortly thereafter and production of rudimentary images beginning in 2015. When complete, the facility will consist of ten 1.4 m diameter relocatable telescopes laid out in an equilateral-Y configuration, with 28 separate telescope pads to accommodate array reconfiguration (Creech-Eakman et al. 2010b). Full descriptions of the MROI capabilities and progress have been presented recently by Santoro et al. (2010), Jorgensen and Mozurkewich (2010), Farris et al. (2010), and Fisher et al. (2010).

Fig. 6 A recent photograph of the MROI beam combining facility. *To the left in the photograph* extends the single pass delay lines in a 190 m long building. *To the right in the photograph* is the location of the center of the array arms to be laid out in an equilateral-Y with the longest baseline attaining nearly 345 m (adapted from Creech-Eakman et al. 2008)

In broad terms, the MROI will utilize two separate beam combiners running simultaneously: one, a pairwise correlator optimized for faint source fringe tracking, will monitor the atmospheric perturbations between nearest-neighbor telescopes (in either the H or K_s near-IR band), while the other, a multi-beam closure phase combiner, will collect science data in another bandpass of interest. The current design is for two different science combiners, one optimized for the near-IR windows with another offering a capability in the R and I optical bandpasses. The goal for the science combiners is to permit full sampling of all possible interferometer baselines within 8 minutes, allowing the MROI to deliver deep images with high dynamic range in a *snapshot* mode routinely.

MROI IR science instrument, SIRCUS (Creech-Eakman et al. 2010b), will come online in about 2014, and will be capable of spectral resolutions of $R \simeq 30$ and $R \simeq 300$ on objects as faint as $H = 14$, with dynamic range of at least 5 more magnitudes within the image itself. A snapshot image with SIRCUS could be produced about every 8 minutes (where about 2 minutes of this is actual on-source integration) using beams from six of the MROI telescopes.

The Key Science Mission for the MROI is targeted on three main areas of astrophysical interest, all of which would be revolutionized were very high angular resolution imaging routinely achievable (Creech-Eakman et al. 2010a). For all three core areas, many of the physical processes occurring remain poorly understood, requiring complex imaging to be better understood. One of the cornerstones of the MROI Key Science mission is the study of star formation in low- and high-mass molecular clouds and the evidence of the earliest stages of planetary formation during this period of the star early life. In order to make a substantial contribution to our understanding of these YSOs, the MROI has been designed to be capable of making images of targets in the nearest star formation regions (for the northern hemisphere) on AU and sub-AU scales.

The MROI will be able to access hundreds of YSOs, not only due to the long baselines, unprecedented sensitivity and baseline bootstrapping capabilities of the reconfigurable array, but also because of MROI ability to offset point from optical objects down to about $V = 16$ within a few tens of arcseconds from objects for which fringes are to be tracked. This is crucial for YSOs due to their heavy dust enshrouding and because YSO cores are often just becoming observable in the IR/optical for only the most evolved objects.

4.2 Exemplary sciences cases

While the observations described in Sect. 3 have been key in confirming and improving current theories of planet formation, much is left to understand and characterize about circumstellar disks. Key questions that need to be addressed concern the surface density profile and three-dimensional dust distribution in the inner regions of protoplanetary disks prior to planet formation, and the presence of, e.g., planet-induced asymmetries in the inner few AU of any type of disks (see Sect. 2.3). To unambiguously address these issues, resolved images at the highest possible resolution are a necessary step forward.

Obtaining high-resolution images of the inner regions of protoplanetary disks can hardly be achieved with the next generation of large telescopes. For example, with a 42 m ground-based telescope providing diffraction-limited images in the near-IR, the highest linear resolution that can be achieved in a distance of 140 pc is about 1 AU, so that only a few resolution elements will cover the entire planet-forming region. Furthermore, the disk will remain embedded in the glare of the central star. Only long-baseline interferometry offers the promise of imaging of disks with a linear resolution on the order of 0.1 AU.

4.2.1 The diversity of planet-forming regions

With milliarcsecond angular resolution long-baseline interferometry has proven to be an ideal tool to study protoplanetary disks (see e.g. Millan-Gabet et al. 2007). It has refined the vision of the inner astronomical unit structure of a disk, revealing the emission discontinuity a the dust sublimation distance, the putative presence of hot gas accreting onto the star and/or wind emission and refractory dust (Benisty et al. 2010). The current sensitivity of VLTI instruments limits the exploration of protoplanetary disks to the brightest ones and therefore mainly intermediate-mass stars. The essential limitation comes from (1) the availability of a reference in the isopistonic field and (2) the fact that there are only two Fringe Sensing Units that will limit the observations to one spatial frequency visibility (one baseline) per observation. PRIMA opens the possibility to use a reference star close to the young star to phase the interferometer. This opens the way to longer integrations on fainter targets or with increased spectral resolution.

One of the most evident interesting things would be to increase the sample of solar-mass pre-main-sequence stars (T Tauri stars) for which disks near-IR size and inclination can be estimated. As shown by Pinte et al. (2008), sampling the emission from disks around low-mass stars would certainly bring significant constraints on disk energy balance through radiative transfer modeling. Also, astrometric detection of multiplicity among young stars for which radial-velocity surveys are less efficient (e.g. because of line veiling) would allow one to probe the properties of disks in binary/multiple environments.

As outlined in Sect. 3.1.2, most of the disk studies published so far have been focused on intermediate-mass pre-main sequence stars and few interferometric studies have been sensitive enough to observe protoplanetary disks around T Tauri stars. GRAVITY's sensitivity should allow the sample of observed young-stellar objects to be increased considerably and span the entire range of stellar masses. This will therefore open the way to statistical studies on disk morphologies and their relation with the central stars properties. On the favorable case where the disks are largely spatially resolved by the VLTI, image reconstruction of the K band emission in the continuum and in the lines will be the source of important information. This has already been carried by several authors (Renard et al. 2010; Kraus et al. 2010) with AMBER but the addition of a new telescope significantly increases the mapping efficiency. The predominant lines for disk studies in the K band are Brγ and CO overtone. Several questions will be addressed thanks to the GRAVITY ability to map the K band emission with a certain dynamical range:

1. What is the nature of the disk inner rim (dust distribution vs. gas distribution)?
2. Can we constrain the inner disk vertical structure (e.g. flaring, inner edge width, temperature radial dependence)?
3. Can we use the CO emission lines to constrain disk dynamics at the astronomical unit level?
4. Can we detect structures in the emission that can be related to the planet formation mechanisms (density waves, clumpiness)?
5. Can we relate the Brγ emission to the accretion ejection mechanisms?
6. Can we constrain the mass loss morphology (wind/jet) and therefore constrain the physical mechanisms at play at planetary formation spatial scales? Does mass loss affect planetary formation?

GRAVITY's contribution should be seen as complementary to MATISSE and the combination of the two should be a powerful tool to constrain the disk physical conditions within the central astronomical unit of a protoplanetary disk.

At KI, the high differential precision of visibilities and phases in spectroscopic operation (currently offered as SPR, but DFPR spectroscopy is also conceivable) allows one to distinguish different constituents of circumstellar disks, and measure their (differential) kinematic properties. Earth rotation and repeated observations will minimize the limitations of the single baseline on full two-dimensional kinematics and astrometry. Furthermore, the ASTRA upgrade provides the single-baseline KI with a series of new observing capabilities. In particular, the sensitivity of the KI fringe tracker and LGS-AO operation open up for the first time the observation of faint and red targets at the 10–15 mag level (K band) to the tool of long-baseline interferometry in the near-IR. Due to the increased sensitivity in DFPR (off-axis fringe tracking) mode, the current exemplary studies of the brightest nearby targets can be extended to more systematic surveys of larger samples of circumstellar disks.

4.2.2 The potential of interferometric imaging of the planet-forming region

The importance of simultaneous multi-baseline observations In terms of spatial resolution, a major progress has been achieved with MIDI and AMBER in the recent years. Given the typical distance of nearby star-forming regions of ∼140–200 pc and the spatial resolution achievable with the *Very Large Telescope Interferometer* (VLTI) in the 8–13 μm atmospheric window of 10–20 mas, these instruments are best suited to study the planet-forming region in circumstellar disks. One of the first exciting results achieved with MIDI was to show the difference in the dust grain evolution between the “inner” disk (represented by the correlated flux) and the outer disk (net flux), using the low-resolution spectroscopy observing mode (van Boekel et al. 2004). However, given the intrinsic limitations of the analysis of single-baseline observations (interpretation of visibilities, such as in the case of MIDI), one has only weak constraints on the structure and size of the emitting region: The interpretation is based on models, which in turn are weakly constrained in the inner disk region because of the lack of adequate observations since the main constraints are given at best by mid-infrared SEDs in a few cases. The situation becomes even more difficult if visibilities are used to constrain more than the geometrical parameters, such as the inner emissivity profile of circumstellar disks. High angular resolution images at infrared wavelengths are of decisive importance to distinguish between various existing disk models.

True surface brightness profile in circumstellar disks around T Tauri/HAe/Be stars Two-telescope interferometers allow one to derive the "mean" disk size and the approximate inclination of the disk. In this data analysis it is usually assumed that iso-brightness contours are centered on the location of the central star. In contrast, multi-baseline interferometers will allow studies of circumstellar disks that are not exactly seen face-on, and show a brightness profile which cannot be described by iso-brightness contours centered on the star.

In the mid-infrared, this will allow one to derive the radial temperature profile of the hot dust on the disk surface and the inner disk rim. This profile will provide information about the radial and vertical structure of the disk, and thus also about the importance of viscous heating (in addition to the stellar heating) and hence on the interior density structure in the potential planet-forming region of the disk.

Complex structures on large and small scale Thanks to the increasing spatial resolution of optical to mid-infrared images of young circumstellar disks it becomes more and more evident that these disks are highly structured. Moreover, the inner region of circumstellar disks is expected—but not yet proven—to show large-scale (sub-AU–AU sized) density fluctuations/inhomogeneities. Locally increased densities and the resulting locally increased disk scale height have direct impact on the heating of the disk by the central star and are expected to show up as local brightness variation (due to increased absorption/shadowing effects) in the mid-infrared images.

Evidence for dust grain growth and sedimentation The most reliable conclusions about grain growth—as the first stage of planet formation—are based on the millimeter slope in the SED of circumstellar disks (Beckwith et al. 1990) and more recently on images of dust disks provided by millimeter interferometry, such as the Butterfly Star in Taurus (Wolf et al. 2003) and CQ Tau (Testi et al. 2003). These images reveal grain growth up to particles of cm size. Clearly missing, however, are (a) observational constraints on the region, where dust grain growth is presumably fastest, and (b) detailed knowledge of the vertical distribution of the dust particles. The scattering parameter of dust grains significantly changes from sub-micron to micron-size (or larger) grains in the wavelength range of stellar emission. Together with the dust density structure, the forward- vs. backward-scattering behavior of dust grains determines the temperature structure of the disk which in turn controls the vertical structure of the disk.

As simulations of dust settling in circumstellar disks show that the disk flaring and, thus, the ability to absorb stellar radiation even at large distances from the star depend on the grain size distribution in the upper disk layers (e.g., Dullemond and Dominik 2004). Conclusions about the importance of this effect may be derived by comparing the average intensity profile for a large sample of sources (see e.g., Sauter and Wolf 2011).

Evidence for the presence of planets Once (proto-)planets have been formed, they may significantly alter the surface density profile of the disk and thus cause signatures that are much easier to find than the planets themselves. The appearance and type of these signatures depend on the mass and orbit of the planet, but even more on the relevant physical processes (e.g., turbulence) and the disk properties (e.g., mass, viscosity, magnetic fields) and thus on the evolutionary stage of the circumstellar disk.

Status of disk clearing within the inner few AU Depending on the temperature and luminosity of the central star, the sublimation radius for dust grains is of the order of 0.1–1.0 AU (T Tauri–Herbig Ae/Be stars)—a spatial resolution which can be approximately reached with MATISSE in the L band in the case of nearby YSOs. However, inner cavities in disks—dust depletion regions with radii which are much larger than the sublimation radius of interstellar medium-like grains—have been found (see Sect. 2.3.2).

Imaging: an MROI case study In the following, we present a case study which illustrates the potential of next-generation interferometers in the domain of imaging through adequate sampling of the uv plane and state-of-the-art image reconstruction. As described in Sect. 3.1.1, YSOs have flared disk geometries with puffed-up inner walls at the location where the accretion disk makes its closest approach to the star (Millan-Gabet et al. 2007; Pinte et al. 2008). These flared disk models tend to imply that most of the near-IR continuum emission comes from a narrow annular region where dust is sublimating. As a consequence, there is a large contrast between the brightness of the central star to that of the outermost parts of the disk, causing the detection of gaps within the disk to be challenging. In particular, we refer the reader to the models of Wolf et al. (2002) in which radiative transfer images of disks around YSOs were derived (for much longer wavelengths) using hydrodynamical simulations and various intensity fall-offs were derived assuming the presence of a Jupiter-mass planet at $\simeq$5 AU around a solar-mass protostar. Using these models, simulated data has been generated for the near-IR continuum emission from a Herbig Ae/Be star in a face-on presentation with a central cavity due to dust sublimation. For comparison, in some simulations a gap of 0.7 AU was superimposed in the dust at 2.1 AU from the star, putatively due to the presence of a Jupiter-mass planet. The ratio of disk to stellar flux was 3.35.

The simulated dataset was prepared by evaluating the discrete Fourier transform of the model image at spatial frequencies corresponding to the measured projected baselines, converting to MROI observables (squared visibilities and bispectra), and adding Gaussian noise appropriate for bright ($K \simeq 5$) targets. These simulated dataset were used as input to the BSMEM maximum entropy imaging code (Baron and Young 2008) and a point source image was used as the default. A six-telescope MROI was used with telescopes place at stations West 0, 1, and 4, North 1 and 3 and South 2, which resulted in a baseline range of 7.8 to 32 meters. The lowest spectral resolution of SIRCUS (R $\simeq 30$) was used with assumed uncorrelated visibility calibration errors of $\Delta V/V = 0.02$. A 6 hour observation duration was assumed for a target at +25° and MROI at 33.98° latitude such that a set of 42 visibility amplitudes and 70 closure phase measures was obtained every 20 minutes (Fig. 7).

As can be seen in the images, the uv coverage for the MROI on such a target is excellent, and the performance of SIRCUS on MROI results in reconstructed images with a dynamic range of 1000:1. Further, a degree of super-resolution has been obtained, as is demonstrated by the resolution of the 7 mas diameter inner cavity. The presence of the dust gap, indicative of a putative Jupiter-mass planet, is clearly evident from the reconstructed images. This type of work will be very complimentary to similar work done with e.g. ALMA, where MROI is highly suited to imaging the inner hot disk, and ALMA to the outer, cooler disk regions. For the nearest seven star-forming regions observable from the northern hemisphere, the MROI will be able to resolve structures down to the 0.15 to 1 AU scales in the IR.

In phase II implementation of MROI, the facility will deploy optical capabilities (in the R and I bandpasses) and bring online the final four telescopes of the array. Once optical imaging is possible, angular resolutions of less than a milliarcsecond will be routinely possible, and in particular, emission line imaging to trace shocked regions and magnetically channeled accretion in YSOs will become feasible. No other facility-class optical interferometers current or planned are expected to work at optical wavelengths, therefore MROI will deliver a unique capability unparalleled by ELT employing adaptive optics or space-based facilities.

4.2.3 Analysis of the mineralogy and gas in protoplanetary disks with MATISSE

In L band (∼3.0–4.1 μm), interferometric observations of the H_2O ice broad band feature (2.7–4.0 μm) and PAHs: 3.3 μm, 3.4 μm; nano-diamonds: 3.52 μm will become possible, while in M band (∼4.6–4.8 μm) CO fundamental transition series (4.6–4.78 μm), CO ice features 4.6–4.7 μm, and recombination lines, e.g., Pfβ at 4.65 μm, can be investigated with "interferometric resolution". In N band (∼8–13 μm), spectral features to be investigated with MATISSE will be very similar to those studied with MIDI. However, MATISSE will allow one to constrain the spatial distribution in much more detail.

4.2.4 Disks around massive stars

While several prominent low-mass star-forming regions can be found at distances of 150–300 pc from the Sun, most of the currently active high-mass star-forming regions are located at distances beyond 1 kpc, distances of 3 to 7 kpc are quite common. Furthermore, massive stars predominantly form in the densest regions of young-stellar clusters. Recent investigations estimate typical number densities of 5×10^4 stars/pc^3 (Orion Trapezium Cluster, McCaughrean and Stauffer 1994) or even higher values

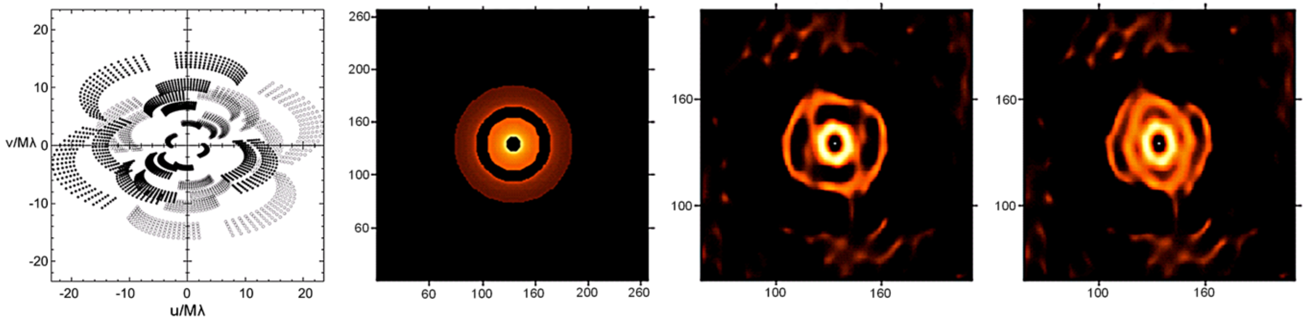

Fig. 7 *From left to right the panels* show: (**a**) UV coverage of the simulation for a YSO at a distance of 140 pc using a 6-telescope configuration of MROI with SIRCUS during a 6-hour observation. (**b**) The original image on which the simulations are modeled with a 0.7 AU gap present and employing an intensity fall-off of r^{-2}. (**c**) A six-telescope SIRCUS image of the YSO with the gap, and (**d**) The same six-telescope YSO image without the gap. *The color scale* is logarithmic and covers only the range of intensities in the disk, whereas *the central point* source is actually 130 times brighter than the brightest pixels in the reconstructed disk images

(Eisenhauer et al. 1998; Stolte et al. 2002). Although more and more theoretical investigations point towards the formation of high-mass stars by disk accretion (e.g., Yorke 2004), clear observational evidence for the existence of such disks remains rather scarce. Convincing cases were mainly found by radio interferometry (e.g., Shepherd et al. 2001; Cesaroni et al. 2005; Schreyer et al. 2006). Disks around young massive stars are probably short-lived since they are ablated by the strong UV flux and winds of the central star on time scales of $\leq 10^5$ years (Hollenbach et al. 1994). Thus, the best chance to detect such disks is to catch those systems in an early phase of evolution. As high-mass star formation is associated with high extinction, mid-infrared interferometry is the ultimate tool for investigating such disks.

In general, disks around massive stars are expected to be relatively massive themselves (e.g., Yorke and Bodenheimer 1999). As a consequence, they are increasingly susceptible to gravitational instabilities. Numerical simulations, including realistic cooling conditions (e.g., Durisen et al. 2001; Johnson and Gammie 2003) and MHD turbulence (e.g., Fromang et al. 2004; Fromang 2005) show that sufficiently massive disks tend to form dense spiral arms, arclets, ridges and similar kinds of surface distortions. For disk–star systems with a mass ratio $M_{\rm disk}/M_* > 0.3$, the disk might even begin to fragment into distinct blobs. As it is impossible to constrain these predicted complex structures on the basis of simple visibility measurements, high-resolution imaging is essential to make progress.

With the success of the mission for characterizing star-forming regions in the IR, there is a tremendous number of new objects available for studying with interferometry as identified in the GLIMPSE surveys in particular (Churchwell et al. 2009). An area in which interferometry has only recently shown success is the study of massive YSOs, for which competing theories of formation scenarios are still strongly debated (Zinnecker and Yorke 2007). The existence of the so-called "green-band emission" at the IRAC 4.5 μm band, a possible tracer of shocked gaseous regions, could readily be compared with the locations of pre-forming stellar cores. Identification of massive YSOs is being accomplished in the submillimeter and radio where the YSO shocked gases are evident and extinctions are much lower (Araya et al. 2007; Hofner et al. 2007; Beuther et al. 2002), and so the complementarity of these IR and radio techniques is again quite promising. Nevertheless, studies of core multiplicities, which could help sort among competing formation mechanisms, are still in their early stages as they require very high angular resolution in the IR.

Cyganowski et al. (2011) have catalogued nearly 300 possible massive YSOs candidates from the GLIMPSE survey. In their Table 1 they list 97 *likely* candidates. Of these candidates which are north of $-10°$ declination and therefore readily available to the MROI, 19 (67 %) have integrated fluxes above 11.5 magnitudes at IRAC 3.6, 4.5 and 5.8 μm bands. If these sources suffer less than 2.5 magnitudes extinction between the IRAC bands and the MROI tracking wavelengths of H and K_s, there is a high likelihood that the MROI will be able to image these regions and help contribute to our understanding of multiplicity and therefore help sort among competing formation scenarios. Such success has recently been demonstrated using VLTI AMBER in the near-IR (Kraus et al. 2010) and MIDI in the mid-IR (Vehoff et al. 2010) on two massive YSOs using instruments much less sensitive than MROI is predicted to perform by $\simeq$2015.

4.2.5 *Astrometric detection of exoplanets*

As an astrometric instrument, PRIMA is designed to measure the displacement of the star on the sky plane due to the gravitational influence of companions, hopefully of planetary nature (see, e.g., Fig. 5). The expected reflex motion of a host star of mass M_* located at a distance d from earth and orbited by a planetary companion of mass $M_{\rm P}$ with orbital radius $a_{\rm P}$ is given by the following formula:

$$\Delta\alpha = 0.33\left(\frac{a_{\rm P}}{1\ \rm AU}\right)\left(\frac{M_{\rm P}}{1\ \rm M_{\oplus}}\right)\left(\frac{M_*}{1\ \rm M_{\odot}}\right)^{-1}\left(\frac{d}{10\ \rm pc}\right)^{-1}\ \mu\rm as. \qquad (2)$$

The astrometric detection parameter space of PRIMA brings evident complementarity to radial-velocity observations. The further away from the star, the stronger the astrometric signal (with a longer period to sample). As presented by Launhardt (2009) PRIMA can be used to address several issues:

1. Obtain the inclination of the planetary orbit to derive the planetary mass (constrained by radial-velocity surveys only).
2. Confirm long-period planets candidates in radial-velocity surveys.
3. Measure the relative orbit inclinations in multiple planetary systems.
4. Perform an inventory of planets around stars with different mass and age, in particular planets around young stars (age <300 Myr).

A preliminary list of 900 candidates has been selected by the ESPRI consortium while the final list will be probably much reduced. Indeed, the final planetary mass detection performance will be directly linked to the ability to find a reference star at 10″ to 30″ and to the astrometric precision. Astrometric accuracies of 100 μas have been demonstrated at the Palomar Tested Interferometer (Colavita et al. 1999) with the PHASES program (Muterspaugh et al. 2006). It is hoped that PRIMA will be able to track on K ∼ 9 stars on a routine basis as it was done during commissioning (Sahlmann et al. 2009). The precision of 10 μas was the initial goal but this was done with an incomplete description of the instrument. A precision of a few 10 μas would already permit significant contributions such as the detection of Jupiter mass planets at a distance of 1–5 AU.

As an astrometric device, GRAVITY will be sensitive to the wobble of a star under the gravitational influence of its planetary system. Given its sensitivity, detecting Jupiter and Saturn mass planets at ∼1 AU from their parent star should be within reach. The strength with respect to PRIMA is the redundancy provided by the simultaneous six baselines observation. However, the limited 2″ field-of-view will restrict such studies to those objects having a suitable fringe tracking reference.

As an interferometer, GRAVITY provides the capability to measure precise closure phases. It has been shown (Renard et al. 2008) that using four UT telescopes with GRAVITY one can reach a sufficient closure phase precision to directly detect hot Jupiters with favorable stellar to planet brightness ratio. Moreover, a moderate spectral resolution capability might allow the detection of molecular features such as methane/water absorption in the planet spectrum to be detected.

At KI, the envisaged precision level of 50 μas of the ASTRA astrometry mode will allow for the detection of on-sky reflex motion of exoplanet hosting stars. While large astrometric exoplanet surveys such as ESPRI (Launhardt et al. 2008) are most efficiently done with two orthogonal baselines and smaller apertures, ASTRA-AST observations will have a high impact with the detailed study of fainter and complex multi-planet systems aligned with the KI baseline.

4.2.6 Direct imaging of exoplanets: a challenge for interferometry

Direct imaging and observations of exoplanets with optical interferometers are inherently challenging due to the very large contrasts between the star and exoplanet. However, interferometry offers access to measurements impossible with conventional telescopes. CHARA has recently contributed to our understanding of fundamental physical scales in confirmed exoplanet systems by making accurate measurements of the host star diameters (Baines et al. 2009). As interferometers continue to characterize planet-bearing stars, and in particular features such as stellar spots and limb-darkening, we will gain better understanding of basic parameters associated with planet transits and the environments in which these planets exist. More challenging yet would be the actual characterization of the exoplanets themselves via spectroscopy, which could in principle be accomplished using differential closure phase techniques.

Studies have been undertaken to determine the feasibility of such measurements, including investigations of the potential of existing interferometric instruments: VLTI using AMBER (Joergens and Quirrenbach 2005) and PIONIER (Absil et al. 2011), and CHARA using MIRC (Zhao et al. 2010). These studies suggest that characterization of closure phases with milli-radian level precision will yield information on both orbital geometries and spectral energy distributions in the exoplanetary atmospheres. These measurements are presently limited by interferometric systematics which presently prevent these facilities from attaining required closure phase precisions. Other potential complications include the need for adequate models for the host stars, which are most likely resolved by the interferometers, and how to adequately address changes in the orbital geometries of the star–exoplanet systems which are likely on the order of Earth rotation synthesis time scales for so-called hot Jupiter candidates. The MROI will have advantages over existing interferometers, in particular in that the array telescopes can be deployed and optimally baseline bootstrapped in order to match MROI intrinsic angular resolution to the systems being measured. Further, the high dynamic range and fidelity in SIRCUS images (with 10 telescopes it collects 36 independent closure phases every 8 minutes), will be produced via stabilized fringes delivered as a matter of course. With MROI planned observing scenarios, it may be possible to produce useful closure phase measurements on these systems, but this will certainly require more study and simulations once the MROI is operational.

It is clear that interferometry will remain the only feasible method to obtain sub-mas angular resolutions in the optical and IR on these types of object for at least the next decade. Because circumstellar environments of YSOs are expected to be complex, and exoplanets will likely require high-precision differential closure phases, imaging interferometers in particular are likely the only viable tools to make any significant progress understanding the contiguous environments of nearby systems.

5 The role of selected complementary observatories

One caveat of optical/infrared measurements is that protoplanetary disks are extremely optically thick in this wavelength range, so that it will remain impossible to *directly* probe the midplane in the inner regions of the disk. Over the next few years, ALMA will greatly expand our ability to spatially resolve protoplanetary and debris disks at (sub)millimeter wavelengths. For protoplanetary disks, this will allow one to extend the study of surface density profile and dust segregation down to the inner few AU.

Another shortcoming inherent to existing and planned optical/infrared long-baseline interferometers is the low sensitivity compared to that of large-aperture telescopes operating at the same wavelengths. Both, planned large-aperture ground-based (e.g., E-ELT[18]) and space-based observatories (e.g., JWST,[19] SPICA[20]) are therefore essential to achieve a comprehensive understanding of circumstellar disk physics by tracing the low-luminosity outer disk regions. In turn, interferometric observations—both at optical/infrared and (sub)millimeter wavelengths—will reduce the uncertainties related to the inward extrapolation of the outer surface density profile.

5.1 ALMA: the Atacama Large Millimetre Array

The Atacama Large Millimeter/submillimeter Array (ALMA) has been designed to be the leading ground-based observatory at millimeter and submillimeter wavelengths in the foreseeable future. ALMA will initially be composed of 54 × 12-m and 12 × 7-m diameter antennas located on the Chajnantor Altiplano at an altitude of 5000 m in Northern Chile. The plateau offers a relatively constant altitude site for arranging the ALMA antennas in several different configurations. In the most compact configuration the longest available baseline will be of only ∼150 m, in the most extended it will be up to ∼15 km. To fully exploit the excellent conditions on the site for submillimeter observations, ten receiver bands covering all the atmospheric transparency windows from 30 GHz to 1 THz are planned. The six highest priority bands will be available from the start of full science operations in early 2013. The remaining frequency bands will be added later to the array. Detailed descriptions of the ALMA system and performances have been published in Kurz et al. (2002) and Haupt and Rykaczewski (2007). When fully operational, ALMA will be 10–100 more sensitive and have 10–100 times better angular resolution than existing (sub-)millimeter instruments.

One of the three high-level science requirements by which the design of the ALMA system is determined is directly related to the observation of protoplanetary disks: Imaging the gas kinematics in protostars and protoplanetary disks around young Sun-like stars at a distance of 150 pc, enabling the study of their physical, chemical and magnetic field structures and to detect the tidal gaps created by planets

[18] European Extremely Large Telescope (Ramsay et al. 2010).

[19] James Webb Space Telescope (Mather 2010).

[20] Space Infrared Telescope for Cosmology and Astrophysics (Nakagawa 2011).

undergoing formation in the disks. Protoplanetary disks feature prominently in the high-level ALMA science goals and in the ALMA DRSP[21] and are a key science theme where ALMA is expected to provide a significant step forward, both for the study of the solid and gas components.

5.1.1 Dust in protoplanetary disks

At submillimeter and especially millimeter wavelengths, the dust thermal emission in protoplanetary disks is mostly optically thin to its own emission. The only possible exception being the innermost regions of the disk close to the star. Observing at these wavelengths offers the possibility of probing the bulk of the solids in the disks, especially at the disk midplane where most of the material is located and where planet formation is thought to occur. This methodology has been applied with success to estimate the total disk mass, the distribution of the material in the disk and to put constraints on the evolution of dust, in particular grain growth towards the formation of planetesimals (Beckwith et al. 1990; Beckwith and Sargent 1991; Dutrey et al. 1996; Wilner et al. 2000; Testi et al. 2001; Natta et al. 2007; Hughes et al. 2008; Isella et al. 2009; Andrews et al. 2009).

ALMA will also allow one to study of disk properties as a function of the central star parameters (age, mass), the evolution of disk structure and the relationship with planet formation processes and environment, and a proper understanding of the dust evolution processes. The presence and properties of circumstellar disks in the substellar mass domain and around the higher mass protostars are still debated. These systems are currently difficult to probe but ALMA is expected to overcome the current limitations (Natta and Testi 2008; Testi and Leurini 2008). Simulations show that ALMA will allow one to probe the diversity of disk properties at the bottom of the mass function, but it will still be hard to resolve spatially these disks and probe their structure. In the high-mass regime, ALMA should clarify the role of disk in the formation of these objects by detecting and resolving the disk structure (Cesaroni 2008; Krumholz et al. 2007).

5.1.2 Protoplanets

In the solar-mass star regime, ALMA will provide the sensitivity and resolution to detect forming protoplanets if they do exist in nearby star-forming regions (Wolf and D'Angelo 2005). Current observations show that grain growth is a relatively common process and many disks show evidence for very large grains in the midplane (e.g. Lommen et al. 2009; Ricci et al. 2010a, 2010b), suggesting also that large grains can remain on the disk for long times. These findings are at odds with model predictions of grain growth and migration in disks, which suggest that large grains should be efficiently removed from the outer regions of disks (Brauer et al. 2008b). Observations and theory could be reconciled if large grain migration is halted or slowed

[21] ALMA Design Reference Science Plan; a collection of the science projects that can be expected to be carried over during the initial years of ALMA full science operations. The latest version of the DRSP is available on the ESO webpages: http://www.eso.org/sci/facilities/alma/science/drsp/; for a high-level analysis of the DRSP content, see Hogerheijde (2006) and Testi (2008).

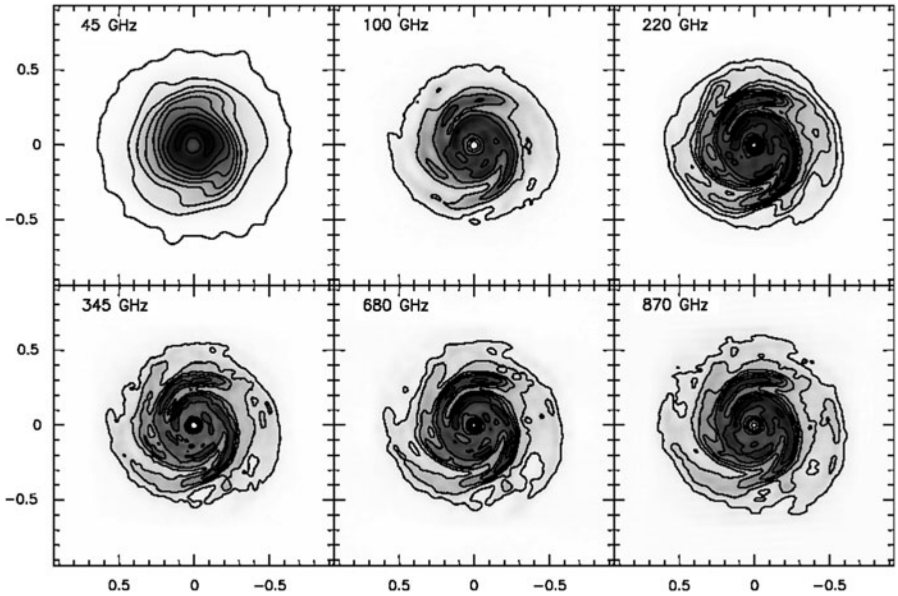

Fig. 8 Simulated ALMA observations of a self-gravitating circumstellar disk in the Taurus Star Forming Region. Axis scales are in arcseconds (adapted from Cossins et al. 2010)

down (e.g. Birnstiel et al. 2010). To constrain theoretical expectations it is necessary to resolve grain growth as a function of radius in disks and to observe the possible patterns in disks that may be responsible for slowing inward grain drift. Initial attempts in this respect are being performed with current instruments (Isella et al. 2010; Banzatti et al. 2011; Guilloteau et al. 2011), but ALMA will put the initial findings on a firmer ground. As an example, Cossins et al. (2010) simulated ALMA observations of a self-gravitating disks which develops a pattern of spiral structures that trap large grains and slow or halt migration (see Fig. 8). The simulations demonstrate that, once completed, ALMA will not only allow one to detect such features in protoplanetary disks, but also to derive the dust properties in the high and low density regions of the disk constraining selective dust trapping.

5.1.3 Tracing the spatial distribution and kinematics of molecules

One major unknown in planet formation scenarios is the radial and vertical distribution of the gas and its evolution with time in the regions <20–50 AU. Furthermore, the mass and dynamics of disks surrounding young low-mass stars are gas dominated[22] but the main gas component, H_2, remains difficult to observe. The quadrupolar H_2 rotational transitions in the mid-IR only trace the warm material which is located at the disk surface. Hence, there is no simple way to get a reliable estimate of the cold gas mass. One has to rely on indirect tracers such as CO or rarer molecules

[22]The gas-to-dust ratio is supposed to be of the order of 100 in a disk of 1 Myr.

whose observations are sensitivity limited. This situation will drastically improve with ALMA, thanks to its very large collecting area.

In the early 1990s, CO J = 1–0 and J = 2–1 maps not only revealed that disks are in Keplerian rotation around T Tauri (Koerner et al. 1993) and Herbig Ae stars (Piétu et al. 2005) but led to the first quantitative studies of the physical conditions of the gas in disks, provided an adequate data analysis is used (e.g. Dutrey et al. 2007). Multi-line multi-isotope study of CO can unveil the vertical structure of gas disks, in particular the temperature. This has been illustrated by Dartois et al. (2003) and Piétu et al. (2007) who showed that the "CO disk surface", traced by an opacity of $\sim$1 in the ^{12}CO J = 2–1 transition located at about 3–5 scale height, is significantly warmer than the mid-plane. This method using higher CO transitions would sample the disk atmosphere (Qi et al. 2004, 2006) revealing the impact of X-rays and UV irradiation on the disk properties. The disk surface can be reasonably approximated by models of photo-dissociation regions, while the colder disk interior reflects a chemistry close to that of dense clouds. In all T Tauri disks where CO has been mapped, the gas temperature in the mid-plane appears to be below the CO freeze out point (17 K), suggesting that the vertical turbulence should play an important role by providing chemical mixing between the vertical molecular layers. Direct studies of the turbulence will also be possible with ALMA by quantifying the non-thermal component of molecular line broadening.

Rarer molecules are more difficult to detect. Moreover, most of them may have transitions which are in non-LTE conditions, contrary to first rotational lines of CO. These molecules can provide invaluable information on disk density structures provided the excitation conditions are understood and properly modeled (Dutrey et al. 1997). Several groups (Kastner et al. 1997; van Zadelhoff et al. 2001) have conducted molecular surveys, but they are sensitivity limited to the most abundant molecules found in molecular clouds. In addition to CO, ^{13}CO and C^{18}O, only HCO^+, $H^{13}CO^+$, DCO^+, CS, HCN, HNC, DCN, CN, H_2CO, N_2H^+ and C_2H have been firmly detected. As soon as the full ALMA array is operational, the number of detected and mapped molecules will increase revealing the complexity of the disk molecular chemistry and the vertical stratification of molecules (Semenov et al. 2008). For example, mapping of molecular ions such as N_2H^+ or HCO^+ and its isotopomers should provide the first quantitative information on the ionization fraction, one key element to characterize the dead zone.

5.2 Infrared space observatories

Space observatories benefit from a much more stable image quality, with no seeing-degradation point spread function (PSF), and also usually better sensitivities for a given size of the primary mirror. To illustrate the potential of near-future infrared observations from space to provide complementary insights on the topic of circumstellar disks and planets, we make use of the well-advanced preparatory science studies for the JWST, which is designed to replace the Hubble Space Telescope.

The JWST primary mirror will be larger in size than that of the Hubble Space Telescope (6.5 m compared to 2.4 m) and its range of wavelength coverage will shift towards the IR (0.6–28 μm). While ground-based instruments suffer in this wavelength range from an incomplete coverage due to the atmospheric absorbing bands as well as a limited sensitivity with a large thermal background beyond ∼2 μm, JWST will have access to any wavelength in the range mentioned above and will be limited by zodiacal light up to 16 μm. Beyond this wavelength, its sensitivity will be constrained by the sunshield thermal radiation and the telescope proper emission. More information concerning the telescope and its specificities can be found in Gardner et al. (2006).

The JWST comprises a suite of three instruments and a Fine Guidance Sensor (FGS) that can be also used to obtain scientific observations. The FGS features narrow band Fabry–Pérot spectro-imaging (Doyon et al. 2008) and pupil interferometry by a Non Redundant Mask (NRM) (Sivaramakrishnan et al. 2009). Occulting masks are also available and can be combined with apodization masks to produce 10^{-4} (at an angular distance larger than $2''$) contrast ratio coronagraphic images in the near-IR range. The NIRCam instrument is in principal an imager observing in the near-IR range (0.6–5.0 μm) with a set of broad, intermediate, and narrow band filters. It is equipped with a set of coronagraphic occulters (three apodized spots and two apodized wedges with sizes ranging from 2 to 6 λ/D) that allow the NIRCam instrument to conduct high-contrast imaging observations (Krist et al. 2007). In addition, NIRCAM offers also the possibility to produce slitless spectra using a set of grisms (2.4–5 μm) with R ∼ 2000 spectral resolution. The NIRSPEC instrument features a multi-object spectrometer, an integral field unit (IFU), and a long-slit mode. The spectral resolutions range from R = 100 to R = 2700. Finally, MIRI is the mid-IR instrument (5–28 μm) observing both in imaging and spectroscopic modes. The MIRI imager sub-instrument is equipped with focal plane coronagraphic masks, three four-quadrant phase masks and one Lyot mask (Baudoz et al. 2006) particularly designed to observe exoplanets and circumstellar disks, respectively, at wavelengths of 10.65/11.4/15.5/23 μm. It offers also slit and slitless prism modes (R = 100); the spectrometer sub-instrument is an IFU with higher spectral resolution (R = 3000).

5.2.1 Protoplanetary disks

Its remarkable sensitivity to faint diffuse objects coupled with a good angular resolution at IR wavelength comparable to that of ground-based instruments make the JWST a first choice facility for the study of protoplanetary and debris disks. Its high-level spectroscopic capabilities at medium resolution (R ∼ 2500) will allow one to study the gas chemistry in protoplanetary disks and the dust content in protoplanetary and debris disks in detail, and to search for leftover warm gas in debris disks. Furthermore, some spatial information will also be obtained in the case of the closest objects ($d \lesssim 50$ pc).

Important science questions regarding the physical state and evolution of protoplanetary disks can be tackled using the JWST capabilities in order to constrain the physical conditions (depending on the star mass) that lead to planet formation. In the case of the JWST, at least three science cases/questions can be identified. The first one deals with the large scale (50–500 AU) vertical structure of protoplanetary disks. The second one is the dust sedimentation process, which is a prerequisite to planet formation through core accretion. Finally, MIRI and NIRCAM have both, and for the first time ever, the angular resolution, the sensitivity and the stability to directly detect thin/weak structures imprinted in the disks by already formed giant planets.

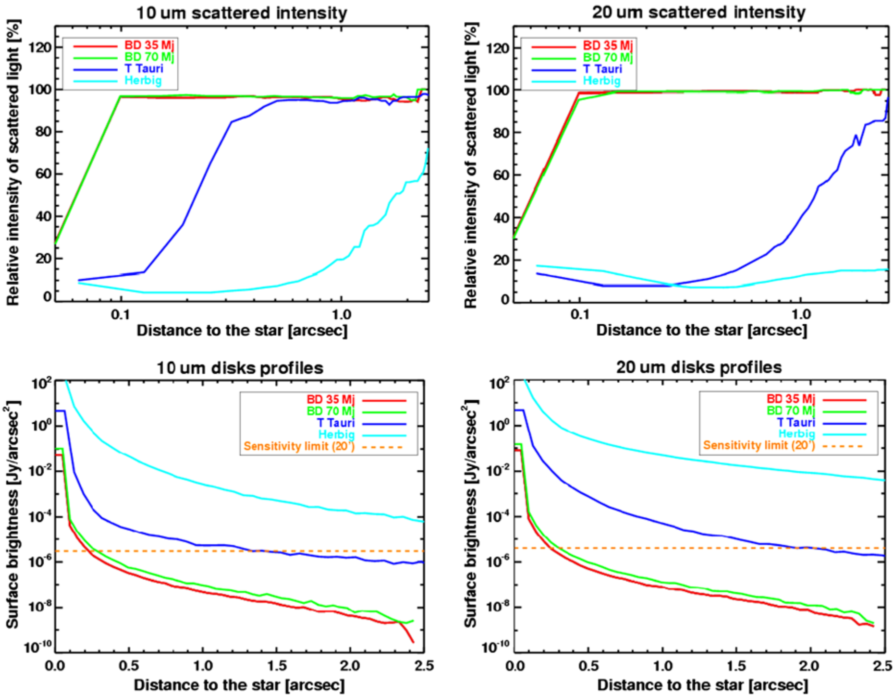

Fig. 9 *Upper panel*: Relative proportions of (inner rim) scattered light (10 and 20 μm) with respect to the total emission. *The lower panel*: Displays the protoplanetary disks total emission (10 and 20 μm) as a function of the angular distance to the star for an object at 140 pc. Different types of star are considered: a Herbig Ae star (A0e, $L = 40\ L_{\odot}$), a T Tauri star ($T_{\rm eff} = 3900$ K, $R_* = 3\ R_{\odot}$), and two brown dwarves (70 and 35 Jupiter masses, respectively)

In relatively short integration sequences, the IFU spectrometer in MIRI will be able to measure the abundances and temperatures of species in gaseous form with an amazing precision. The observations of atomic line like the [NeII], [NeIII] and possibly [SI] (Gorti and Hollenbach 2008) signatures at 12.81 and 15.55 and 17.4 μm, respectively, will allow one to trace the physical state (e.g., temperature, heating mechanism) of the upper tenuous layers of the disks. At deeper levels in the inner few AUs, the molecular layer contains among others H_2 (the major constituent of giant exoplanets), water, OH, C_2H_2 and HCN molecules. The observation of water lines in non-LTE state (Salyk et al. 2008; Pontoppidan et al. 2010) provides an important diagnostic of the layers where the gas and the dust start to couple in the disks. In parallel, the MIRI high-sensitivity imaging capabilities, coupled with an excellent inner working angle (IWA = 1 λ/D) of the 4QPM coronagraph, will be particularly efficient to angularly resolve the disks in the mid-IR range. At these wavelengths the thermal emission dominates. However, given MIRI's extreme sensitivity, the (unresolved) inner rim light scattered by the dust particles at the surface will start dominating at distances from the star fixed by the stars luminosity (see Fig. 9). MIRI will have a major role to expand our knowledge concerning the lower-mass stars disks. The intermediate-mass stars have a pure thermal emission that dominates up to more than $\sim 2''$ from the star at 10 μm ($r \gg 2$ at 20 μm, respectively). The lower-mass T Tauri stars have a scattered light emission that starts to dominate above a distance of $\sim 0.2''$ at a wavelength of 10 μm ($\sim 1.2''$ at 20 μm, respectively). Finally, MIRI observations of disks around brown dwarves (BD) will be dominated by the scattered light emission at any distance/wavelength. However, if the extended disk emission should be easily detectable in relatively short integrations times ($t \sim 1$ h) in the cases of Herbig and T Tauri stars, brown dwarf disks extended emission will require fairly long integration times ($\sim$3 h at the most favorable wavelength of 23 μm; see Fig. 9). Albeit so that a fairly large observing time will be needed in the latter case, it will be worth spending it as JWST/MIRI will be the unique facility able to detect and resolve BDs disks emission at these wavelengths in the next decade. Observing a mixture of star and inner rim scattered light, the NIRCAM imager will typically achieve in coronagraphic mode at 2.5 μm a 230/70 μJy/arcsec^2 ($\sim$16.2/17.5 arcsec^{-2}) surface brightness magnitude sensitivity, respectively, at distances of 0.3 and $0.5''$ from a 10th magnitude star ($0.3''$ corresponds to the IWA ($4\,\lambda/D$) of the NIRCAM wedge coronagraphic mode at a median wavelength of 2.5 μm). These detection limits will allow one to easily detect and resolve protoplanetary disks around Herbig and T Tauri type stars in the closest star-forming regions. However, in the case of disks around brown dwarves it will remain extremely difficult. Nonetheless, there is some hope that in the most favorable cases (closest and brightest ones e.g. around TW Hya) they should be resolved at a level of few spatial resolution elements; given the very red color of the disks, the multi-color PSF subtraction should be particularly interesting to apply in this case. The resolved images of the disks will be used to derive several physical parameters. The first and most immediate ones are the physical size (outer radius, or a least an lower limit on it), the disk inclination and position angle by measuring them directly on the images. Using a slightly more evolved analysis of the isophots centering w.r.t. the star position, one can also derive the disks thickness and their flaring angle as a function of the distance to the star (Lagage et al. 2006).

The inner zones of disks ($a \leq 10$ AU) have a surprisingly rich chemistry, as revealed in recent years by mid-IR spectroscopy (Lahuis et al. 2006; Carr and Najita 2008; Salyk et al. 2008). Features from H_2O, OH, HCN, C_2H_2 and CO_2 have been detected, implying abundances that are orders of magnitude higher than in the outer disk or in protostellar clouds which indicates an active high-temperature chemistry. There is evidence for differences in the observed spectra between disks around Herbig Ae, T Tauri stars and brown dwarves as well as among disks around T Tauri stars themselves which can be partly understood in terms of stellar irradiation. A complete inventory of their content in ingredients (e.g. NH_3, CH_4, C_6H_6, HCO^+ or HCN) to form prebiotic molecules will be established in *a large number of targets* by the MIRI instrument. At shorter wavelengths, the NIRSpec instrument will observe the forests of rovibrational ^{12}CO, ^{13}CO and C^{18}O line emission allowing one to establish accurate excitation diagrams and determine with precision the vibrational temperature(s). Finally, even with the moderate resolution of NIRSPEC and MIRI resolved observations spectrally (e.g. by spectro-astrometry technique; Pontoppidan et al. 2008) will be also a source of valuable information.

Based on numerical simulations of the dynamical evolution of the disk structure, one expects that massive planets embedded into disks strongly modify their appearance, sculpting and structuring them: inner voids, gaps, walls, asymmetries (Nelson et al. 2000; Edgar and Quillen 2008, see also Sect. 3.1.2). There are more and more indirect convincing indications e.g. from the modeling of the SED, from velocity-resolved observations of the gas phase (Acke et al. 2005), or interferometric measurements (Fedele et al. 2008) that many protoplanetary disks are structured. Some disks display inner depleted regions (the so-called transitional disks, see e.g. Brown et al. 2009; Sicilia-Aguilar et al. 2009; Muzerolle et al. 2010). Some others have or are believed to feature intermediate large walls (as opposed to the inner rims at the dust sublimation radius, typically a fraction of an AU) at the limit between an inner and an outer massive, optically thick disk (Bouwman et al. 2003; Thalmann et al. 2010; Verhoeff et al. 2011). Finally, dynamical simulations show that giant planets embedded in disks would not only carve a gap but also launch large-scale spiral waves (Edgar and Quillen 2008). Since the density waves induce a local heating of the disk they produce in turn thermal emission features that can be best detected in the mid-IR range. The JWST instruments do not in general have the required angular resolution to directly image these gaps, walls, and spiral structures. However, given their extreme sensitivity and stability it will be possible to obtain indirect indications of the presence of e.g. a spiral structure or a wall at projected distances larger than $\sim 0.2''$ by searching for surface brightness asymmetries in the disk.

5.2.2 Debris disks

Due to the complexity and aberrations in the JWST PSF, the ultimate contrast achieved with the NIRCam coronagraph is expected to be about 10 times worse than that achieved by the coronagraphs on the Hubble Space Telescope (for instance the ACS coronagraph). Therefore, the JWST is not meant to search for and resolve previously unseen debris disks in scattered light, as most of the candidate targets have already been observed with the Hubble Space Telescope at better contrast levels. In non-thermal emission imaging, JWST's primary contribution will be the characterization of known debris disks at previously unobtainable wavelengths (2.5–5 μm). This characterization shall probably mainly be focused on the sizes/shapes/composition of the dust grains and the study of structures in the surface density produced by giant planets. On the other hand, the MIRI instrument will map the debris disks in the thermal (and possibility scattering far away from the star) IR regime with an angular resolution and sensitivity by far better than anything that will have been achieved before. MIRI will be for instance able to map at 23 μm with an angular resolution ($\sim 0.9''$) 7 times better than *Spitzer* the VEGA archetype, a disk which is currently unobservable from the ground given its low surface brightness. This disk appears featureless at modest spatial resolutions ($\sim 7''$; Su et al. 2005; Sibthorpe et al. 2010). This will offer the possibility to search for planet footprints at an $\sim$7 AU spatial scale in the disk.

5.2.3 Exoplanets studies

One of the major science cases for the JWST is that of the exoplanet studies. The JWST is particularly well adapted for this task because of an extreme sensitivity, a very stable point spread function, and covers the IR 1–28 μm wavelength range where numerous molecular emission features are found. Besides, observations are generally easier in the IR range where the thermal emission of the planet dominates, because of a reduced star-planet contrast (10^5–10^7 in the case of giant planets) in comparison with the visible range (10^9–10^{11}).

Given the very high contrast to deal with in the IR range, direct imaging observations of exoplanets with the JWST will require the use of coronagraphic modes to efficiently reject the starlight. Multi-wavelength/multi-epoch observations using the different instrument will have to be combined to unambiguously confirm the planetary nature of the sources discovered. However, even though the JWST segmented-mirror producing considerable additional diffraction structures is not primarily designed to conduct coronagraphic observations, the very high stability of its point spread function combined with superb sensitivity performances at wavelengths where the thermal emission of giant exoplanets emerges make the JWST a very good competitor to specifically designed instruments on ground-based larger telescopes. This stability can be efficiently exploited to achieve better rejection performances through multi-wavelength observations using e.g. the TFI coronagraphic mode. As a general rule, the niche for JWST imaging programs lies in searching and characterizing giant planets on fairly large orbits around faint late-type stars (M and later). One of the major scientific goals will be to disentangle hot-start (Baraffe et al. 2003) and core-accretion proposed models (Fortney et al. 2008b) for giant planets formation. Simulated performances of the NIRCAM coronagraphic mode show that old (1 Gyr and more), narrow orbit ($a \geq 5$ AU), self-luminous giant exoplanets detection/characterization will best be conducted at 4.5–5 μm around close-by late-type (M and brown dwarves) stars (Green et al. 2005). Self-luminous giant planets of age younger than 100 Myr will be observable at orbital radii larger than 25 AU around a few hundred young stars within 25–150 pc. Using Monte-Carlo simulations, Beichman et al. (2010) have computed the success rate in terms of detectability for two representative samples: around nearby (age $\leq$100 Myr, 25–140 pc) young stars and around nearby M stars (ages between several Myr and 5 Gyr, $d \leq 15$ pc). Concerning telluric planets, although typical super-Earth exoplanets should not be detectable by the JWST because their emission is weak and they are probably found at narrower angular separations from the star, two "non-classical" cases appear to be favorable for direct imaging detection. First, the presence of a dusty circumplanetary ring should boost the mid-IR flux by an order of magnitude around late-type stars. A second interesting case deals with high-temperature telluric planets after a major catastrophic impact event. Depending on the presence (or not) or a residual atmosphere, the cooling time shall be long enough (several Myr) for such exoplanets to be observed by direct imaging around 3.8 μm (Miller-Ricci et al. 2009). Finally, one should also mention the possibility provided by MIRI and NIRSpec IFUs spectrometers to perform spectral deconvolution (Thatte et al. 2007), a starlight rejection technique which is complementary to coronagraphic imaging.

While direct imaging of exoplanets will deal with large separation objects ($d \gtrsim 1''$), a very larger amount of information will come from the study of transiting objects. Transit spectroscopy of these objects on relatively narrow orbits by essence, will provide a unique set of information to characterize them. The main advantages of JWST observations over ground-based ones lie in the stability (no variable atmospheric absorption) and access to longer wavelengths where molecular signatures are numerous. Typical relative precisions achievable from the ground are of the order of 0.1 % and are limited by systematic errors due to the atmosphere. In the case of space-born observatories, systematic errors also exist and limit the relative precision achievable to a few 10^{-4}, so well above the photon noise limit still. When *Spitzer*/IRS or *Spitzer*/IRAC observations of exoplanets were limited to bright objects and low-resolution spectra, JWST observations of fainter targets or at higher spectral resolution should be possible. All things remaining equal, a crude estimate based on the ratio of telescope apertures (6.5 m vs. 90 cm) shows that high-resolution (R = 3500) spectroscopic observations will be possible on targets for which *Spitzer* was limited to photometric or low-resolution spectroscopic observations. Two JWST instruments include slitless spectroscopic modes (grisms mode in NIRCAM, low-resolution spectroscopy in MIRI imager). While shorter wavelengths (1–5 μm) are best suited for primary eclipse observations, longer wavelengths are more adequate to determine the effective temperature of exoplanets by means of secondary transit or detect phase modulation signals in the case of tidally locked out-of-plane exoplanets. Also even though emission spectra produce potentially larger signals than transmission spectra, features in transmission spectra will always be present whatever is the structure of the exoplanet atmosphere. As opposed to that, isothermal atmospheric profiles would produce featureless emission spectra. Depending on the size of the planet, its distance to the star, and the star brightness, NIRSpec and NIRCam can be used to obtain spectra (narrow band photometric measurements) in a spectral range where signatures of H_2, H_2O, CH_4, CO and CO_2 are present. MIRI imager and spectrometer will probe slightly cooler objects in a wavelength range where NH_3, CO_2, H_2O, CH_4, and O_3 signatures are present. Simulated observations by the JWST show that a significant SNR of 3 is achievable on a single primary transit observation with NIRSpec ($\lambda = 3$ μm, R = 100) of a Jupiter-sized planet. The same detection limit is reached at 3 μm on Neptune-sized planets up to a distance of 10 pc (Belu et al. 2011). Around 10 μm, MIRI low-resolution spectrometer (R = 100) achieves a 3-σ detection limit on Neptune-sized exoplanets ($d = 10$ pc) by combining few transits. In the case of telluric planets, by combining 20 transit observations with NIRSpec, a 10^{-5} relative precision is achieved at a spectral resolution of R $\sim$ 100 which allows the characterization of the atmosphere of a hydrogen rich super-Earth exoplanet (Clampin 2009). CO_2 4.3 μm (15 μm, respectively) signatures of super-Earths at 10 pc are detectable by NIRSpec (MIRI resp.) if *all* its primary transits ($\sim$50) are combined over the JWST lifetime. In this case, planets in the habitable zone are found around stars with spectral types later than M2. Maybe more interesting, the ozone feature at 9.6 μm of a super-Earth planet around a M4V (or later type) star 6.7 pc away is detectable again by summing the signals of all the transit events (Belu et al. 2011). However, the expected number of planets in such a favorable configuration is only on the order of 1 when considering all the M stars of the solar neighborhood. Finally, the TFI mode of the FGS allows one also to obtain spectro-imaging (1.5–5 μm, R = 100) data; its (NRM) sub-λ/D imaging capability and its relatively simple coronagraphic mode could provide in some cases very useful complementary data to the instruments already cited.

6 Concluding remarks

The major limitation of the current studies of the planet formation process is the insufficient spatial resolution of existing imaging telescopes, at optical to millimeter wavelength range. High-resolution imaging as it will be possible with the next generation of multi-baseline interferometers is therefore of essential importance for planet formation and evolution studies. The ability to investigate the inner regions of protoplanetary and debris disks in unprecedented detail will provide insight into planetary systems at various stages of their evolution. Questions about disk evolution and planet formation belong to the key science cases for the presented interferometers which are therefore designed also to meet the requirements in sensitivity and accuracy.

The presented tasks for the next generation of long-baseline optical to infrared interferometers and exemplary case studies are by no means comprehensive, but illustrate the potential of these type of astronomical observations. Moreover, as pointed out, the combination of individual interferometers with those operating at other wavelengths and single telescopes which provide significant higher sensitivity and field-of-view is essential to connect small and large scales and to trace the complex interplay of different physical processes in protoplanetary disks. From this point of view, currently existing and planned large ground-based telescopes and (sub)millimeter interferometers in combination with space observatories provide the perfect frame for the next-generation long-baseline optical to infrared interferometers.

Acknowledgements The work on this article was initiated during the workshop "Circumstellar disks and planets—Science cases for the second generation VLTI instrumentation" (University of Kiel, 2010), funded through the "Optical Interferometry Networking Activity" (European Community's Seventh Framework Programme under Grant Agreement 226604). RDA acknowledges support from the Science & Technology Facilities Council (STFC) through an Advanced Fellowship (ST/G00711X/1). C.M. acknowledges the valuable discussions with H. Klahr, Y. Alibert, W. Benz, Ch. Ormel, K.-M. Dittkrist, and A. Reufer during the preparation of Sect. 2.2. C.M. acknowledges financial support by the Swiss National Science Foundation and the financial support as a fellow of the Alexander von Humboldt Foundation. The realization of the KI-ASTRA upgrade is supported by the NSF MRI grant, AST-0619965. The W.M. Keck Observatory is operated as a scientific partnership among the California Institute of Technology, the University of California and the National Aeronautics and Space Administration. The Observatory was made possible by the generous financial support of the W.M. Keck Foundation. The authors wish to recognize and acknowledge the very significant cultural role and reverence that the summit of Mauna Kea has always had within the indigenous Hawaiian community. The KI is funded by the National Aeronautics and Space Administration as part of its Exoplanet Exploration program Funded by NASA, the KI is developed and operated by JPL,[23] NExScI[24] and the W.M. Keck Observatory (WMKO).[25] ASTRA is funded by the National Science Foundation (NSF) Major Research Instrumentation (MRI) program.[26] Besides the NSF engagement, a number of science institutes contribute to the ASTRA collaboration to advance and profit from large-aperture OLBI (UC Berkeley, UCLA, Caltech, NExScI, JPL, University of Arizona). The design and deployment of the MROI facility is being directed from a Project Office at the New Mexico Institute of Mining and Technology. The MROI main collaborator on the project is the former COAST interferometer group at the Cavendish Laboratory, University of Cambridge, UK. S.W. acknowledges the tremendous work done by the MATISSE Science Group (Phase A); selected parts of this article are based

[23] Jet Propulsion Laboratory; http://planetquest.jpl.nasa.gov/Keck/keck_index.cfm.

[24] NASA Exoplanet Science Institute; http://nexsci.caltech.edu.

[25] http://keckobservatory.org.

[26] Wizinowich, P., Graham, J., Woillez, J., et al. NSF-MRI Award Abstract #0619965.

on the "MATISSE, Sciences Cases" (Doc. No. VLT-TRE-MAT-15860-432, Wolf et al., 2007). We wish to thank W. Brandner, T. Herbst, F. Ménard, and K. Stapelfeldt for fruitful discussions during the preparation of this article.

References

Absil O, Mawet D (2010) Formation and evolution of planetary systems: the impact of high-angular resolution optical techniques. Astron Astrophys Rev 18:317–382. doi:10.1007/s00159-009-0028-y. arXiv:0912.3915

Absil O, Le Bouquin J-B, Lebreton J, Augereau J-C, Benisty M, Chauvin G, Hanot C, Mérand A, Montagnier G (2010) Deep near-infrared interferometric search for low-mass companions around β Pictoris. Astron Astrophys 520:L2. doi:10.1051/0004-6361/201015156. arXiv:1009.1245. URL: http://adsabs.harvard.edu/abs/2010A%26A...520L...2A. Provided by the SAO/NASA Astrophysics Data System

Absil O, Le Bouquin JB, Berger JP, Lagrange AM, Chauvin G, Lazareff B, Zins G, Haguenauer P, Jocou L, Kern P, Millan-Gabet R, Rochat S, Traub W (2011) Searching for faint companions with VLTI/PIONIER. I. Method and first results. Astron Astrophys 535:A68. doi:10.1051/0004-6361/201117719. arXiv:1110.1178. http://adsabs.harvard.edu/abs/2011A%26A...535A..68A. Provided by the SAO/NASA Astrophysics Data System

Acke B, van den Ancker ME, Dullemond CP (2005) [O I] 6300 Å emission in Herbig Ae/Be systems: signature of Keplerian rotation. Astron Astrophys 436:209–230. doi:10.1051/0004-6361:20042484. arXiv:astro-ph/0502504

Akeson RL, Boden AF, Monnier JD, Millan-Gabet R, Beichman C, Beletic J, Calvet N, Hartmann L, Hillenbrand L, Koresko C, Sargent A, Tannirkulam A (2005) Keck interferometer observations of classical and weak-line T Tauri stars. Astrophys J 635:1173–1181. doi:10.1086/497436

Alencar SHP, Teixeira PS, Guimarães MM, McGinnis PT, Gameiro JF, Bouvier J, Aigrain S, Flaccomio E, Favata F (2010) Accretion dynamics and disk evolution in NGC 2264: a study based on CoRoT photometric observations. Astron Astrophys 519:A88. doi:10.1051/0004-6361/201014184. arXiv:1005.4384

Alexander R (2008a) From discs to planetesimals: evolution of gas and dust discs. New Astron Rev 52:60–77. doi:10.1016/j.newar.2008.04.004. arXiv:0712.0388

Alexander RD (2008b) [NeII] emission-line profiles from photoevaporative disc winds. Mon Not R Astron Soc 391:L64–L68. doi:10.1111/j.1745-3933.2008.00556.x. arXiv:0809.0316

Alexander RD, Armitage PJ (2009) Giant planet migration, disk evolution, and the origin of transitional disks. Astrophys J 704:989–1001. doi:10.1088/0004-637X/704/2/989. arXiv:0909.0004

Alexander RD, Clarke CJ, Pringle JE (2004) On the origin of ionizing photons emitted by T Tauri stars. Mon Not R Astron Soc 348:879–884. doi:10.1111/j.1365-2966.2004.07401.x. arXiv:astro-ph/0311276

Alexander RD, Clarke CJ, Pringle JE (2005) Constraints on the ionizing flux emitted by T Tauri stars. Mon Not R Astron Soc 358:283–290. doi:10.1111/j.1365-2966.2005.08786.x. arXiv:astro-ph/0501100

Alexander RD, Clarke CJ, Pringle JE (2006a) Photoevaporation of protoplanetary DISCS—I. Hydrodynamic models. Mon Not R Astron Soc 369:216–228. doi:10.1111/j.1365-2966.2006.10293.x. arXiv:astro-ph/0603253

Alexander RD, Clarke CJ, Pringle JE (2006b) Photoevaporation of protoplanetary discs—II. Evolutionary models and observable properties. Mon Not R Astron Soc 369:229–239. doi:10.1111/j.1365-2966.2006.10294.x. arXiv:astro-ph/0603254

Alibert Y, Mordasini C, Benz W (2004) Migration and giant planet formation. Astron Astrophys 417:L25

Alibert Y, Mordasini C, Benz W, Winisdoerffer C (2005a) Models of giant planet formation with migration and disc evolution. Astron Astrophys 434:343

Alibert Y, Mousis O, Mordasini C, Benz W (2005b) New Jupiter and Saturn formation models meet observations. Astrophys J 626:L57

Alibert Y, Mordasini C, Benz W (2011) Extrasolar planet population synthesis III. Formation of planets around stars of different masses. Astron Astrophys 526:A63. doi:10.1051/0004-6361/201014760. arXiv:1101.0513. URL: http://adsabs.harvard.edu/abs/2011A%26A...526A..63A. Provided by the SAO/NASA Astrophysics Data System

Andrews SM, Williams JP (2005) Circumstellar dust disks in Taurus-Auriga: the submillimeter perspective. Astrophys J 631:1134–1160. doi:10.1086/432712. arXiv:astro-ph/0506187

Andrews SM, Williams JP (2007) High-resolution submillimeter constraints on circumstellar disk structure. Astrophys J 659:705–728. doi:10.1086/511741. arXiv:astro-ph/0610813

Andrews SM, Wilner DJ, Hughes AM, Qi C, Dullemond CP (2009) Protoplanetary disk structures in Ophiuchus. Astrophys J 700:1502–1523. doi:10.1088/0004-637X/700/2/1502. arXiv:0906.0730

Andrews SM, Wilner DJ, Hughes AM, Qi C, Dullemond CP (2010) Protoplanetary disk structures in Ophiuchus. II. Extension to fainter sources. Astrophys J 723:1241–1254. doi:10.1088/0004-637X/723/2/1241. arXiv:1007.5070

Araya E, Hofner P, Sewiło M, Goss WM, Linz H, Kurtz S, Olmi L, Churchwell E, Rodríguez LF, Garay G (2007) An H_2CO 6 cm maser pinpointing a possible circumstellar torus in IRAS 18566+0408. Astrophys J 669:1050–1057. doi:10.1086/521576. arXiv:0708.3832

Armitage PJ (2007) Lecture notes on the formation and early evolution of planetary systems. arXiv:astro-ph/0701485

Armitage PJ (2010) Astrophysics of planet formation. Cambridge University Press, Cambridge

Armitage PJ, Livio M, Pringle JE (2001) Episodic accretion in magnetically layered protoplanetary discs. Mon Not R Astron Soc 324:705–711. doi:10.1046/j.1365-8711.2001.04356.x. arXiv:astro-ph/0101253

Bacciotti F, Testi L, Marconi A, Garcia PJV, Ray TP, Eislöffel J, Dougados C (2003) Unveiling the launching region of YSO jets with AMBER. Astrophys Space Sci 286:157–162. doi:10.1023/A:1026151304959

Baines EK, McAlister HA, ten Brummelaar TA, Sturmann J, Sturmann L, Turner NH, Ridgway ST (2009) Eleven exoplanet host star angular diameters from the Chara array. Astrophys J 701:154–162. doi:10.1088/0004-637X/701/1/154. arXiv:0906.2702

Balbus SA (2009) Magnetohydrodynamics of protostellar disks. In: Garcia P (ed) Physical processes in circumstellar disks around young stars. arXiv:0906.0854

Balbus SA, Hawley JF (1991) A powerful local shear instability in weakly magnetized disks. I—Linear analysis. II—Nonlinear evolution. Astrophys J 376:214–233. doi:10.1086/170270

Balbus SA, Hawley JF (1998) Instability, turbulence, and enhanced transport in accretion disks. Rev Mod Phys 70:1–53

Banzatti A, Testi L, Isella A, Natta A, Neri R, Wilner DJ (2011) New constraints on dust grain size and distribution in CQ Tauri. Astron Astrophys 525:A12. doi:10.1051/0004-6361/201015206. arXiv:1009.2697

Baraffe I, Chabrier G, Barman TS, Allard F, Hauschildt PH (2003) Evolutionary models for cool brown dwarfs and extrasolar giant planets. The case of HD 209458. Astron Astrophys 402:701–712. doi:10.1051/0004-6361:20030252. arXiv:astro-ph/0302293

Baron F, Young JS (2008) Image reconstruction at Cambridge University. In: Society of photo-optical instrumentation engineers (SPIE) conference series, vol 7013. doi:10.1117/12.789115

Batygin K, Stevenson DJ (2010) Inflating Hot Jupiters with ohmic dissipation. Astrophys J 714:L238–L243. doi:10.1088/2041-8205/714/2/L238. arXiv:1002.3650

Baudoz P, Boccaletti A, Riaud P, Cavarroc C, Baudrand J, Reess JM, Rouan D (2006) Feasibility of the four-quadrant phase mask in the mid-infrared on the James Webb space telescope. Publ Astron Soc Pac 118:765–773. doi:10.1086/503124

Beckwith SVW, Sargent AI (1991) Particle emissivity in circumstellar disks. Astrophys J 381:250–258. doi:10.1086/170646

Beckwith SVW, Sargent AI, Chini RS, Guesten R (1990) A survey for circumstellar disks around young stellar objects. Astron J 99:924–945. doi:10.1086/115385

Begelman MC, McKee CF, Shields GA (1983) Compton heated winds and coronae above accretion disks. I. Dynamics. Astrophys J 271:70–88. doi:10.1086/161178

Beichman CA, Krist J, Trauger JT, Greene T, Oppenheimer B, Sivaramakrishnan A, Doyon R, Boccaletti A, Barman TS, Rieke M (2010) Imaging young giant planets from ground and space. Publ Astron Soc Pac 122:162–200 doi:10.1086/651057. arXiv:1001.0351

Belu AR, Selsis F, Morales JC, Ribas I, Cossou C, Rauer H (2011) Primary and secondary eclipse spectroscopy with JWST: exploring the exoplanet parameter space. Astron Astrophys 525:A83. doi:10.1051/0004-6361/201014995. arXiv:1008.0028

Benisty M, Natta A, Isella A, Berger J, Massi F, Le Bouquin J, Mérand A, Duvert G, Kraus S, Malbet F, Olofsson J, Robbe-Dubois S, Testi L, Vannier M, Weigelt G (2010) Strong near-infrared emission in the sub-AU disk of the Herbig Ae star HD 163296: evidence of refractory dust? Astron Astrophys 511:A74. doi:10.1051/0004-6361/200912898. arXiv:0911.4363

Beuther H, Schilke P, Menten KM, Motte F, Sridharan TK, Wyrowski F (2002) High-mass protostellar candidates. II. Density structure from dust continuum and CS emission. Astrophys J 566:945–965. doi:10.1086/338334. arXiv:astro-ph/0110370

Birnstiel T, Ricci L, Trotta F, Dullemond CP, Natta A, Testi L, Dominik C, Henning T, Ormel CW, Zsom A (2010) Testing the theory of grain growth and fragmentation by millimeter observations of protoplanetary disks. Astron Astrophys 516:L14. doi:10.1051/0004-6361/201014893. arXiv:1006.0940

Boccaletti A, Augereau JC, Marchis F, Hahn J (2003) Ground-based near-infrared imaging of the HD 141569 circumstellar disk. Astrophys J 585:494–501. doi:10.1086/346019. arXiv:astro-ph/0211648

Bodenheimer P, Pollack JB (1986) Calculations of the accretion and evolution of giant planets: the effects of solid cores. Icarus 67:391

Bodenheimer P, Hubickyj O, Lissauer JJ (2000) Models of the in situ formation of detected extrasolar giant planets. Icarus 143:2

Boley AC (2009) The two modes of gas giant planet formation. Astrophys J Lett 695:L53

Boss AP (2007) Testing disk instability models for giant planet formation. Astrophys J 661:L73–L76

Bouvier J, Alencar SHP, Boutelier T, Dougados C, Balog Z, Grankin K, Hodgkin ST, Ibrahimov MA, Kun M, Magakian TY, Pinte C (2007) Magnetospheric accretion-ejection processes in the classical T Tauri star AA Tauri. Astron Astrophys 463:1017–1028. doi:10.1051/0004-6361:20066021. arXiv:astro-ph/0611787

Bouwman J, de Koter A, Dominik C, Waters LBFM (2003) The origin of crystalline silicates in the Herbig Be star HD 100546 and in comet Hale-Bopp. Astron Astrophys 401:577–592. doi:10.1051/0004-6361:20030043. arXiv:astro-ph/0301254

Bowler BP, Liu MC, Dupuy TJ, Cushing MC (2010) Near-infrared Spectroscopy of the extrasolar planet HR 8799 b. Astrophys J 723:850–868. doi:10.1088/0004-637X/723/1/850. arXiv:1008.4582

Brauer F, Dullemond CP, Henning T (2008a) Coagulation, fragmentation and radial motion of solid particles in protoplanetary disks. Astron Astrophys 480:859–877

Brauer F, Henning T, Dullemond CP (2008b) Planetesimal formation near the snow line in MRI-driven turbulent protoplanetary disks. Astron Astrophys 487:L1–L4. doi:10.1051/0004-6361:200809780. arXiv:0806.1646

Brown JM, Blake GA, Qi C, Dullemond CP, Wilner DJ, Williams JP (2009) Evidence for dust clearing through resolved submillimeter imaging. Astrophys J 704:496–502. doi:10.1088/0004-637X/704/1/496. arXiv:0909.5595

Buenzli E, Thalmann C, Vigan A, Boccaletti A, Chauvin G, Augereau JC, Meyer MR, Ménard F, Desidera S, Messina S, Henning T, Carson J, Montagnier G, Beuzit JL, Bonavita M, Eggenberger A, Lagrange AM, Mesa D, Mouillet D, Quanz SP (2010) Dissecting the Moth: discovery of an off-centered ring in the HD 61005 debris disk with high-resolution imaging. Astron Astrophys 524:L1. doi:10.1051/0004-6361/201015799. arXiv:1011.2496

Burrows CJ, Stapelfeldt KR, Watson AM, Krist JE, Ballester GE, Clarke JT, Crisp D, Gallagher JS III, Griffiths RE, Hester JJ, Hoessel JG, Holtzman JA, Mould JR, Scowen PA, Trauger JT, Westphal JA (1996) Hubble space telescope observations of the disk and jet of HH 30. Astrophys J 473:437. doi:10.1086/178156

Cai K, Pickett MK, Durisen RH, Milne AM (2010) Giant planet formation by disk instability: a comparison simulation with an improved radiative scheme. Astrophys J 716:L176–L180

Carr JS, Najita JR (2008) Organic molecules and water in the planet formation region of young circumstellar disks. Science 319:1504. doi:10.1126/science.1153807

Casse F, Ferreira J (2000) Magnetized accretion-ejection structures. IV. Magnetically-driven jets from resistive, viscous, Keplerian discs. Astron Astrophys 353:1115–1128

Cesaroni R (2008) High-mass star forming regions: an ALMA view. Astrophys Space Sci 313:23–28. doi:10.1007/s10509-007-9596-3

Cesaroni R, Neri R, Olmi L, Testi L, Walmsley CM, Hofner P (2005) A study of the Keplerian accretion disk and precessing outflow in the massive protostar IRAS 20126+4104. Astron Astrophys 434:1039–1054. doi:10.1051/0004-6361:20041639

Chiang E, Murray-Clay R (2007) Inside-out evacuation of transitional protoplanetary discs by the magneto-rotational instability. Nat Phys 3:604–608. doi:10.1038/nphys661. arXiv:0706.1241

Chiang EI, Joung MK, Creech-Eakman MJ, Qi C, Kessler JE, Blake GA, van Dishoeck EF (2001) Spectral energy distributions of passive T Tauri and Herbig Ae disks: grain mineralogy, parameter dependences, and comparison with infrared space observatory LWS observations. Astrophys J 547:1077–1089. doi:10.1086/318427. arXiv:astro-ph/0009428

Chin JCY, Stalcup T, Wizinowich P, Panteleev S, Neyman C, Tsubota K, Summers D, Stomski P, Medeiros D, Nance C, Grace K, Cooper A, Wetherell E, Doyle S (2010) Keck I laser guide star AO system integration. In: Society of photo-optical instrumentation engineers (SPIE) conference series, vol 7736. doi:10.1117/12.857598

Churchwell E, Babler BL, Meade MR, Whitney BA, Benjamin R, Indebetouw R, Cyganowski C, Robitaille TP, Povich M, Watson C, Bracker S (2009) The Spitzer/GLIMPSE surveys: a new view of the Milky Way. Publ Astron Soc Pac 121:213–230. doi:10.1086/597811

Cieza LA, Swift JJ, Mathews GS, Williams JP (2008) The masses of transition circumstellar disks: observational support for photoevaporation models. Astrophys J 686:L115–L118. doi:10.1086/592965. arXiv:0809.0030

Clampin M (2009) Comparative planetology: transiting exoplanet science with JWST. In: astro2010: the astronomy and astrophysics decadal survey. Astronomy, vol 2010, p 46

Clampin M, Krist JE, Ardila DR, Golimowski DA, Hartig GF, Ford HC, Illingworth GD, Bartko F, Benítez N, Blakeslee JP, Bouwens RJ, Broadhurst TJ, Brown RA, Burrows CJ, Cheng ES, Cross NJG, Feldman PD, Franx M, Gronwall C, Infante L, Kimble RA, Lesser MP, Martel AR, Menanteau F, Meurer GR, Miley GK, Postman M, Rosati P, Sirianni M, Sparks WB, Tran HD, Tsvetanov ZI, White RL, Zheng W (2003) Hubble space telescope ACS coronagraphic imaging of the circumstellar disk around HD 141569A. Astron J 126:385–392. doi:10.1086/375460. arXiv:astro-ph/0303605

Clarke CJ (2009) Pseudo-viscous modelling of self-gravitating discs and the formation of low mass ratio binaries. Mon Not R Astron Soc 396:1066–1074. doi:10.1111/j.1365-2966.2009.14774.x. arXiv:0904.3549

Clarke CJ, Gendrin A, Sotomayor M (2001) The dispersal of circumstellar discs: the role of the ultraviolet switch. Mon Not R Astron Soc 328:485–491. doi:10.1046/j.1365-8711.2001.04891.x

Colavita MM, Wallace JK, Hines BE, Gursel Y, Malbet F, Palmer DL, Pan XP, Shao M, Yu JW, Boden AF, Dumont PJ, Gubler J, Koresko CD, Kulkarni SR, Lane BF, Mobley DW, van Belle GT (1999) The Palomar testbed interferometer. Astrophys J 510:505–521. doi:10.1086/306579. arXiv:astro-ph/9810262

Colavita MM, Serabyn E, Booth AJ, Crawford SL, Garcia-Gathright JI, Ligon ER, Mennesson BL, Paine CG, Wizinowich PL, Ragland S, Appleby EC, Berkey BC, Cooper A, Dahl W, Gathright JT, Hrynevych MA, Medeiros DW, Morrison D, Panteleeva T, Smith B, Summers KR, Tsubota K, Tyau C, Wetherell E, Woillez JM, Akeson RL, Millan-Gabet R, Felizardo C, Koresko CD, Herstein JS (2008) Keck interferometer nuller update. In: Society of photo-optical instrumentation engineers (SPIE) conference series, vol 7013. doi:10.1117/12.789476

Cossins P, Lodato G, Testi L (2010) Resolved images of self-gravitating circumstellar discs with ALMA. Mon Not R Astron Soc 407:181–188. doi:10.1111/j.1365-2966.2010.16934.x. arXiv:1004.5389

Cowan NB, Agol E (2011) The statistics of albedo and heat recirculation on hot exoplanets. Astrophys J 729:54. doi:10.1088/0004-637X/729/1/54. arXiv:1001.0012

Creech-Eakman MJ, Romero V, Westpfahl D, Cormier C, Haniff C, Buscher D, Bakker E, Berger L, Block E, Coleman T, Festler P, Jurgenson C, King R, Klinglesmith D, McCord K, Olivares A, Parameswariah C, Payne I, Paz T, Ryan E, Salcido C, Santoro F, Selina R, Shtromberg A, Steenson J, Baron F, Boysen R, Coyne J, Fisher M, Seneta E, Sun X, Thureau N, Wilson D, Young J (2008) Magdalena Ridge Observatory Interferometer: progress toward first light. In: Society of photo-optical instrumentation engineers (SPIE) conference series, vol 7013. doi:10.1117/12.789859

Creech-Eakman M, Young J, Haniff C, Buscher D, Elvis M, Chiavassa A, Schartmann M (2010a) Imaging simulations of selected science with the Magdalena ridge observatory interferometer. In: Society of photo-optical instrumentation engineers (SPIE) conference series, vol 7734. doi:10.1117/12.858359

Creech-Eakman MJ, Romero V, Payne I, Haniff C, Buscher D, Aitken C, Anderson C, Bakker E, Coleman T, Dahl C, Farris A, Jiminez S, Jurgenson C, King R, Klinglesmith D III, McCord K, McCracken T, Nyland K, Olivares A, Richmond M, Romero M, Salcido C, Sandoval J, Santoro F, Seamons J, Selina R, Shtromberg A, Steenson J, Torres N, Westpfahl D, Baron F, Fisher M, Seneta E, Sun X, Wilson D, Young J (2010b) Magdalena ridge observatory interferometer: advancing to first light and new science. In: Society of photo-optical instrumentation engineers (SPIE) conference series, vol 7734. doi:10.1117/12.857359

Crida A, Morbidelli A (2007) Cavity opening by a giant planet in a protoplanetary disc and effects on planetary migration. Mon Not R Astron Soc 377:1324–1336

Cuzzi JN, Hogan RC, Shariff K (2008) Toward planetesimals: dense chondrule clumps in the protoplanetary nebula. Astrophys J 687:1432–1447

Cyganowski CJ Brogan CL, Hunter TR, Churchwell E, Zhang Q (2011) Bipolar molecular outflows and hot cores in glimpse extended green objects (EGOs). Astrophys J 729:124. doi:10.1088/0004-637X/729/2/124. arXiv:1012.0851

D'Alessio P, Calvet N, Hartmann L, Muzerolle J, Sitko M (2004) Models of accretion disks around young stars. In: Burton MG, Jayawardhana R, Bourke TL (eds) Star formation at high angular resolution. IAU Symposium, vol 221, p 403. arXiv:astro-ph/0309590

D'Angelo G, Durisen RH, Lissauer JJ (2010) Giant planet formation. arXiv:1006.5486

Dartois E, Dutrey A, Guilloteau S (2003) Structure of the DM Tau Outer disk: probing the vertical kinetic temperature gradient. Astron Astrophys 399:773–787. doi:10.1051/0004-6361:20021638

Delplancke F (2008) The PRIMA facility phase-referenced imaging and micro-arcsecond astrometry. New Astron Rev 52:199–207. doi:10.1016/j.newar.2008.04.016

Dougados C (2009) Magnetic jets from young stars: high-angular resolution observations. In: Heydari-Malayeri M, Reyl'E C, Samadi R (eds) SF2A-2009: proceedings of the annual meeting of the French society of astronomy and astrophysics, p 3

Dougados C, Bouvier J, Duvert G, Garcia PJV, Folha DFM (2003) Probing the magnetosphere in young stars with AMBER/VLTI. Astrophys Space Sci 286:151–156. doi:10.1023/A:1026147204051

Doyon R, Rowlands N, Hutchings J, Evans CE, Greenberg E, Scott AD, Touhari D, Beaulieu M, Abraham R, Ferrarese L, Fullerton AW, Jayawardhana R, Johnston D, Meyer MR, Pipher J, Sawicki M (2008) The JWST tunable filter imager (TFI). In: Society of photo-optical instrumentation engineers (SPIE) conference series, vol 7010. doi:10.1117/12.789504

Duchêne G, Ghez AM, McCabe C (2002) Resolved near-infrared spectroscopy of the mysterious pre-main-sequence binary system T Tauri S. Astrophys J 568:771–778. doi:10.1086/338987. arXiv:astro-ph/0112103

Duchêne G, McCabe C, Ghez AM, Macintosh BA (2004) A multiwavelength scattered light analysis of the dust grain population in the GG Tauri circumbinary ring. Astrophys J 606:969–982. doi:10.1086/383126. arXiv:astro-ph/0401560

Dullemond CP, Dominik C (2004a) Flaring vs self-shadowed disks: the SEDs of Herbig Ae/Be stars. Astron Astrophys 417:159–168. doi:10.1051/0004-6361/20031768. arXiv:astro-ph/0401495

Dullemond CP, Dominik C (2004b) The effect of dust settling on the appearance of protoplanetary disks. Astron Astrophys 421:1075–1086. doi:10.1051/0004-6361:20040284. arXiv:astro-ph/0405226

Dullemond CP, Dominik C, Natta A (2001) Passive irradiated circumstellar disks with an inner hole. Astrophys J 560:957–969. doi:10.1086/323057. arXiv:astro-ph/0106470

Dullemond CP, Hollenbach D, Kamp I, D'Alessio P (2007) Models of the structure and evolution of protoplanetary disks. In: Protostars and planets V, pp 555–572. arXiv:astro-ph/0602619

Durán-Rojas MC, Watson AM, Stapelfeldt KR, Hiriart D (2009) The polarimetric and photometric variability of HH 30. Astron J 137:4330–4338. doi:10.1088/0004-6256/137/5/4330

Durisen RH, Mejia AC, Pickett BK, Hartquist TW (2001) Gravitational instabilities in the disks of massive protostars as an explanation for linear distributions of methanol masers. Astrophys J 563:L157–L160. doi:10.1086/338738

Dutrey A, Guilloteau S, Duvert G, Prato L, Simon M, Schuster K, Menard F (1996) Dust and gas distribution around T Tauri stars in Taurus-Auriga. I. Interferometric 2.7 mm continuum and 13CO J = 1–0 observations. Astron Astrophys 309:493–504

Dutrey A, Guilloteau S, Guelin M (1997) Chemistry of protosolar-like nebulae: the molecular content of the DM Tau and GG Tau disks. Astron Astrophys 317:L55–L58

Dutrey A, Guilloteau S, Ho P (2007) Interferometric spectroimaging of molecular gas in protoplanetary disks. In: Protostars and planets V, pp 495–506

Dzyurkevich N, Flock M, Turner NJ, Klahr H, Henning T (2010) Trapping solids at the inner edge of the dead zone: 3-D global MHD simulations. Astron Astrophys 515:A70

Edgar RG, Quillen AC (2008) The vertical structure of planet-induced gaps in protoplanetary discs. Mon Not R Astron Soc 387:387–396. doi:10.1111/j.1365-2966.2008.13242.x. arXiv:0709.1649

Eisenhauer F, Quirrenbach A, Zinnecker H, Genzel R (1998) Stellar content of the Galactic starburst template NGC 3603 from adaptive optics observations. Astrophys J 498:278. doi:10.1086/305552

Eisner JA (2007) Water vapour and hydrogen in the terrestrial-planet-forming region of a protoplanetary disk. Nature 447:562–564. doi:10.1038/nature05867. arXiv:0706.1239

Eisner JA, Hillenbrand LA, White RJ, Akeson RL, Sargent AI (2005) Observations of T Tauri disks at sub-AU radii: implications for magnetospheric accretion and planet formation. Astrophys J 623:952–966. doi:10.1086/428828

Eisner JA, Chiang EI, Hillenbrand LA (2006) Spatially resolving the inner disk of TW Hydrae. Astrophys J 637:L133–L136. doi:10.1086/500689. arXiv:astro-ph/0601034

Eisner JA, Chiang EI, Lane BF, Akeson RL (2007a) Spectrally dispersed K-band interferometric observations of Herbig Ae/Be sources: inner disk temperature profiles. Astrophys J 657:347–358. doi:10.1086/510833

Eisner JA, Hillenbrand LA, White RJ, Bloom JS, Akeson RL, Blake CH (2007b) Near-infrared interferometric, spectroscopic, and photometric monitoring of T Tauri inner disks. Astrophys J 669:1072–1084. doi:10.1086/521874

Eisner JA, Graham JR, Akeson RL, Najita J (2009) Spatially resolved spectroscopy of sub-AU-sized regions of T Tauri and Herbig Ae/Be disks. Astrophys J 692:309–323. doi:10.1088/0004-637X/692/1/309

Eisner JA, Monnier JD, Woillez J, Akeson RL, Millan-Gabet R, Graham JR, Hillenbrand LA, Pott J, Ragland S, Wizinowich P (2010) Spatially and spectrally resolved hydrogen gas within 0.1 AU of T Tauri and Herbig Ae/Be stars. Astrophys J 718:774–794. doi:10.1088/0004-637X/718/2/774. arXiv:1006.1651

Ercolano B, Owen JE (2010) Theoretical spectra of photoevaporating protoplanetary discs: an atlas of atomic and low-ionization emission lines. Mon Not R Astron Soc 406:1553–1569. doi:10.1111/j.1365-2966.2010.16798.x. arXiv:1004.1203

Ercolano B, Clarke CJ, Drake JJ (2009) X-ray irradiated protoplanetary disk atmospheres. II. Predictions from models in hydrostatic equilibrium. Astrophys J 699:1639–1649. doi:10.1088/0004-637X/699/2/1639. arXiv:0905.1001

Farris A, Klinglesmith D, Seamons J, Torres N, Buscher D, Young J (2010) Software architecture of the Magdalena Ridge Observatory Interferometer. In: Society of photo-optical instrumentation engineers (SPIE) conference series, vol 7740. doi:10.1117/12.856497

Fedele D, van den Ancker ME, Acke B, van den Plas G, van Boekel R, Wittkowski M, Henning T, Bouwman J, Meeus G, Rafanelli P (2008) The structure of the protoplanetary disk surrounding three young intermediate mass stars. II. Spatially resolved dust and gas distribution. Astron Astrophys 491:809–820. doi:10.1051/0004-6361:200810126. arXiv:0809.3947

Fedele D, van den Ancker ME, Henning T, Jayawardhana R, Oliveira JM (2010) Timescale of mass accretion in pre-main-sequence stars. Astron Astrophys 510:A72. doi:10.1051/0004-6361/200912810. arXiv:0911.3320

Fischer DA, Valenti J (2005) The planet-metallicity correlation. Astrophys J 622:1102–1117. doi:10.1086/428383

Fisher M, Boysen RC, Buscher DF, Haniff CA, Seneta EB, Sun X, Wilson DMA, Young JS (2010) Design of the MROI delay line optical path compensator. In: Society of photo-optical instrumentation engineers (SPIE) conference series, vol 7734. doi:10.1117/12.857168

Fitzgerald MP, Kalas PG, Duchêne G, Pinte C, Graham JR (2007a) The AU Microscopii debris disk: multiwavelength imaging and modeling. Astrophys J 670:536–556. doi:10.1086/521344. arXiv:0705.4196

Fitzgerald MP, Kalas PG, Graham JR (2007b) A ring of warm dust in the HD 32297 debris disk. Astrophys J 670:557–564. doi:10.1086/521699. arXiv:0707.3295

Font AS, McCarthy IG, Johnstone D, Ballantyne DR (2004) Photoevaporation of circumstellar disks around young stars. Astrophys J 607:890–903. doi:10.1086/383518. arXiv:astro-ph/0402241

Fortney JJ, Marley MS, Hubickyj O, Bodenheimer PH, Lissauer JJ (2005) Young Jupiters are faint: new models of the early evolution of giant planets. Astron Nachr 326:925

Fortney JJ, Lodders K, Marley MS, Freedman RS (2008a) A unified theory for the atmospheres of the hot and very hot Jupiters: two classes of irradiated atmospheres. Astrophys J 678:1419–1435. doi:10.1086/528370. arXiv:0710.2558

Fortney JJ, Marley MS, Saumon D, Lodders K (2008b) Synthetic spectra and colors of young giant planet atmospheres: effects of initial conditions and atmospheric metallicity. Astrophys J 683:1104–1116. doi:10.1086/589942. arXiv:0805.1066

Fromang S (2005) The effect of MHD turbulence on massive protoplanetary disk fragmentation. Astron Astrophys 441:1–8. doi:10.1051/0004-6361:20053080. arXiv:astro-ph/0506216

Fromang S, Balbus SA, Terquem C, De Villiers JP (2004) Evolution of self-gravitating magnetized disks. II. Interaction between magnetohydrodynamic turbulence and gravitational instabilities. Astrophys J 616:364–375. doi:10.1086/424829. arXiv:astro-ph/0409404

Fukagawa M, Hayashi M, Tamura M, Itoh Y, Hayashi SS, Oasa Y, Takeuchi T, Morino Ji, Murakawa K, Oya S, Yamashita T, Suto H, Mayama S, Naoi T, Ishii M, Pyo TS, Nishikawa T, Takato N, Usuda T, Ando H, Iye M, Miyama SM, Kaifu N (2004) Spiral structure in the circumstellar disk around AB Aurigae. Astrophys J 605:L53–L56. doi:10.1086/420699

Gammie CF (1996) Layered accretion in T Tauri disks. Astrophys J 457:355. doi:10.1086/176735
Gammie CF (2001) Nonlinear outcome of gravitational instability in cooling, gaseous disks. Astrophys J 553:174–183
Gardner JP, Mather JC, Clampin M, Doyon R, Greenhouse MA, Hammel HB, Hutchings JB, Jakobsen P, Lilly SJ, Long KS, Lunine JI, McCaughrean MJ, Mountain M, Nella J, Rieke GH, Rieke MJ, Rix HW, Smith EP, Sonneborn G, Stiavelli M, Stockman HS, Windhorst RA, Wright GS (2006) Science with the James Webb space telescope. In: Society of photo-optical instrumentation engineers (SPIE) conference series, vol 6265. doi:10.1117/12.670492
Gillessen S, Eisenhauer F, Perrin G, Brandner W, Straubmeier C, Perraut K, Amorim A, Schöller M, Araujo-Hauck C, Bartko H, Baumeister H, Berger J, Carvas P, Cassaing F, Chapron F, Choquet E, Clenet Y, Collin C, Eckart A, Fedou P, Fischer S, Gendron E, Genzel R, Gitton P, Gonte F, Gräter A, Haguenauer P, Haug M, Haubois X, Henning T, Hippler S, Hofmann R, Jocou L, Kellner S, Kervella P, Klein R, Kudryavtseva N, Lacour S, Lapeyrere V, Laun W, Lena P, Lenzen R, Lima J, Moratschke D, Moch D, Moulin T, Naranjo V, Neumann U, Nolot A, Paumard T, Pfuhl O, Rabien S, Ramos J, Rees JM, Rohloff R, Rouan D, Rousset G, Sevin A, Thiel M, Wagner K, Wiest M, Yazici S, Ziegler D (2010) GRAVITY: a four-telescope beam combiner instrument for the VLTI. In: Society of photo-optical instrumentation engineers (SPIE) conference series. Society of photo-optical instrumentation engineers (SPIE) conference, vol 7734. doi:10.1117/12.856689. arXiv:1007.1612
Gilmozzi R, Spyromilio J (2008) The 42m European ELT: status. In: Society of photo-optical instrumentation engineers (SPIE) conference series, vol 7012. doi:10.1117/12.790801
Glauser AM, Ménard F, Pinte C, Duchêne G, Güdel M, Monin JL, Padgett DL (2008) Multiwavelength studies of the gas and dust disc of IRAS 04158+2805. Astron Astrophys 485:531–540. doi:10.1051/0004-6361:20065685. arXiv:0804.3483
Glindemann A, Algomedo J, Amestica R, Ballester P, Bauvir B, Bugueño E, Correia S, Delgado F, Delplancke F, Derie F, Duhoux P, di Folco E, Gennai A, Gilli B, Giordano P, Gitton P, Guisard S, Housen N, Huxley A, Kervella P, Kiekebusch M, Koehler B, Lévêque S, Longinotti A, Ménardi S, Morel S, Paresce F, Phan Duc T, Richichi A, Schöller M, Tarenghi M, Wallander A, Wittkowski M, Wilhelm R (2003) The VLTI—a status report. Astrophys Space Sci 286:35–44. doi:10.1023/A:1026145709077
Goldreich P, Tremaine S (1980) Disk-satellite interactions. Astrophys J 241:425
Goldreich P, Ward WR (1973) The formation of planetesimals. Astrophys J 183:1051–1062
Goldreich P, Lithwick Y, Sari R (2004) Final stages of planet formation. Astrophys J 614:497
Golimowski DA, Ardila DR, Krist JE, Clampin M, Ford HC, Illingworth GD, Bartko F, Benítez N, Blakeslee JP, Bouwens RJ, Bradley LD, Broadhurst TJ, Brown RA, Burrows CJ, Cheng ES, Cross NJG, Demarco R, Feldman PD, Franx M, Goto T, Gronwall C, Hartig GF, Holden BP, Homeier NL, Infante L, Jee MJ, Kimble RA, Lesser MP, Martel AR, Mei S, Menanteau F, Meurer GR, Miley GK, Motta V, Postman M, Rosati P, Sirianni M, Sparks WB, Tran HD, Tsvetanov ZI, White RL, Zheng W, Zirm AW (2006) Hubble space telescope ACS multiband coronagraphic imaging of the debris disk around β pictoris. Astron J 131:3109–3130. doi:10.1086/503801. arXiv:astro-ph/0602292
Goodman AA, Benson PJ, Fuller GA, Myers PC (1993) Dense cores in dark clouds. VIII—Velocity gradients. Astrophys J 406:528–547. doi:10.1086/172465
Gorti U, Hollenbach D (2008) Line emission from gas in optically thick dust disks around young stars. Astrophys J 683:287–303. doi:10.1086/589616. arXiv:0804.3381
Gorti U, Hollenbach D (2009) Photoevaporation of circumstellar disks by far-ultraviolet, extreme-ultraviolet and X-ray radiation from the central star. Astrophys J 690:1539–1552. doi:10.1088/0004-637X/690/2/1539. arXiv:0809.1494
Gorti U, Dullemond CP, Hollenbach D (2009) Time evolution of viscous circumstellar disks due to photoevaporation by far-ultraviolet, extreme-ultraviolet, and X-ray radiation from the central star. Astrophys J 705:1237–1251. doi:10.1088/0004-637X/705/2/1237. arXiv:0909.1836
Gould A, Dorsher S, Gaudi BS, Udalski A (2006) Frequency of hot Jupiters and very hot Jupiters from the OGLE-III transit surveys toward the Galactic Bulge and Carina. Acta Astron 56:1–50. arXiv:astro-ph/0601001
Gräfe C, Wolf S, Roccatagliata V, Sauter J, Ertel S (2011) Mid-infrared observations of the transitional disks around DH Tau, DM Tau, and GM Aur. arXiv:1108.2373
Graham JR, Kalas PG, Matthews BC (2007) The signature of primordial grain growth in the polarized light of the AU Microscopii debris disk. Astrophys J 654:595–605. doi:10.1086/509318. arXiv:astro-ph/0609332

Green JJ, Beichman C, Basinger SA, Horner S, Meyer M, Redding DC, Rieke M, Trauger JT (2005) High contrast imaging with the JWST NIRCAM coronagraph. In: Coulter DR (ed) Society of photo-optical instrumentation engineers (SPIE) conference series, vol 5905, pp 185–195. doi:10.1117/12.619343
Guilloteau S, Dutrey A, Piétu V, Boehler Y (2011) A dual-frequency sub-arcsecond study of protoplanetary disks at mm wavelengths: first evidence for radial variations of the dust properties. Astron Astrophys 529:A105. doi:10.1051/0004-6361/201015209. arXiv:1103.1296
Gullbring E, Hartmann L, Briceno C, Calvet N (1998) Disk accretion rates for T Tauri stars. Astrophys J 492:323. doi:10.1086/305032
Haisch KE Jr, Lada EA, Lada CJ (2001) Disk frequencies and lifetimes in young clusters. Astrophys J 553:L153–L156. doi:10.1086/320685. arXiv:astro-ph/0104347
Hartigan P, Edwards S, Ghandour L (1995) Disk accretion and mass loss from young stars. Astrophys J 452:736. doi:10.1086/176344
Hartmann L, Hewett R, Calvet N (1994) Magnetospheric accretion models for T Tauri stars. 1: Balmer line profiles without rotation. Astrophys J 426:669–687. doi:10.1086/174104
Hartmann L, Calvet N, Gullbring E, D'Alessio P (1998) Accretion and the evolutiion of T Tauri disks. Astrophys J 495:385. doi:10.1086/305277
Haupt C, Rykaczewski H (2007) Progress of the ALMA project. Messenger 128:25
Hayashi C (1981) Structure of the solar nebula, growth and decay of magnetic fields and effects of magnetic and turbulent viscosities on the nebula. Prog Theor Phys Suppl 70:35
Herczeg GJ (2007) Observational constraints on disk photoevaporation by the central star. In: Bouvier J, Appenzeller I (eds) IAU Symposium, vol 243, pp 147–154. doi:10.1017/S1743921307009507
Hofner P, Jordan E, Araya E, Kurtz S (2007) The 44 GHz methanol maser line in massive star forming regions. In: Chapman JM, Baan WA (eds) IAU Symposium, vol 242, pp 160–161. doi:10.1017/S174392130701280X
Hogerheijde M (2006) The ALMA design reference science plan. Messenger 123:20
Hollenbach D, Johnstone D, Lizano S, Shu F (1994) Photoevaporation of disks around massive stars and application to ultracompact H II regions. Astrophys J 428:654–669. doi:10.1086/174276
Honda M, Inoue AK, Fukagawa M, Oka A, Nakamoto T, Ishii M, Terada H, Takato N, Kawakita H, Okamoto YK, Shibai H, Tamura M, Kudo T, Itoh Y (2009) Detection of water ice grains on the surface of the circumstellar disk around HD 142527. Astrophys J 690:L110–L113. doi:10.1088/0004-637X/690/2/L110
Howard AW, Marcy GW, Johnson JA, Fischer DA, Wright JT, Isaacson H, Valenti JA, Anderson J, Lin DNC, Ida S (2010) The occurrence and mass distribution of close-in Super-Earths, Neptunes, and Jupiters. Science 330:653. doi:10.1126/science.1194854. arXiv:1011.0143
Hughes AM, Wilner DJ, Calvet N, D'Alessio P, Claussen MJ, Hogerheijde MR (2007) An inner hole in the disk around TW Hydrae resolved in 7 mm dust emission. Astrophys J 664:536–542. doi:10.1086/518885. arXiv:0704.2422
Hughes AM, Wilner DJ, Qi C, Hogerheijde MR (2008) Gas and dust emission at the outer edge of protoplanetary disks. Astrophys J 678:1119–1126. doi:10.1086/586730. arXiv:0801.4763
Hughes AM, Andrews SM, Espaillat C, Wilner DJ, Calvet N, D'Alessio P, Qi C, Williams JP, Hogerheijde MR (2009) A spatially resolved inner hole in the disk around GM Aurigae. Astrophys J 698:131–142. doi:10.1088/0004-637X/698/1/131. arXiv:0903.4455
Hughes AM, Wilner DJ, Andrews SM, Qi C, Hogerheijde MR (2011) Empirical constraints on turbulence in protoplanetary accretion disks. Astrophys J 727:85. doi:10.1088/0004-637X/727/2/85. arXiv:1011.3826
Ida S, Lin DNC (2004a) Toward a deterministic model of planetary formation. I. A desert in the mass and semimajor axis distributions of extrasolar planets. Astrophys J 604:388
Ida S, Lin DNC (2004b) Toward a deterministic model of planetary formation. II. The formation and retention of gas giant planets around stars with a range of metallicities. Astrophys J 616:567
Ida S, Makino J (1993) Scattering of planetesimals by a protoplanet—slowing down of runaway growth. Icarus 106:210
Inaba S, Tanaka H, Nakazawa K, Wetherill GW, Kokubo E (2001) High-accuracy statistical simulation of planetary accretion: II. Comparison with N-body simulation. Icarus 149:235–250
Ingleby L, Calvet N, Bergin E, Yerasi A, Espaillat C, Herczeg G, Roueff E, Abgrall H, Hernández J, Briceño C, Pascucci I, Miller J, Fogel J, Hartmann L, Meyer M, Carpenter J, Crockett N, McClure M (2009) Far-ultraviolet H_2 emission from circumstellar disks. Astrophys J 703:L137–L141. doi:10.1088/0004-637X/703/2/L137. arXiv:0909.0688
Ireland MJ, Kraus AL (2008) The disk around CoKu Tauri/4: circumbinary, not transitional. Astrophys J 678:L59–L62. doi:10.1086/588216. arXiv:0803.2044

Isella A, Natta A (2005) The shape of the inner rim in proto-planetary disks. Astron Astrophys 438:899–907. doi:10.1051/0004-6361:20052773. arXiv:astro-ph/0503635

Isella A, Tatulli E, Natta A, Testi L (2008) Gas and dust in the inner disk of the Herbig Ae star MWC 758. Astron Astrophys 483:L13–L16. doi:10.1051/0004-6361:200809641

Isella A, Carpenter JM, Sargent AI (2009) Structure and evolution of pre-main-sequence circumstellar disks. Astrophys J 701:260–282. doi:10.1088/0004-637X/701/1/260. arXiv:0906.2227

Isella A, Carpenter JM, Sargent AI (2010) Investigating planet formation in circumstellar disks: CARMA observations of Ry Tau and Dg Tau. Astrophys J 714:1746–1761. doi:10.1088/0004-637X/714/2/1746. arXiv:1003.4318

Joergens V, Quirrenbach A (2005) Towards characterization of exoplanetary atmospheres with the VLT interferometer. In: Favata F, Hussain GAJ, Battrick B (eds) 13th Cambridge workshop on cool stars, Stellar systems and the Sun. ESA special publication, vol 560, p 677

Johansen A, Klahr H, Henning T (2006) Gravoturbulent formation of planetesimals. Astrophys J 636:1121–1134

Johansen A, Oishi JS, Low MMM, Klahr H, Henning T, Youdin A (2007) Rapid planetesimal formation in turbulent circumstellar disks. Nature 448:1022

Johnson BM, Gammie CF (2003) Nonlinear outcome of gravitational instability in disks with realistic cooling. Astrophys J 597:131–141. doi:10.1086/378392. arXiv:astro-ph/0312507

Johnstone D, Hollenbach D, Bally J (1998) Photoevaporation of disks and clumps by nearby massive stars: application to disk destruction in the Orion Nebula. Astrophys J 499:758. doi:10.1086/305658

Jorgensen AM, Mozurkewich D (2010) Coherent integration: to real time or not to real time? That is the question. In: Society of photo-optical instrumentation engineers (SPIE) conference series, vol 7734. doi:10.1117/12.858277

Kalas P, Graham JR, Clampin M (2005) A planetary system as the origin of structure in Fomalhaut's dust belt. Nature 435:1067–1070. doi:10.1038/nature03601. arXiv:astro-ph/0506574

Kalas P, Duchene G, Fitzgerald MP, Graham JR (2007a) Discovery of an extended debris disk around the F2 V star HD 15745. Astrophys J 671:L161–L164. doi:10.1086/525252. arXiv:0712.0378

Kalas P, Fitzgerald MP, Graham JR (2007b) Discovery of extreme asymmetry in the debris disk surrounding HD 15115. Astrophys J 661:L85–L88. doi:10.1086/518652. arXiv:0704.0645

Kalas P, Graham JR, Chiang E, Fitzgerald MP, Clampin M, Kite ES, Stapelfeldt K, Marois C, Krist J (2008) Optical images of an exosolar planet 25 light-years from earth. Science 322:1345. doi:10.1126/science.1166609. arXiv:0811.1994

Kama M, Min M, Dominik C (2009) The inner rim structures of protoplanetary discs. Astron Astrophys 506:1199–1213. doi:10.1051/0004-6361/200912068. arXiv:0908.1692

Kastner JH, Zuckerman B, Weintraub DA, Forveille T (1997) X-ray and molecular emission from the nearest region of recent star formation. Science 277:67–71. doi:10.1126/science.277.5322.67

Kenyon SJ, Hartmann L (1995) Pre-main-sequence evolution in the Taurus-Auriga molecular cloud. Astrophys J Suppl Ser 101:117. doi:10.1086/192235

Kitamura Y, Momose M, Yokogawa S, Kawabe R, Tamura M, Ida S (2002) Investigation of the physical properties of protoplanetary disks around T Tauri stars by a 1 arcsecond imaging survey: evolution and diversity of the disks in their accretion stage. Astrophys J 581:357–380. doi:10.1086/344223

Klahr H, Bodenheimer P (2006) Formation of giant planets by concurrent accretion of solids and gas inside an anticyclonic vortex. Astrophys J 639:432

Klahr H, Brandner W (2006) Planet formation. Cambridge University Press, Cambridge

Klahr H, Kley W (2006) 3d-radiation hydro simulations of disk-planet interactions. I. Numerical algorithm and test cases. Astron Astrophys 445:747

Kley W, Bitsch B, Klahr H (2009) Planet migration in three-dimensional radiative discs. Astron Astrophys 506:971–987

Knutson HA, Charbonneau D, Cowan NB, Fortney JJ, Showman AP, Agol E, Henry GW, Everett ME, Allen LE (2009) Multiwavelength constraints on the day-night circulation patterns of HD 189733b. Astrophys J 690:822–836. doi:10.1088/0004-637X/690/1/822. arXiv:0802.1705

Koerner DW, Sargent AI, Beckwith SVW (1993) A rotating gaseous disk around the T Tauri star GM Aurigae. Icarus 106:2. doi:10.1006/icar.1993.1154

Koerner DW, Ressler ME, Werner MW, Backman DE (1998) Mid-infrared imaging of a circumstellar disk around HR 4796: mapping the debris of planetary formation. Astrophys J 503:L83. doi:10.1086/311525. arXiv:astro-ph/9806268

Kraus S, Hofmann KH, Benisty M, Berger JP, Chesneau O, Isella A, Malbet F, Meilland A, Nardetto N, Natta A, Preibisch T, Schertl D, Smith M, Stee P, Tatulli E, Testi L, Weigelt G (2008) The origin of hydrogen line emission for five Herbig Ae/Be stars spatially resolved by VLTI/AMBER spectro-interferometry. Astron Astrophys 489:1157–1173. doi:10.1051/0004-6361:200809946

Kraus S, Hofmann KH, Menten KM, Schertl D, Weigelt G, Wyrowski F, Meilland A, Perraut K, Petrov R, Robbe-Dubois S, Schilke P, Testi L (2010) A hot compact dust disk around a massive young stellar object. Nature 466:339–342. doi:10.1038/nature09174. arXiv:1007.5062

Krist JE, Beichman CA, Trauger JT, Rieke MJ, Somerstein S, Green JJ, Horner SD, Stansberry JA, Shi F, Meyer MR, Stapelfeldt KR, Roellig TL (2007) Hunting planets and observing disks with the JWST NIRCam coronagraph. In: Society of photo-optical instrumentation engineers (SPIE) conference series, vol 6693. doi:10.1117/12.734873

Krumholz MR, Klein RI, McKee CF (2007) Molecular line emission from massive protostellar disks: predictions for ALMA and EVLA. Astrophys J 665:478–491. doi:10.1086/519305. arXiv:0705.0536

Kurz R, Guilloteau S, Shaver P (2002) The Atacama large millimetre array. Messenger 107:7–12

Lagage PO, Doucet C, Pantin E, Habart E, Duchêne G, Ménard F, Pinte C, Charnoz S, Pel JW (2006) Anatomy of a flaring proto-planetary disk around a young intermediate-mass star. Science 314:621–623. doi:10.1126/science.1131436

Lagrange AM, Gratadour D, Chauvin G, Fusco T, Ehrenreich D, Mouillet D, Rousset G, Rouan D, Allard F, Gendron É, Charton J, Mugnier L, Rabou P, Montri J, Lacombe F (2009) A probable giant planet imaged in the β Pictoris disk VLT/NaCo deep L$'$-band imaging. Astron Astrophys 493:L21–L25. doi:10.1051/0004-6361/200811325. arXiv:0811.3583

Lahuis F, van Dishoeck EF, Boogert ACA, Pontoppidan KM, Blake GA, Dullemond CP, Evans NJ II, Hogerheijde MR, Jørgensen JK, Kessler-Silacci JE, Knez C (2006) Hot organic molecules toward a young low-mass star: a look at inner disk chemistry. Astrophys J 636:L145–L148. doi:10.1086/500084. arXiv:astro-ph/0511786

Lai D, Foucart F, Lin DNC (2011) Evolution of spin direction of accreting magnetic protostars and spin–orbit misalignment in exoplanetary systems. Mon Not R Astron Soc 412:2790–2798. doi:10.1111/j.1365-2966.2010.18127.x. arXiv:1008.3148

Lammer H, Bredehöft JH, Coustenis A, Khodachenko ML, Kaltenegger L, Grasset O, Prieur D, Raulin F, Ehrenfreund P, Yamauchi M, Wahlund JE, Grießmeier JM, Stangl G, Cockell CS, Kulikov YN, Grenfell JL, Rauer H (2009) What makes a planet habitable? Astron Astrophys Rev 17:181–249. doi:10.1007/s00159-009-0019-z

Launhardt R (2009) Exoplanet search with astrometry. New Astron Rev 53:294–300. doi:10.1016/j.newar.2010.07.006. arXiv:0904.1100

Launhardt R, Queloz D, Henning T, Quirrenbach A, Delplancke F, Andolfato L, Baumeister H, Bizenberger P, Bleuler H, Chazelas B, Dérie F, Di Lieto L, Duc TP, Duvanel O, Elias NM II, Fluery M, Geisler R, Gillet D, Graser U, Koch F, Köhler R, Maire C, Mégevand D, Michellod Y, Moresmau JM, Müller A, Müllhaupt P, Naranjo V, Pepe F, Reffert S, Sache L, Ségransan D, Salvadé Y, Schulze-Hartung T, Setiawan J, Simond G, Sosnowska D, Stilz I, Tubbs B, Wagner K, Weber L, Weise P, Zago L (2008) The ESPRI project: astrometric exoplanet search with PRIMA. In: Society of photo-optical instrumentation engineers (SPIE) conference series, vol 7013. doi:10.1117/12.789318

Leinert C, Graser U, Przygodda F, Waters LBFM, Perrin G, Jaffe W, Lopez B, Bakker EJ, Böhm A, Chesneau O, Cotton WD, Damstra S, de Jong J, Glazenborg-Kluttig AW, Grimm B, Hanenburg H, Laun W, Lenzen R, Ligori S, Mathar RJ, Meisner J, Morel S, Morr W, Neumann U, Pel JW, Schuller P, Rohloff RR, Stecklum B, Storz C, von der Lühe O, Wagner K (2003) MIDI—the 10 \mum instrument on the VLTI. Astrophys Space Sci 286:73–83. doi:10.1023/A:1026158127732

Leinert C, van Boekel R, Waters LBFM, Chesneau O, Malbet F, Köhler R, Jaffe W, Ratzka T, Dutrey A, Preibisch T, Graser U, Bakker E, Chagnon G, Cotton WD, Dominik C, Dullemond CP, Glazenborg-Kluttig AW, Glindemann A, Henning T, Hofmann K, de Jong J, Lenzen R, Ligori S, Lopez B, Meisner J, Morel S, Paresce F, Pel J, Percheron I, Perrin G, Przygodda F, Richichi A, Schöller M, Schuller P, Stecklum B, van den Ancker ME, von der Lühe O, Weigelt G (2004) Mid-infrared sizes of circumstellar disks around Herbig Ae/Be stars measured with MIDI on the VLTI. Astron Astrophys 423:537–548. doi:10.1051/0004-6361/20047178

Lestrade JF, Wyatt MC, Bertoldi F, Menten KM, Labaigt G (2009) Search for cold debris disks around M-dwarfs. II. Astron Astrophys 506:1455–1467. doi:10.1051/0004-6361/200912306. arXiv:0907.4782

Liffman K (2003) The gravitational radius of an irradiated disk. Publ Astron Soc Aust 20:337–339. doi:10.1071/AS03019

Lin DNC, Papaloizou JCB (1986) On the tidal interaction between protoplanets and the protoplanetary disk. III—Orbital migration of protoplanets. Astrophys J 309:846

Lissauer JJ (1993) Planet formation. Annu Rev Astron Astrophys 31:129

Lissauer JJ, Hubickyj O, D'Angelo G, Bodenheimer P (2009) Models of Jupiter's growth incorporating thermal and hydrodynamic constraints. Icarus 199:338–350

Lissauer JJ, Ragozzine D, Fabrycky DC, Steffen JH, Ford EB, Jenkins JM, Shporer A, Holman MJ, Rowe JF, Quintana EV, Batalha NM, Borucki WJ, Bryson ST, Caldwell DA, Carter JA, Ciardi D, Dunham EW, Fortney JJ, Gautier TN III, Howell SB, Koch DG, Latham DW, Marcy GW, Morehead RC, Sasselov D (2011) Architecture and dynamics of Kepler's candidate multiple transiting planet systems. Astrophys J Suppl Ser 197:8. doi:10.1088/0067-0049/197/1/8. arXiv:1102.0543

Lodato G (2008) Classical disc physics. New Astron Rev 52:21–41. doi:10.1016/j.newar.2008.04.002

Lodato G, Rice WKM (2004) Testing the locality of transport in self-gravitating accretion discs. Mon Not R Astron Soc 351:630–642. doi:10.1111/j.1365-2966.2004.07811.x. arXiv:astro-ph/0403185

Lodato G, Rice WKM (2005) Testing the locality of transport in self-gravitating accretion discs—II. The massive disc case. Mon Not R Astron Soc 358:1489–1500. doi:10.1111/j.1365-2966.2005.08875.x. arXiv:astro-ph/0501638

Lommen D, Maddison ST, Wright CM, van Dishoeck EF, Wilner DJ, Bourke TL (2009) Large grains in discs around young stars: ATCA observations of WW Chamaeleontis, RU Lupi, and CS Chamaeleontis. Astron Astrophys 495:869–879. doi:10.1051/0004-6361:200810999. arXiv:0812.3849

Lopez B, Lagarde S, Wolf S, Jaffe W, Weigelt G, Antonelli P, Abraham P, Augereau JC, Beckman U, Behrend J, Berruyer N, Bresson Y, Chesneau O, Clausse JM, Connot C, Danchi WC, Delbo M, Demyk K, Domiciano A, Dugué M, Glazenborg A, Graser U, Hanenburg H, Henning T, Heininger M, Hofmann KH, Hugues Y, Jankov S, Kraus S, Laun W, Leinert C, Linz H, Matter A, Mathias P, Meisenheimer K, Menut JL, Millour F, Mosoni L, Neumann U, Niedzielski A, Nussbaum E, Petrov R, Ratzka T, Robbe-Dubois S, Roussel A, Schertl D, Schmider FX, Stecklum B, Thiebaut E, Vakili F, Wagner K, Waters LBFM, Absil O, Hron J, Nardetto N, Olofsson J, Valat B, Vannier M, Goldman B, Hönig S, Cotton WD (2009) Matisse. In: Moorwood A (ed) Science with the VLT in the ELT era, p 353. doi:10.1007/978-1-4020-9190-259

Lovis C, Segransan D, Mayor M, Udry S, Benz W, Bertaux JL, Bouchy F, Correia ACM, Laskar J, Curto GL, Mordasini C, Pepe F, Queloz D, Santos NC (2011) The harps search for southern extra-solar planets XXVII. Up to seven planets orbiting HD 10180: probing the architecture of low-mass planetary systems. Astron Astrophys 528:A112

Lubow SH, Seibert M, Artymowicz P (1999) Disk accretion onto high-mass planets. Astrophys J 526:1001

Lynden-Bell D, Pringle JE (1974) The evolution of viscous discs and the origin of the nebular variables. Mon Not R Astron Soc 168:603–637

Malbet F, Benisty M, de Wit WJ, Kraus S, Meilland A, Millour F, Tatulli E, Berger JP, Chesneau O, Hofmann K-H, et al (2007) Disk and wind interaction in the young stellar object <ASTROBJ>MWC 297</ASTROBJ> spatially resolved with AMBER/VLTI. Astron Astrophys 464:43–53. doi:10.1051/0004-6361:20053924

Malbet F, Buscher D, Weigelt G, Garcia P, Gai M, Lorenzetti D, Surdej J, Hron J, Neuhäuser R, Kern P, Jocou L, Berger JP, Absil O, Beckmann U, Corcione L, Duvert G, Filho M, Labeye P, Le Coarer E, Li Causi G, Lima J, Perraut K, Tatulli E, Thiébaut E, Young J, Zins G, Amorim A, Aringer B, Beckert T, Benisty M, Bonfils X, Cabral A, Chelli A, Chesneau O, Chiavassa A, Corradi R, De Becker M, Delboulbé A, Duchêne G, Forveille T, Haniff C, Herwats E, Hofmann KH, Le Bouquin JB, Ligori S, Loreggia D, Marconi A, Moitinho A, Nisini B, Petrucci PO, Rebordao J, Speziali R, Testi L, Vitali F (2008) VSI: the VLTI spectro-imager. In: Society of photo-optical instrumentation engineers (SPIE) conference series, vol 7013. doi:10.1117/12.789710. arXiv:0807.1062

Maness HL, Fitzgerald MP, Paladini R, Kalas P, Duchene G, Graham JR (2008) CARMA millimeter-wave aperture synthesis imaging of the HD 32297 debris disk. Astrophys J 686:L25–L28. doi:10.1086/592783. arXiv:0808.3582

Marcy G, Butler RP, Fischer D, Vogt S, Wright JT, Tinney CG, Jones HRA (2005) Observed properties of exoplanets: masses, orbits, and metallicities. Prog Theor Phys Suppl 158:24–42. doi:10.1143/PTPS.158.24. arXiv:astro-ph/0505003

Marois C, Macintosh B, Barman T, Zuckerman B, Song I, Patience J, Lafrenière D, Doyon R (2008) Direct imaging of multiple planets orbiting the star HR 8799. Science 322:1348. doi:10.1126/science.1166585. arXiv:0811.2606

Mather JC (2010) The James Webb space telescope mission. In: Whalen DJ, Bromm V, Yoshida N (eds) American institute of physics conference series, vol 1294, pp 1–8. doi:10.1063/1.3518853

Mayer L, Quinn T, Wadsley J, Stadel J (2004) The evolution of gravitationally unstable protoplanetary disks: fragmentation and possible giant planet formation. Astrophys J 609:1045

Mazeh T, Zucker S, Pont F (2005) An intriguing correlation between the masses and periods of the transiting planets. Mon Not R Astron Soc 356:955–957. doi:10.1111/j.1365-2966.2004.08511.x. arXiv:astro-ph/0411701
McCabe C, Duchêne G, Ghez AM (2003) The first detection of spatially resolved mid-infrared scattered light from a protoplanetary disk. Astrophys J 588:L113–L116. doi:10.1086/375632. arXiv:astro-ph/0304083
McCabe C, Duchêne G, Pinte C, Stapelfeldt KR, Ghez AM, Ménard F (2011) Spatially resolving the HK Tau B edge-on disk from 1.2 to 4.7 μm: a unique scattered light disk. Astrophys J 727:90. doi:10.1088/0004-637X/727/2/90
McCaughrean MJ, Stauffer JR (1994) High resolution near-infrared imaging of the trapezium: a stellar census. Astron J 108:1382–1397. doi:10.1086/117160
Meeus G, Waters LBFM, Bouwman J, van den Ancker ME, Waelkens C, Malfait K (2001) ISO spectroscopy of circumstellar dust in 14 Herbig Ae/Be systems: towards an understanding of dust processing. Astron Astrophys 365:476–490. doi:10.1051/0004-6361/20000144. arXiv:astro-ph/0012295
Meyer MR, Carpenter JM, Mamajek EE, Hillenbrand LA, Hollenbach D, Moro-Martin A, Kim JS Silverstone MD, Najita J, Hines DC, Pascucci I, Stauffer JR, Bouwman J, Backman DE (2008) Evolution of mid-infrared excess around sun-like stars: constraints on models of terrestrial planet formation. Astrophys J 673:L181–L184. doi:10.1086/527470. arXiv:0712.1057
Millan-Gabet R, Malbet F, Akeson R, Leinert C, Monnier J, Waters R (2007) The circumstellar environments of young stars at AU scales. In: Protostars and planets V, pp 539–554. arXiv:astro-ph/0603554
Millan-Gabet R, Serabyn E, Mennesson B, Traub WA, Barry RK, Danchi WC, Kuchner M, Stark CC, Ragland S, Hrynevych M, Woillez J, Stapelfeldt K, Bryden G, Colavita MM, Booth AJ (2011) Exozodiacal dust levels for nearby main-sequence stars: a survey with the Keck interferometer nuller. Astrophys J 734:67. doi:10.1088/0004-637X/734/1/67
Miller-Ricci E, Meyer MR, Seager S, Elkins-Tanton L (2009) On the emergent spectra of hot protoplanet collision afterglows. Astrophys J 704:770–780. doi:10.1088/0004-637X/704/1/770. arXiv:0907.2931
Mizuno H, Nakazawa K, Hayashi C (1978) Instability of a gaseous envelope surrounding a planetary core and formation of giant planets. Prog Theor Phys 60:699
Monnier JD (2000) An introduction to closure phases. In: Lawson PR (ed) Principles of long baseline stellar interferometry, p 203
Monnier JD, Berger JP, Millan-Gabet R, ten Brummelaar TA (2004) The Michigan infrared combiner (MIRC): IR imaging with the CHARA array. In: Traub WA (ed) Society of photo-optical instrumentation engineers (SPIE) conference series, vol 5491, p 1370
Monnier JD, Millan-Gabet R, Billmeier R, Akeson RL, Wallace D, Berger JP, Calvet N, D'Alessio P, Danchi WC, Hartmann L, et al (2005) The near-infrared size-luminosity relations for Herbig Ae/Be disks. Astrophys J 624:832–840. doi:10.1086/429266
Monnier JD, Berger J, Millan-Gabet R, Traub WA, Schloerb FP, Pedretti E, Benisty M, Carleton NP, Haguenauer P, Kern P, Labeye P, Lacasse MG, Malbet F, Perraut K, Pearlman M, Zhao M (2006) Few skewed disks found in first closure-phase survey of Herbig Ae/Be stars. Astrophys J 647:444–463. doi:10.1086/505340. arXiv:astro-ph/0606052
Morbidelli A, Bottke WF, Nesvorný D, Levison HF (2009) Asteroids were born big. Icarus 204:558–573
Mordasini C, Alibert Y, Benz W (2009a) Extrasolar planet population synthesis I: Method, formation tracks and mass-distance distribution. Astron Astrophys 501:1139–1160
Mordasini C, Alibert Y, Benz W, Naef D (2009b) Extrasolar planet population synthesis II: Statistical comparison with observation. Astron Astrophys 501:1161–1184
Mordasini C, Alibert Y, Benz W, Klahr H, Henning T (in prep.) Extrasolar planet population synthesis IV. Correlations with disk metallicity, mass and lifetime
Mouillet D, Larwood JD, Papaloizou JCB, Lagrange AM (1997) A planet on an inclined orbit as an explanation of the warp in the Beta Pictoris disc. Mon Not R Astron Soc 292:896. arXiv:astro-ph/9705100
Mouillet D, Lagrange AM, Augereau JC, Ménard F (2001) Asymmetries in the HD 141569 circumstellar disk. Astron Astrophys 372:L61–L64. doi:10.1051/0004-6361/20010660
Mourard D, Tallon M, Bério P, Bonneau D, Chesneau O, Clausse JM, Delaa O, Nardetto N, Perraut K, Spang A, Stee P, Tallon-Bosc I, McAlister H, Ten Brummelaar T, Sturmann J, Sturmann L, Turner N, Farrington C, Goldfinger PJ (2010) Performances and first science results with the VEGA/CHARA visible instrument. In: Society of photo-optical instrumentation engineers (SPIE) conference series, vol 7734. doi:10.1117/12.856100

Muterspaugh MW, Lane BF, Konacki M, Wiktorowicz S, Burke BF, Colavita MM, Kulkarni SR, Shao M (2006) PHASES differential astrometry and iodine cell radial velocities of the κ Pegasi Triple star system. Astrophys J 636:1020–1032. doi:10.1086/498209. arXiv:astro-ph/0509406
Muzerolle J, Briceño C, Calvet N, Hartmann L, Hillenbrand L, Gullbring E (2000) Detection of disk accretion at the substellar limit. Astrophys J 545:L141–L144. doi:10.1086/317877
Muzerolle J, D'Alessio P, Calvet N, Hartmann L (2004) Magnetospheres and disk accretion in Herbig Ae/Be stars. Astrophys J 617:406–417. doi:10.1086/425260. arXiv:astro-ph/0409008
Muzerolle J, Allen LE, Megeath ST, Hernández J, Gutermuth RA (2010) A Spitzer census of transitional protoplanetary disks with AU-scale inner holes. Astrophys J 708:1107–1118. doi:10.1088/0004-637X/708/2/1107. arXiv:0911.2704
Najita JR, Strom SE, Muzerolle J (2007) Demographics of transition objects. Mon Not R Astron Soc 378:369–378. doi:10.1111/j.1365-2966.2007.11793.x. arXiv:0704.1681
Najita JR, Doppmann GW, Carr JS, Graham JR, Eisner JA (2009) High-resolution K-band spectroscopy of MWC 480 and V1331 Cyg. Astrophys J 691:738–748. doi:10.1088/0004-637X/691/1/738. arXiv:0809.4267
Nakagawa T (2011) SPICA: the space infrared telescope for cosmology and astrophysics. In: American astronomical society meeting abstracts, vol 218, p 314.01
Naoz S, Farr WM, Lithwick Y, Rasio FA, Teyssandier J (2011) Hot Jupiters from secular planet-planet interactions. Nature 473:187–189. doi:10.1038/nature10076. arXiv:1011.2501
Natta A, Testi L (2008) The study of young substellar objects with ALMA. Astrophys Space Sci 313:113–117. doi:10.1007/s10509-007-9635-0
Natta A, Prusti T, Neri R, Wooden D, Grinin VP, Mannings V (2001) A reconsideration of disk properties in Herbig Ae stars. Astron Astrophys 371:186–197. doi:10.1051/0004-6361:20010334
Natta A, Testi L, Calvet N, Henning T, Waters R, Wilner D (2007) Dust in protoplanetary disks: properties and evolution. In: Protostars and planets V, pp 767–781. arXiv:astro-ph/0602041
Nelson RP, Papaloizou JCB, Masset F, Kley W (2000) The migration and growth of protoplanets in protostellar discs. Mon Not R Astron Soc 318:18–36. doi:10.1046/j.1365-8711.2000.03605.x. arXiv:astro-ph/9909486
Okamoto YK, Kataza H, Honda M, Fujiwara H, Momose M, Ohashi N, Fujiyoshi T, Sakon I, Sako S, Yamashita T, Miyata T, Onaka T (2009) Direct detection of a flared disk around a young massive star HD200775 and its 10 to 1000 AU scale properties. Astrophys J 706:665–675. doi:10.1088/0004-637X/706/1/665. arXiv:0910.4328
Olofsson J, Benisty M, Augereau JC, Pinte C, Ménard F, Tatulli E, Berger JP, Malbet F, Merín B, van Dishoeck EF, Lacour S, Pontoppidan KM, Monin JL, Brown JM, Blake GA (2011) Warm dust resolved in the cold disk around T Chamaeleontis with VLTI/AMBER. Astron Astrophys 528:L6. doi:10.1051/0004-6361/201016074. arXiv:1102.4976
Ormel CW, Dullemond CP, Spaans M (2010) Accretion among preplanetary bodies: the many faces of runaway growth. arXiv:1006.3186
Owen JE, Ercolano B, Clarke CJ, Alexander RD (2010) Radiation-hydrodynamic models of X-ray and EUV photoevaporating protoplanetary discs. Mon Not R Astron Soc 401:1415–1428. doi:10.1111/j.1365-2966.2009.15771.x. arXiv:0909.4309
Owen JE, Ercolano B, Clarke CJ (2011) Protoplanetary disc evolution and dispersal: the implications of X-ray photoevaporation. Mon Not R Astron Soc 412:13–25. doi:10.1111/j.1365-2966.2010.17818.x. arXiv:1010.0826
Paardekooper S, Baruteau C, Crida A, Kley W (2010) A torque formula for non-isothermal type I planetary migration—I. Unsaturated horseshoe drag. Mon Not R Astron Soc 401:1950–1964
Papaloizou JCB, Nelson RP (2005) Models of accreting gas giant protoplanets in protostellar disks. Astron Astrophys 433:247–265
Papaloizou JCB, Terquem C (1999) Critical protoplanetary core masses in protoplanetary disks and the formation of short-period giant planets. Astrophys J 521:823
Papaloizou JCB, Terquem C (2006) Planet formation and migration. Rep Prog Phys 69:119
Pascucci I, Sterzik M (2009) Evidence for disk photoevaporation driven by the central star. Astrophys J 702:724–732. doi:10.1088/0004-637X/702/1/724. arXiv:0908.2367
Pascucci I, Sterzik M, Alexander RD, Alencar SHP, Gorti U, Hollenbach D, Owen J, Ercolano B, Edwards S (2011) The photoevaporative wind from the disk of TW Hya. Astrophys J 736:13. doi:10.1088/0004-637X/736/1/13. arXiv:1105.0045
Pedretti E, Traub WA, Monnier JD, Schuller PA, Ragland S, Berger J, Millan-Gabet R, Wallace G, Burke M, Lacasse MG, Thureau ND, Carleton N (2008) Last technology and results from the

IOTA interferometer. In: Society of photo-optical instrumentation engineers (SPIE) conference series, vol 7013. doi:10.1117/12.789751
Perri F, Cameron AGW (1974) Hydrodynamic instability of the solar nebula in the presence of a planetary core. Icarus 22:416
Perrin G, Woillez J, Lai O, Guérin J, Kotani T, Wizinowich PL, Le Mignant D, Hrynevych M, Gathright J, Léna P, Chaffee F, Vergnole S, Delage L, Reynaud F, Adamson AJ, Berthod C, Brient B, Collin C, Crétenet J, Dauny F, Deléglise C, Fédou P, Goeltzenlichter T, Guyon O, Hulin R, Marlot C, Marteaud M, Melse BT, Nishikawa J, Reess JM, Ridgway ST, Rigaut F, Roth K, Tokunaga AT, Ziegler D (2006a) Interferometric coupling of the Keck telescopes with single-mode fibers. Science 311:194. doi:10.1126/science.1120249
Perrin MD, Duchêne G, Kalas P, Graham JR (2006b) Discovery of an optically thick, edge-on disk around the Herbig Ae star PDS 144N. Astrophys J 645:1272–1282. doi:10.1086/504510. arXiv:astro-ph/0603667
Perrin MD, Schneider G, Duchene G, Pinte C, Grady CA, Wisniewski JP, Hines DC (2009) The case of AB Aurigae's disk in polarized light: is there truly a gap? Astrophys J 707:L132–L136. doi:10.1088/0004-637X/707/2/L132. arXiv:0911.1130
Pesenti N, Dougados C, Cabrit S, O'Brien D, Garcia P, Ferreira J (2003) Near-IR [Fe II] emission diagnostics applied to cold disk winds in young stars. Astron Astrophys 410:155–164. doi:10.1051/0004-6361/20031131
Petrov RG, The AMBER Consortium (2003) Introducing the near infrared VLTI instrument AMBER to its users. Astrophys Space Sci 286:57–67. doi:10.1023/A:1026102009986
Petrov RG, Malbet F, Weigelt G, Antonelli P, Beckmann U, Bresson Y, Chelli A, Dugué M, Duvert G, Gennari S, Glück L, Kern P, Lagarde S, Le Coarer E, Lisi F, Millour F, Perraut K, Puget P, Rantakyrö F, Robbe-Dubois S, Roussel A, Salinari P, Tatulli E, Zins G, Accardo M, Acke B, Agabi K, Altariba E, Arezki B, Aristidi E, Baffa C, Behrend J, Blöcker T, Bonhomme S, Busoni S, Cassaing F, Clausse J, Colin J, Connot C, Delboulbé A, Domiciano de Souza A, Driebe T, Feautrier P, Ferruzzi D, Forveille T, Fossat E, Foy R, Fraix-Burnet D, Gallardo A, Giani E, Gil C, Glentzlin A, Heiden M, Heininger M, Hernandez Utrera O, Hofmann K, Kamm D, Kiekebusch M, Kraus S, Le Contel D, Le Contel J, Lesourd T, Lopez B, Lopez M, Magnard Y, Marconi A, Mars G, Martinot-Lagarde G, Mathias P, Mège P, Monin J, Mouillet D, Mourard D, Nussbaum E, Ohnaka K, Pacheco J, Perrier C, Rabbia Y, Rebattu S, Reynaud F, Richichi A, Robini A, Sacchettini M, Schertl D, Schöller M, Solscheid W, Spang A, Stee P, Stefanini P, Tallon M, Tallon-Bosc I, Tasso D, Testi L, Vakili F, von der Lühe O, Valtier J, Vannier M, Ventura N (2007) AMBER the near-infrared spectro-interferometric three-telescope VLTI instrument. Astron Astrophys 464:1–12. doi:10.1051/0004-6361/20066496
Piétu V, Guilloteau S, Dutrey A (2005) Sub-arcsec imaging of the AB Aur molecular disk and envelope at millimeter wavelengths: a non Keplerian disk. Astron Astrophys 443:945–954. doi:10.1051/0004-6361/20042050. arXiv:astro-ph/0504023
Piétu V, Dutrey A, Guilloteau S, Chapillon E, Pety J (2006) Resolving the inner dust disks surrounding LkCa 15 and MWC 480 at mm wavelengths. Astron Astrophys 460:L43–L47. doi:10.1051/0004-6361/20065968. arXiv:astro-ph/0610200
Piétu V, Dutrey A, Guilloteau S (2007) Probing the structure of protoplanetary disks: a comparative study of DM Tau, LkCa 15, and MWC 480. Astron Astrophys 467:163–178. doi:10.1051/0004-6361/20066537. arXiv:astro-ph/0701425
Pinte C, Ménard F, Berger JP, Benisty M, Malbet F (2008) The inner radius of T Tauri disks estimated from near-infrared interferometry: the importance of scattered light. Astrophys J 673:L63–L66. doi:10.1086/527378. arXiv:0712.0012
Pinte C, Padgett DL, Ménard F, Stapelfeldt KR, Schneider G, Olofsson J, Panić O, Augereau JC, Duchêne G, Krist J, Pontoppidan K, Perrin MD, Grady CA, Kessler-Silacci J, van Dishoeck EF, Lommen D, Silverstone M, Hines DC, Wolf S, Blake GA, Henning T, Stecklum B (2008b) Probing dust grain evolution in IM Lupi's circumstellar disc. Multi-wavelength observations and modelling of the dust disc. Astron Astrophys 489:633–650. doi:10.1051/0004-6361:200810121. arXiv:0808.0619
Pollack JB, Hubickyj O, Bodenheimer P, Lissauer JJ, Podolak M, Greenzweig NC (1996) Formation of the giant planets by concurrent accretion of solids and gas. Icarus 124:62
Pont F (2009) Empirical evidence for tidal evolution in transiting planetary systems. Mon Not R Astron Soc 396:1789–1796. doi:10.1111/j.1365-2966.2009.14868.x. arXiv:0812.1463
Pontoppidan KM, Blake GA, van Dishoeck EF, Smette A, Ireland MJ, Brown J (2008) Spectroastrometric imaging of molecular gas within protoplanetary disk gaps. Astrophys J 684:1323–1329. doi:10.1086/590400. arXiv:0805.3314

Pontoppidan KM, Salyk C, Blake GA, Käufl HU (2010) Spectrally resolved pure rotational lines of water in protoplanetary disks. Astrophys J 722:L173–L177. doi:10.1088/2041-8205/722/2/L173. arXiv:1009.3259
Pott JU, Woillez J, Akeson RL, Berkey B, Colavita MM, Cooper A, Eisner JA, Ghez AM, Graham JR, Hillenbrand L, Hrynewych M, Medeiros D, Millan-Gabet R, Monnier J, Morrison D, Panteleeva T, Quataert E, Randolph B, Smith B, Summers K, Tsubota K, Tyau C, Weinberg N, Wetherell E, Wizinowich PL (2009) Astrometry with the Keck interferometer: the ASTRA project and its science. New Astron Rev 53:363–372. doi:10.1016/j.newar.2010.07.009. arXiv:0811.2264
Pott JU, Woillez J, Ragland S, Wizinowich PL, Eisner JA, Monnier JD, Akeson RL, Ghez AM, Graham JR, Hillenbrand LA, Millan-Gabet R, Appleby E, Berkey B, Colavita MM, Cooper A, Felizardo C, Herstein J, Hrynevych M, Medeiros D, Morrison D, Panteleeva T, Smith B, Summers K, Tsubota K, Tyau C, Wetherell E (2010) Probing local density inhomogeneities in the circumstellar disk of a Be star using the new spectro-astrometry mode at the Keck interferometer. Astrophys J 721:802–808. doi:10.1088/0004-637X/721/1/802. arXiv:1008.1727
Pringle JE (1981) Accretion discs in astrophysics AR. Astron Astrophys 19:137–162. doi:10.1146/annurev.aa.19.090181.001033
Qi C, Ho PTP, Wilner DJ, Takakuwa S, Hirano N, Ohashi N, Bourke TL, Zhang Q, Blake GA, Hogerheijde M, Saito M, Choi M, Yang J (2004) Imaging the disk around TW Hydrae with the submillimeter array. Astrophys J 616:L11–L14. doi:10.1086/421063. arXiv:astro-ph/0403412
Qi C, Wilner DJ, Calvet N, Bourke TL, Blake GA, Hogerheijde MR, Ho PTP, Bergin E (2006) CO J = 6–5 observations of TW Hydrae with the submillimeter array. Astrophys J 636:L157–L160. doi:10.1086/500241. arXiv:astro-ph/0512122
Rafikov RR (2003) The growth of planetary embryos: orderly, runaway, or oligarchic? Astron J 125:942
Rafikov RR (2005) Can giant planets form by direct gravitational instability? Astrophys J 621:L69–L72
Rafikov RR (2009) Properties of gravitoturbulent accretion disks. Astrophys J 704:281–291. doi:10.1088/0004-637X/704/1/281. arXiv:0901.4739
Ragland S, Wizinowich P, Akeson R, Colavita M, Appleby E, Berkey B, Booth A, Cooper A, Crawford S, Dahl W, Felizardo C, Garcia-Gathright J, Gathright J, Herstein J, Hrynevych M, Koresko C, Ligon R, Medeiros D, Mennesson B, Millan-Gabet R, Morrison D, Paine C, Parvin B, Panteleeva T, Serabyn E, Smith B, Summers K, Tsubota K, Tyau C, Wetherell E, Woillez J (2008) Recent progress at the Keck interferometer: operations and V^2 science. In: Society of photo-optical instrumentation engineers (SPIE) conference series, vol 7013. doi:10.1117/12.788070
Ramsay S, D'Odorico S, Casali M, González JC, Hubin N, Kasper M, Käufl HU, Kissler-Patig M, Marchetti E, Paufique J, Pasquini L, Siebenmorgen R, Richichi A, Vernet J, Zerbi FM (2010) An overview of the E-ELT instrumentation programme. In: Society of photo-optical instrumentation engineers (SPIE) conference series, vol 7735. doi:10.1117/12.857037
Ratzka T, Leinert C, Henning T, Bouwman J, Dullemond CP, Jaffe W (2007) High spatial resolution mid-infrared observations of the low-mass young star TW Hydrae. Astron Astrophys 471:173–185. doi:10.1051/0004-6361/20077357. arXiv:0707.0193
Raymond SN, Scalo J, Meadows VS (2007) A decreased probability of habitable planet formation around low-mass stars. Astrophys J 669:606–614. doi:10.1086/521587. arXiv:0707.1711
Raymond SN, Barnes R, Mandell AM (2008) Observable consequences of planet formation models in systems with close-in terrestrial planets. Mon Not R Astron Soc 384:663–674
Raymond SN, O'Brien DP, Morbidelli A, Kaib NA (2009) Building the terrestrial planets: constrained accretion in the inner Solar System. Icarus 203:644–662
Reche R, Beust H, Augereau JC (2009) Investigating the flyby scenario for the HD 141569 system. Astron Astrophys 493:661–669. doi:10.1051/0004-6361/200810419. arXiv:0809.4421
Renard S, Absil O, Berger J, Bonfils X, Forveille T, Malbet F (2008) Prospects for near-infrared characterisation of hot Jupiters with the VLTI Spectro-Imager (VSI). In: Society of photo-optical instrumentation engineers (SPIE) conference series, vol 7013. doi:10.1117/12.790494. arXiv:0807.3014
Renard S, Malbet F, Benisty M, Thiébaut E, Berger J (2010) Milli-arcsecond images of the Herbig Ae star HD 163296. Astron Astrophys 519:A26. doi:10.1051/0004-6361/201014910. arXiv:1007.2930
Ricci L, Testi L, Natta A, Brooks KJ (2010a) Dust grain growth in ρ-Ophiuchi protoplanetary disks. Astron Astrophys 521:A66. doi:10.1051/0004-6361/201015039. arXiv:1008.1144
Ricci L, Testi L, Natta A, Neri R, Cabrit S, Herczeg GJ (2010b) Dust properties of protoplanetary disks in the Taurus-Auriga star forming region from millimeter wavelengths. Astron Astrophys 512:A15. doi:10.1051/0004-6361/200913403. arXiv:0912.3356
Safronov VS (1969) Evolution of the protoplanetary cloud and formation of the earth and the planets. Nauka, Moscow

Sahlmann J, Ménardi S, Abuter R, Accardo M, Mottini S, Delplancke F (2009) The PRIMA fringe sensor unit. Astron Astrophys 507:1739–1757. doi:10.1051/0004-6361/200912271. arXiv:0909.1470

Salyk C, Pontoppidan KM, Blake GA, Lahuis F, van Dishoeck EF, Evans NJ II (2008) H_2O and OH gas in the terrestrial planet-forming zones of protoplanetary disks. Astrophys J 676:L49–L52 doi:10.1086/586894. arXiv:0802.0037

Salyk C, Blake GA, Boogert ACA, Brown JM (2009) High-resolution 5 μm spectroscopy of transitional disks. Astrophys J 699:330–347. doi:10.1088/0004-637X/699/1/330

Santoro FG, Olivares AM, Salcido CD, Jimenez SR, Sun X, Haniff CA, Buscher DF, Creech-Eakman MJ, Jurgenson CA, Shtromberg AV, Bakker EJ, Selina RJ, Fisher M, Young JS, Wilson DMA (2010) Mechanical design of the Magdalena ridge observatory interferometer. In: Society of photo-optical instrumentation engineers (SPIE) conference series, vol 7734. doi:10.1117/12.856591

Santos NC, Israelian G, Mayor M (2004) Spectroscopic [Fe/H] for 98 extra-solar planet-host stars exploring the probability of planet formation. Astron Astrophys 415:1153–1166. doi:10.1051/0004-6361/20034469. arXiv:astro-ph/0311541

Sauter J, Wolf S (2011) Observing dust settling and coagulation in circumstellar discs. Selected constraints from high resolution imaging. Astron Astrophys 527:A27. doi:10.1051/0004-6361/201014546. arXiv:1011.4834

Sauter J, Wolf S, Launhardt R, Padgett DL, Stapelfeldt KR, Pinte C, Duchêne G, Ménard F, McCabe CE, Pontoppidan K, Dunham M, Bourke TL, Chen JH (2009) The circumstellar disc in the Bok globule CB 26. Multi-wavelength observations and modelling of the dust disc and envelope. Astron Astrophys 505:1167–1182. doi:10.1051/0004-6361/200912397. arXiv:0907.1074

Sauty C, Trussoni E, Tsinganos K (2004) Nonradial and nonpolytropic astrophysical outflows. VI. Over-pressured winds and jets. Astron Astrophys 421:797–809. doi:10.1051/0004-6361/20035790

Schegerer AA, Wolf S (2010) Spatially resolved detection of crystallized water ice in a T Tauri object. Astron Astrophys 517:A87. doi:10.1051/0004-6361/200911849

Schegerer AA, Wolf S, Ratzka T, Leinert C (2008) The T Tauri star RY Tauri as a case study of the inner regions of circumstellar dust disks. Astron Astrophys 478:779–793. doi:10.1051/0004-6361:20077049. arXiv:0712.0696

Schegerer AA, Wolf S, Hummel CA, Quanz SP, Richichi A (2009) Tracing the potential planet-forming regions around seven pre-main-sequence stars. Astron Astrophys 502:367–383. doi:10.1051/0004-6361/200810782. arXiv:0905.0565

Schlaufman KC, Lin DNC, Ida S (2009) The signature of the ice line and modest type I migration in the observed exoplanet mass-semimajor axis distribution. Astrophys J 691:1322–1327

Schneider G, Smith BA, Becklin EE, Koerner DW, Meier R, Hines DC, Lowrance PJ, Terrile RJ, Thompson RI, Rieke M (1999) NICMOS imaging of the HR 4796A circumstellar disk. Astrophys J 513:L127–L130. doi:10.1086/311921. arXiv:astro-ph/9901218

Schneider G, Silverstone MD, Hines DC, Augereau JC, Pinte C, Ménard F, Krist J, Clampin M, Grady C, Golimowski D, Ardila D, Henning T, Wolf S, Rodmann J (2006) Discovery of an 86 AU radius debris ring around HD 181327. Astrophys J 650:414–431. doi:10.1086/506507. arXiv:astro-ph/0606213

Schneider G, Weinberger AJ, Becklin EE, Debes JH, Smith BA (2009) STIS imaging of the HR 4796A circumstellar debris ring. Astron J 137:53–61. doi:10.1088/0004-6256/137/1/53. arXiv:0810.0286

Schreyer K, Semenov D, Henning T, Forbrich J (2006) A rotating disk around the very young massive star AFGL 490. Astrophys J 637:L129–L132. doi:10.1086/500732. arXiv:astro-ph/0601270

Selsis F, Kasting JF, Levrard B, Paillet J, Ribas I, Delfosse X (2007) Habitable planets around the star Gliese 581? Astron Astrophys 476:1373–1387. doi:10.1051/0004-6361/20078091. arXiv:0710.5294

Semenov D, Pavlyuchenkov Y, Henning T, Wolf S, Launhardt R (2008) Chemical and thermal structure of protoplanetary disks as observed with ALMA. Astrophys J 673:L195–L198. doi:10.1086/528795. arXiv:0801.1463

Shakura NI, Sunyaev RA (1973) Black holes in binary systems. Observational appearance. Astron Astrophys 24:337–355

Shao M, Colavita MM (1992) Potential of long-baseline infrared interferometry for narrow-angle astrometry. Astron Astrophys 262:353–358

Shepherd DS, Claussen MJ, Kurtz SE (2001) Evidence for a Solar System-size accretion disk around the massive protostar G192.16-3.82. Science 292:1513–1518. doi:10.1126/science.1059475

Showman AP, Guillot T (2002) Atmospheric circulation and tides of "51 Pegasus b-like" planets. Astron Astrophys 385:166–180. doi:10.1051/0004-6361/20020101. arXiv:astro-ph/0202236

Shu F, Najita J, Ostriker E, Wilkin F, Ruden S, Lizano S (1994) Magnetocentrifugally driven flows from young stars and disks. 1: A generalized model. Astrophys J 429:781–796. doi:10.1086/174363

Sibthorpe B, Vandenbussche B, Greaves JS, Pantin E, Olofsson G, Acke B, Barlow MJ, Blommaert JADL, Bouwman J, Brandeker A, Cohen M, De Meester W, Dent WRF, di Francesco J, Dominik C, Fridlund M, Gear WK, Glauser AM, Gomez HL, Hargrave PC, Harvey PM, Henning T, Heras AM, Hogerheijde MR, Holland WS, Ivison RJ, Leeks SJ, Lim TL, Liseau R, Matthews BC, Naylor DA, Pilbratt GL, Polehampton ET, Regibo S, Royer P, Sicilia-Aguilar A, Swinyard BM, Waelkens C, Walker HJ, Wesson R (2010) The Vega debris disc: a view from Herschel. Astron Astrophys 518:L130. doi:10.1051/0004-6361/201014574. arXiv:1005.3543

Sicilia-Aguilar A, Bouwman J, Juhász A, Henning T, Roccatagliata V, Lawson WA, Acke B, Feigelson ED, Tielens AGGM, Decin L, Meeus G (2009) The long-lived disks in the η Chamaeleontis cluster. Astrophys J 701:1188–1203. doi:10.1088/0004-637X/701/2/1188. arXiv:0906.3365

Sicilia-Aguilar A, Henning T, Hartmann LW (2010) Accretion in evolved and transitional disks in CEP OB2: looking for the origin of the inner holes. Astrophys J 710:597–612. doi:10.1088/0004-637X/710/1/597. arXiv:1001.3026

Silber J, Gledhill T, Duchêne G, Ménard F (2000) Near-infrared imaging polarimetry of the GG Tauri circumbinary ring. Astrophys J 536:L89–L92. doi:10.1086/312731. arXiv:astro-ph/0005303

Simon M, Prato L (1995) Disk dissipation in single and binary young star systems in Taurus. Astrophys J 450:824. doi:10.1086/176187

Sing DK, Vidal-Madjar A, Désert JM, Lecavelier des Etangs A, Ballester G (2008) Hubble space telescope STIS optical transit transmission spectra of the hot Jupiter HD 209458b. Astrophys J 686:658–666. doi:10.1086/590075. arXiv:0802.3864

Sivaramakrishnan A, Tuthill PG, Ireland MJ, Lloyd JP, Martinache F, Soummer R, Makidon RB, Doyon R, Beaulieu M, Beichman CA (2009) Planetary system and star formation science with non-redundant masking on JWST. In: Society of photo-optical instrumentation engineers (SPIE) conference series, vol 7440. doi:10.1117/12.826633

Skrutskie MF, Dutkevitch D, Strom SE, Edwards S, Strom KM, Shure MA (1990) A sensitive 10-micron search for emission arising from circumstellar dust associated with solar-type pre-main-sequence stars. Astron J 99:1187–1195. doi:10.1086/115407

Stapelfeldt KR, Krist JE, Menard F, Bouvier J, Padgett DL, Burrows CJ (1998) An edge-on circumstellar disk in the young binary system HK Tauri. Astrophys J 502:L65. doi:10.1086/311479

Stevenson DJ (1982) Formation of the giant planets. Planet Space Sci 30:755–764

Stolte A, Grebel EK, Brandner W, Figer DF (2002) The mass function of the Arches cluster from Gemini adaptive optics data. Astron Astrophys 394:459–478. doi:10.1051/0004-6361/20021118. arXiv:astro-ph/0208321

Stone JM, Hawley JF, Gammie CF, Balbus SA (1996) Three-dimensional magnetohydrodynamical simulations of vertically stratified accretion disks. Astrophys J 463:656. doi:10.1086/177280

Strom KM, Strom SE, Edwards S, Cabrit S, Skrutskie MF (1989) Circumstellar material associated with solar-type pre-main-sequence stars—a possible constraint on the timescale for planet building. Astron J 97:1451–1470. doi:10.1086/115085

Su KYL, Rieke GH, Misselt KA, Stansberry JA, Moro-Martin A, Stapelfeldt KR, Werner MW, Trilling DE, Bendo GJ, Gordon KD, Hines DC, Wyatt MC, Holland WS, Marengo M, Megeath ST, Fazio GG (2005) The Vega debris disk: a surprise from Spitzer. Astrophys J 628:487–500. doi:10.1086/430819. arXiv:astro-ph/0504086

Tanaka H, Takeuchi T, Ward WR (2002) Three-dimensional interaction between a planet and an isothermal gaseous disk. I. Corotation and Lindblad torques and planet migration. Astrophys J 565:1257

Tannirkulam A, Harries TJ, Monnier JD (2007) The inner rim of YSO disks: effects of dust grain evolution. Astrophys J 661:374–384. doi:10.1086/513265. arXiv:astro-ph/0702044

Tannirkulam A, Monnier JD, Harries TJ, Millan-Gabet R, Zhu Z, Pedretti E, Ireland M, Tuthill P, ten Brummelaar T, McAlister H, Farrington C, Goldfinger PJ, Sturmann J, Sturmann L, Turner N (2008) A tale of two Herbig Ae stars, MWC 275 and AB Aurigae: comprehensive models for spectral energy distribution and interferometry. Astrophys J 689:513–531. doi:10.1086/592346. arXiv:0808.1728

Tatulli E, Isella A, Natta A, Testi L, Marconi A, Malbet F, Stee P, Petrov RG, Millour F, Chelli A, et al (2007) Constraining the wind launching region in Herbig Ae stars: AMBER/VLTI spectroscopy of HD 104237. Astron Astrophys 464:55–58. doi:10.1051/0004-6361/20065719

Tatulli E, Malbet F, Ménard F, Gil C, Testi L, Natta A, Kraus S, Stee P, Robbe-Dubois S (2008) Spatially resolving the hot CO around the young Be star 51 Ophiuchi. Astron Astrophys 489:1151–1155. doi:10.1051/0004-6361/200809627

Tatulli E, Benisty M, Ménard F, Varnière P, Martin-Zaïdi C, Thi WF, Pinte C, Massi F, Weigelt G, Hofmann KH, Petrov RG (2011) Constraining the structure of the planet-forming region in the disk

of the Herbig Be star HD 100546. Astron Astrophys 531:A1. doi:10.1051/0004-6361/201016165. arXiv:1104.0905
ten Brummelaar TA, McAlister HA, Ridgway ST, Bagnuolo WG Jr, Turner NH, Sturmann L, Sturmann J, Berger DH, Ogden CE, Cadman R, Hartkopf WI, Hopper CH, Shure MA (2005) First results from the CHARA array. II. A description of the instrument. Astrophys J 628:453–465. doi:10.1086/430729. arXiv:astro-ph/0504082
Terada H, Tokunaga AT, Kobayashi N, Takato N, Hayano Y, Takami H (2007) Detection of water ice in edge-on protoplanetary disks: HK Tauri B and HV Tauri C. Astrophys J 667:303–307. doi:10.1086/520951
Testi L (2008) ALMA science: the ESO-Garching astronomers view. Messenger 131:46–47
Testi L, Leurini S (2008) High angular resolution millimeter observations of circumstellar disks. New Astron Rev 52:105–116. doi:10.1016/j.newar.2008.04.010
Testi L, Natta A, Shepherd DS, Wilner DJ (2001) Constraints on properties of the protoplanetary disks around UX Orionis and CQ Tauri. Astrophys J 554:1087–1094. doi:10.1086/321406. arXiv:astro-ph/0102473
Testi L, Natta A, Shepherd DS, Wilner DJ (2003) Large grains in the disk of CQ Tau. Astron Astrophys 403:323–328. doi:10.1051/0004-6361/20030362. arXiv:astro-ph/0303420
Thalmann C, Grady CA, Goto M, Wisniewski JP, Janson M, Henning T, Fukagawa M, Honda M, Mulders GD, Min M, Moro-Martín A, McElwain MW, Hodapp KW, Carson J, Abe L, Brandner W, Egner S, Feldt M, Fukue T, Golota T, Guyon O, Hashimoto J, Hayano Y, Hayashi M, Hayashi S, Ishii M, Kandori R, Knapp GR, Kudo T, Kusakabe N, Kuzuhara M, Matsuo T, Miyama S, Morino JI, Nishimura T, Pyo TS, Serabyn E, Shibai H, Suto H, Suzuki R, Takami M, Takato N, Terada H, Tomono D, Turner EL, Watanabe M, Yamada T, Takami H, Usuda T, Tamura M (2010) Imaging of a transitional disk gap in reflected light: indications of planet formation around the young solar analog LkCa 15. Astrophys J 718:L87–L91. doi:10.1088/2041-8205/718/2/L87. arXiv:1005.5162
Thatte N, Abuter R, Tecza M, Nielsen EL, Clarke FJ, Close LM (2007) Very high contrast integral field spectroscopy of AB Doradus C: 9-mag contrast at 0.2 arcsec without a coronagraph using spectral deconvolution. Mon Not R Astron Soc 378:1229–1236. doi:10.1111/j.1365-2966.2007.11717.x. arXiv:astro-ph/0703565
Thébault P, Augereau JC (2007) Collisional processes and size distribution in spatially extended debris discs. Astron Astrophys 472:169–185. doi:10.1051/0004-6361/20077709. arXiv:0706.0344
Thommes EW, Duncan M, Levison HF (2003) Oligarchic growth of giant planets. Icarus 162:431
Toomre A (1964) On the gravitational stability of a disk of stars. Astrophys J 139:1217–1238. doi:10.1086/147861
Toomre A (1981) What amplifies the spirals. In: Fall SM, Lynden-Bell D (eds) Structure and evolution of normal Galaxies, pp 111–136
Trilling DE, Bryden G, Beichman CA, Rieke GH, Su KYL, Stansberry JA, Blaylock M, Stapelfeldt KR, Beeman JW, Haller EE (2008) Debris disks around Sun-like stars. Astrophys J 674:1086–1105. doi:10.1086/525514. arXiv:0710.5498
Udry S, Santos NC (2007) Statistical properties of exoplanets. Annu Rev Astron Astrophys 45:397–439. doi:10.1146/annurev.astro.45.051806.110529
van Boekel R, Min M, Leinert C, Waters LBFM, Richichi A, Chesneau O, Dominik C, Jaffe W, Dutrey A, Graser U, Henning T, de Jong J, Köhler R, de Koter A, Lopez B, Malbet F, Morel S, Paresce F, Perrin G, Preibisch T, Przygodda F, Schöller M, Wittkowski M (2004) The building blocks of planets within the 'terrestrial' region of protoplanetary disks. Nature 432:479–482. doi:10.1038/nature03088
van Zadelhoff GJ, van Dishoeck EF, Thi WF, Blake GA (2001) Submillimeter lines from circumstellar disks around pre-main sequence stars. Astron Astrophys 377:566–580. doi:10.1051/0004-6361/20011137. arXiv:astro-ph/0108375
Vehoff S, Hummel CA, Monnier JD, Tuthill P, Nürnberger DEA, Siebenmorgen R, Chesneau O, Duschl WJ (2010) Mid-infrared interferometry of the massive young stellar object NGC 3603—IRS 9A. Astron Astrophys 520:A78. doi:10.1051/0004-6361/200913546. arXiv:1009.1598
Verhoeff AP, Min M, Pantin E, Waters LBFM, Tielens AGGM, Honda M, Fujiwara H, Bouwman J, van Boekel R, Dougherty SM, de Koter A, Dominik C, Mulders GD (2011) The complex circumstellar environment of HD 142527. Astron Astrophys 528:A91. doi:10.1051/0004-6361/201014952. arXiv:1101.5719
Vinković D, Jurkić T (2007) Relation between the luminosity of young stellar objects and their circumstellar environment. Astrophys J 658:462–479. doi:10.1086/511327
Watson AM, Stapelfeldt KR (2007) Asymmetry and variability in the HH 30 circumstellar disk. Astron J 133:845–861. doi:10.1086/510455

Watson AM, Stapelfeldt KR, Wood K, Ménard F (2007) Multiwavelength imaging of young stellar object disks: toward an understanding of disk structure and dust evolution. In: Protostars and planets V, pp 523–538. arXiv:0707.2608

Weidenschilling SJ (1977) Aerodynamics of solid bodies in the solar nebula. Mon Not R Astron Soc 180:57

Weidenschilling SJ, Spaute D, Davis DR, Marzari F, Ohtsuki K (1997) Accretional evolution of a planetesimal swarm. Icarus 128:429

Wilner DJ, Ho PTP, Kastner JH, Rodríguez LF (2000) VLA imaging of the disk surrounding the nearby young star TW Hydrae. Astrophys J 534:L101–L104. doi:10.1086/312642. arXiv:astro-ph/0005019

Winn JN, Fabrycky D, Albrecht S, Johnson JA (2010) Hot stars with hot Jupiters have high obliquities. Astrophys J 718:L145–L149. doi:10.1088/2041-8205/718/2/L145. arXiv:1006.4161

Wizinowich PL, Akeson RL, Colavita MM, Gathright J, Appleby E, Bell J, Booth AJ, Dahl W, Goude P, Hrynevych MA, Lynn I, Millan-Gabet R, Neyman CR, Rudeen AC, Saloga T, Summers K, Tsubota K (2004) Visibility science operations with the Keck interferometer. In: Traub WA (ed) Society of photo-optical instrumentation engineers (SPIE) conference series, vol 5491, p 1678

Woillez J, Akeson R, Colavita M, Eisner J, Ghez A, Graham J, Hillenbrand L, Millan-Gabet R, Monnier J, Pott JU, Ragland S, Wizinowich P, Appleby E, Berkey B, Cooper A, Felizardo C, Herstein J, Hrynevych M, Martin O, Medeiros D, Morrison D, Panteleeva T, Smith B, Summers K, Tsubota K, Tyau C, Wetherell E (2010) ASTRA: astrometry and phase-referencing astronomy on the Keck interferometer. In: Society of photo-optical instrumentation engineers (SPIE) conference series, vol 7734. doi:10.1117/12.857740

Wolf S (2008) Signatures of planets in young and evolved circumstellar disks. Phys Scr T 130(1):014025. doi:10.1088/0031-8949/2008/T130/014025

Wolf S, D'Angelo G (2005) On the observability of giant protoplanets in circumstellar disks. Astrophys J 619:1114–1122. doi:10.1086/426662. arXiv:astro-ph/0410064

Wolf S, Gueth F, Henning T, Kley W (2002) Detecting planets in protoplanetary disks: a prospective study. Astrophys J 566:L97–L99. doi:10.1086/339544. arXiv:astro-ph/0201197

Wolf S, Padgett DL, Stapelfeldt KR (2003) The circumstellar disk of the butterfly star in Taurus. Astrophys J 588:373–386. doi:10.1086/374041. arXiv:astro-ph/0301335

Wolf S, Schegerer A, Beuther H, Padgett DL, Stapelfeldt KR (2008) Submillimeter structure of the disk of the butterfly star. Astrophys J 674:L101–L104. doi:10.1086/529188. arXiv:0801.1422

Wolf S, Lopez B, Jaffe W, Weigelt G, Augereau JC, Berruyer N, Chesneau O, Danchi WC, Delbo M, Demyk K, Domiciano A, Henning T, Hofmann KH, Kraus S, Leinert C, Linz H, Mathias P, Meisenheimer K, Menut JL, Millour F, Mosoni L, Niedzielski A, Petrov R, Ratzka T, Stecklum B, Thiebaut E, Vakili F, Waters LBFM, Absil O, Hron J, Lagarde S, Matter A, Nardetto N, Olofsson J, Valat B, Vannier M (2009) MATISSE science cases. In: Moorwood A (ed) Science with the VLT in the ELT Era, p 359. doi:10.1007/978-1-4020-9190-260

Wolk SJ, Walter FM (1996) A search for protoplanetary disks around naked T Tauri stars. Astron J 111:2066. doi:10.1086/117942

Wuchterl G (1993) The critical mass for protoplanets revisited—massive envelopes through convection. Icarus 106:323–334

Yorke HW (2004) Theory of formation of massive stars via accretion. In: Burton M, Jayawardhana R, Bourke T (eds) Star formation at high angular resolution. IAU Symposium, vol 221, p 141

Yorke HW, Bodenheimer P (1999) The formation of protostellar disks. III. The influence of gravitationally induced angular momentum transport on disk structure and appearance. Astrophys J 525:330–342. doi:10.1086/307867

Youdin AN, Goodman J (2005) Streaming instabilities in protoplanetary disks. Astrophys J 620:459–469

Youdin AN, Mitchell JL (2010) The mechanical greenhouse: burial of heat by turbulence in hot Jupiter atmospheres. Astrophys J 721:1113–1126. doi:10.1088/0004-637X/721/2/1113. arXiv:1008.0645

Zhao M, Monnier JD, Che X, Ten Brummelaar T, Pedretti E, Thureau ND (2010) MIRC closure phase studies for high precision measurements. In: Society of photo-optical instrumentation engineers (SPIE) conference series, vol 7734. doi:10.1117/12.857538

Zhu Z, Hartmann L, Gammie C (2009) Nonsteady accretion in protostars. Astrophys J 694:1045–1055. doi:10.1088/0004-637X/694/2/1045. arXiv:0811.1762

Zinnecker H, Yorke HW (2007) Toward understanding massive star formation. Annu Rev Astron Astrophys 45:481–563. doi:10.1146/annurev.astro.44.051905.092549. arXiv:0707.1279